Genome-wide DNA Methylation and Transcriptome-wide Responses to a Bout of Higher- Versus Lower-load Resistance Training in Previously Trained Men

by

Casey Lee Sexton, PhD(c), CSCS

A dissertation submitted to the Graduate Faculty of
Auburn University
in partial fulfillment of the
requirements for the Degree of
Doctor of Philosophy of Kinesiology

Auburn, Alabama
August 6, 2022

Keywords: skeletal muscle, training volume, DNA methylation, transcriptomics

Approved by

Michael D. Roberts, Ph.D. (Chair) Professor of Kinesiology, Auburn University
C. Brooks Mobley, Ph.D. Assistant Clinical Professor of Kinesiology, Auburn University
Andreas N. Kavazis, Ph.D. Professor of Kinesiology, Auburn University
Kaelin C. Young, Ph.D. Associate Professor of Physiology, Pacific Northwest University of Health Sciences
Adam P. Sharples, Ph.D. Professor of Molecular Physiology and Epigenetics, Norwegian School of Sports Science

Abstract

We sought to determine how genome-wide DNA methylation and transcriptome responses in skeletal muscle differed between one bout of lower-load versus higher-load resistance exercise. Previously trained college-aged males (n=11, age: 23±4 years old, percent body fat: 11.4 ± 6.4%, training experience: 4 ± 3 years, squat strength relative to body weight: 1.7 ± 0.3) performed two bouts of resistance exercise separated by one week. The higher-load bout consisted of 4 sets of back squats and 4 sets of leg extensions to failure using 80% of their estimated one-repetition maximum (Est. 1-RM) (80 Fail), whereas the lower-load bout consisted of this same paradigm using 30% of their Est. 1-RM (30 Fail). Vastus lateralis muscle biopsies were collected before (PRE), 3 hours (3hPOST), and 6 hours (6hrPOST) after each exercise bout. DNA and RNA were batch-isolated from muscle tissue and analyzed for genome-wide DNA methylation and mRNA expression, respectively, using the 850k Illumina MethylationEPIC array and Clariom S mRNA array. The total number of repetitions performed were significantly greater during the 30 Fail versus 80 Fail bout ($p<0.001$); however, total training volume (sets x reps x load) was not significantly different between conditions ($p=0.571$). While 30 Fail training generally led to greater hypomethylation across various promoter regions, the transcriptome-wide responses between bouts were largely similar. Both bouts altered mRNAs involved in inflammatory signaling (e.g., Toll receptor signaling, CCKR signaling, chemokine and cytokine signaling), apoptosis signaling, gonadotropin-releasing hormone signaling, and integrin signaling. Although several studies have examined the muscle-molecular responses to higher- versus lower-load resistance training, this is the first multi-omics comparison of these paradigms. Our transcriptomic data suggest that the molecular signaling events during the early post-exercise period are largely

similar, and this may explain why similar longer-term phenotypes (e.g., myofiber hypertrophy) result from these two resistance training-to-failure modalities.

Acknowledgments

This journey to complete my doctoral degree has been a trial of my grit and resilience, and without the following people, none of it would have been possible. Dr. Michael D. Roberts has been the best mentor I could have asked for. If not for his mentorship and belief in me, I would have never realized my interest in research, nor found a home in his laboratory. I am incredibly grateful for everything you have done for me, so I sincerely thank you. To all my committee members, Dr. Kaelin Young, Dr. Andreas Kavazis, Dr. Adam Sharples, and Dr. C. Brooks Mobley, you all have given me gifts that are invaluable for my future career. Your mentorship, feedback, genuine care, guidance, and friendship will never be forgotten. I would like to give a special thanks to Dr. Adam Sharples for his immense help with this project. You helped execute critical analyses and provided me with unwavering assistance, mentorship, and knowledge. I am forever grateful that you joined my committee. Additionally, Dr. C. Brooks Mobley has given me more guidance, words of encouragement, and intellectual feedback than I could ever hope to repay. You have given me a much wider perspective for my career moving forward and help shape the vision I have for myself. I cannot thank you enough for that.

The Molecular and Applied Sciences Laboratory members past and present, you all have help make this journey fulfilling and meaningful. I want to thank Bradley Ruple, Dr. Shelby Osburn, Nicholas Kontos, Mason McIntosh, Paulo Mesquita, Tony Birikorang, Cleiton Libarti, Blake Hollingsworth, and Philip Agostinelli for all your dedication and hard work on this project. I also want to thank all the other friends I've made here in auburn for keeping me above water and for all the good times we have had. I thank you all for the friendship you've shown me and for being my family away from home. I want to especially thank Joshua Godwin and Dr. Christopher Vann for being the best friends I could have asked for through my time here at Auburn University.

You both have helped shape the person that I am and continue to make me a better person and scientist every day.

I would also like to thank all our collaborators at TruDiagnostics and Thermo Fisher Scientific. You all completed critical arrays that our laboratory could not perform and provided feedback on the project that ultimately led to its overall success. I appreciate all your hard work.

I am also grateful for the participant who volunteered for my study. I know it was grueling and some aspects were very unpleasant, but without you and people like you, there would be no way to move forward to a brighter tomorrow.

I want to also thank Steve and Ann Lambert for their love, generosity, and welcoming me to be a part of their family. My time at Auburn would have never been as special without you and I thank you for all that you have done for me.

I also must give a very special thanks to my parents Billy and Penny Sexton for everything they have done for me. I would have never become the person I am without the inspiration, grit, and resiliency you imparted upon me. I appreciate your unconditional love and belief in me. I hope to continue to make you proud.

Finally, I want to give the biggest thanks to my wonderful wife Stephanie Sexton. You have been my biggest source of courage and inspiration. You've truly been the soul thread keeping my life together and I could never express how deeply and sincerely grateful I have been to have you by my side through this. I love you.

Table of Contents

List of Tables

List of Figures

List of Abbreviations

1-RM	one-repetition maximum
30 Fail	30% 1-RM to failure
3h POST	3 hours post exercise
5-mC	5- methylcytosine
6h POST	6 hours post exercise
80 fail	80% 1-RM to failure
ATP	adenosine triphosphate
cm	centimeters
CpG	cytosine, guanine dinucleotide
CSA	cross-sectional area
DEG	differentially expressed genes
DMP	differentially methylated CpG position
DMR	differentially methylated region
DNMT	DNA methyltransferase
Est. 1-RM	estimated one-repetition maximum
fCSA	muscle fiber cross-sectional area
h	hour
HL	high- load
HV	high- volume
kg	kilograms
mg	milligrams

min	minute
ml	milliliters
mRNA	messenger RNA
ms	millisecond
PRE	prior to exercise
RE	resistance Exercise
RT	resistance Training
s	second
TET	ten-eleven translocase
VL	vastus lateralis
wk	week
μg	micrograms
μl	microliters

Chapter I

Introduction

Resistance training (RT) is one of the most efficacious means to induce skeletal muscle hypertrophy (i.e., accretion of muscle mass and volume) and increase strength [1]. Ultimately, adaptations within skeletal muscle cells, also called myofibers, are a result of environmental stimuli (i.e., overcoming external resistance, producing ATP to meet increased demands, repairing damage, etc.). Alterations in gene expression and increased muscle protein synthesis facilitates molecular adaptations that translate to phenotype outcomes [2, 3]. It has been recognized that RT produces specific molecular signaling based on training intensity (i.e., 0-100% one-repetition maximum (1-RM)) and volume (i.e., sets x repetitions x load) [4]. Further, RT using high loads (≥65% 1-RM) at moderate to low volumes (i.e., 1-5 sets of 1-8 repetitions) generally increases force production capabilities of skeletal muscles, while lower load training (i.e., <65% 1-RM) with high volume (i.e., >3 sets of >10 repetitions) tends to favor glycolytic and mitochondrial adaptations over strength adaptations [5-9]. Several studies to date have observed that a wide range of loads (i.e., high-loads ≥65-80% one-repetition maximum (1RM)) and low loads (20-<65 1-RM) can achieve a similar magnitude of skeletal muscle hypertrophy training to failure [5, 10-14]. However, a divergence in molecular adaptations to different volume-loads of resistance training may occur. For example, in 2019 a study from Lim and colleagues sought to examine several aspects of muscle phenotype after 10 weeks of RT with either: i) 80% of a one-repetition maximum (1-RM) to failure, ii) 30% 1-RM with volume equated to the 80% to failure group, and iii) 30% 1-RM to failure. The authors determined there were similar amounts of hypertrophy, strength increases, and satellite cell number increases across both groups, but mitochondrial adaptations were greater in the 30% 1-RM to failure group [5]. Haun and colleagues reported that a six-week,

lower-load (i.e.,65% 1-RM) extremely high-volume (i.e., week 6 volume: 32 sets of 10 reps, per exercise), full body training program in trained college aged males produced muscle hypertrophy with a disproportionate dilution of myofibrillar proteins [8]. Additionally, these authors reported a significant upregulation in proteins involved with glycolysis. Vann and colleagues subsequently examined the effects of a 10-week higher-load (i.e., >85% 1-RM), moderate- to low-volume, whole body training program in trained college-aged males to that myofibril protein accretion scaled with increases in mean fCSA [15]. These studies have led our laboratory to hypothesize that, during higher volume RT conditions, myofiber hypertrophy occurs due to a disproportionate increase in sarcoplasmic volume [16]. Moreover, we have hypothesized that higher volume RT leads to a more robust metabolic adaptation phenotype. In 2022, Vann and colleagues tested these hypotheses by using a within-subject six-week unilateral leg RT design that compared higher-load (HL; 82.5% to 95% 1-RM, 9 sets of 5 reps each wk) to a lower-load/higher-volume condition (HV; 60% 1-RM, 5 sets of 10 reps at wk 1 to 10 sets of 10 reps at week 6) [17]. There was significant increase in vastus lateralis muscle cross-sectional area (measured by magnetic resonance imaging), and 6-week integrated sarcoplasmic protein synthesis rates were significantly higher in the HV-trained leg. These collective findings suggest that higher- and lower-load training result in divergent molecular adaptations. This, therefore, necessitates more research into this area to determine why molecular outcomes differ.

An acute bout of resistance exercise has been shown to alter activation of signaling pathways (e.g., mTORC1 signaling), elicit epigenetic alterations, and affect the transcription of hundreds to thousands mRNA [18, 19]. One epigenetic mechanism is termed DNA methylation, which is a unique mechanism that alters the ability of RNA polymerase II to transcribe RNA. Several studies have outlined how acute and chronic exercise alters methylation globally and at

specific genes in many different tissues [19-27]. In general, the addition of methyl groups (i.e., hypermethylation) to DNA at repeating cytosine and guanine dinucleotide sites in the promoter region of the gene body (i.e., CpG islands) downregulates mRNA transcription. The opposite is true when DNA promoter regions become hypomethylated (i.e., removal of methyl groups from CpG islands), as this often associated with increased mRNA transcription [21]. Seaborne and colleagues performed a study observing acute and chronic DNA methylation changes by examining young, untrained male subjects through a single bout of training (i.e., the acute condition), followed by a seven-week RE training program (i.e., the chronic condition), which was followed by a seven-week detraining and seven-week retraining period [18, 22]. This training program elicited a significant increase in lean mass with training, a return to baseline with detraining, and a significant increase in lean mass with retraining as compared to the initial training period and baseline. The authors also noted the following: i) after an acute bout of training there were four (i.e., GRINK2, TRAF1, BICC1, and STAG1) genes that became hypomethylated with enhanced gene expression and these genes retained their hypomethylated status throughout the study, ii) after retraining there were roughly twice as many hypomethylated CpG sites compared to the initial training cycle, iii) there were four genes (AXIN1, GRIK2, CAMK4, and TRAF1) that were hypomethylated with enhanced expression after training and maintained this signature throughout the detraining period, and iv) there were five genes (UBR5, RPL35a, HEG1, PLA2G16, and SETD3) that exhibited hypomethylation and enhanced gene expression with training and experienced further hypomethylation and gene expression after retraining [18]. This not only highlights the heterogeneous response of DNA methylation to RT, but also the variable role of DNA methylation in regulating gene expression. Bagley and colleagues [28] subsequently showed that trained participants experienced different changes in methylation status compared to

their untrained counterparts, adding to hypotheses put forth by Seaborne, Turner, and Sharples [18, 19, 21, 22, 24] that prior training plays a role in the DNA methylation responses to exercise. A number of additional studies revealed that additional factors affect DNA methylation including sex [29], nutrition [30], and age [31]. However, the differential alterations in DNA methylation that occur with higher-load versus lower-load resistance exercise have not been characterized.

Given that differential muscle-molecular responses can occur with higher-load and lower-load resistance exercise, it is possible that unique DNA methylation signatures may occur in response to each style of training. Therefore, the purpose of this study is to observe the transient changes in the global and gene-specific methylation statuses between a single bout of failure training using 30% of maximal strength (30FAIL) or failure training using 80% of maximal strength (80FAIL) in previously-trained young adult men. Moreover, we sought to align DNA methylation results to transcriptome-wide analysis to examine how each style of RT affected the transient mRNA responses.

Hypotheses

1. 30FAIL training will elicit a greater hypomethylation compared to 80 Fail training for genes that are related to energy metabolism and a similar methylation status for genes associated with a hypertrophic response.
2. 30FAIL training will cause greater global hypermethylation compared to 80FAIL training.
3. Participants with greater lean mass and muscle fiber size will present less global DNA methylation changes, but a larger and more refined response at the gene specific level, compared to those with lower values.

Chapter II

Literature Review

I will begin this literature review by describing the structure and function of skeletal muscle. Then, I will discuss the differential adaptations of skeletal muscle to higher-load and lower-load resistance training and the studies that have compared the hypertrophic outcome between these conditions. Then, I will give an overview of DNA methylation and its effects on gene expression. Lastly, I will outline the role of DNA methylation in the epigenetic response to an acute bout of resistance training

Structure and Function of Skeletal Muscle

Skeletal muscle possesses high metabolic activity and has the primary functions of locomotion, supporting posture, and producing heat as a byproduct of metabolism. In healthy humans, skeletal muscle makes up approximately 40% of total mass and subsequently 30% of the resting metabolic rate [32]. The focus of this section is on the cellular function and composition of skeletal muscle fibers, as well as the molecular signaling that leads to gene transcription.

Whole muscle (e.g., the vastus lateralis or biceps brachii) is covered in a connective tissue called the epimysium. Within muscle exists bundles of fascicles that are sheathed with perimysium. Fascicles consist of myofiber bundles, with each single myofiber being surrounded by endomysium, otherwise known as the basal lamina [33, 34]. The myofiber has a membrane that is deep to the basal lamina called the sarcolemma, and it acts to retain myocyte organelles (i.e., contractile proteins, sarcoplasmic proteins, ribosomes, intramuscular mitochondria, sarcoplasmic reticulum, etc.) [33, 34]. The epi-, peri-, and endomysium interconnect to form the extracellular

matrix (ECM) of skeletal muscle and the ECM plays important roles in not only tendon to tendon force transduction and microstructure framework, but also in a process termed mechanotransduction (i.e., the process of converting mechanical load into chemical signaling in muscle) that leads to several potential mechanisms of hypertrophy initiation (e.g., nuclear deformation, mTORC1 signaling, muscle protein synthesis, etc.) [1, 33, 35].

Organelles within myofibers play very specific roles in cellular function and maintenance. Myofibrils are the most abundant organelle in myofibers, as estimates suggest that myofibrils occupy ~70-80% of myofiber volume. Sarcomeres exist in series within myofibers and consist of three main bands of proteins which give skeletal muscle its characteristic striated appearance: i) a light-colored isotropic band (I-band) which consists primarily of actin and z-line proteins, ii) a dark-colored anisotropic band (A-band) consisting of overlapping myosin and actin proteins, and iii) the h-zone which contains only myosin. Z-lines exist on both ends of the sarcomere and are made up of rigid interconnecting proteins (i.e., α-actinin) and act as an anchor point for the actin filament. During the power stroke phase of excitation contraction coupling, the z-lines are brought closer together, and I-bands shrink in size as the actin and myosin filaments slide past one another, a hallmark of the sliding filament theory [36, 37]. In studies examining muscle damage, such as those studying the reloading of muscle after disuse during space flight or during eccentric exercise, z-line streaming is often used as confirmation of ultrastructure damage [38].

In addition to myofibrils, a host of other macromolecules exist within myofibers to facilitate proper function. One such macromolecule is the ribosome. Ribosomes consist of 40S and 60S ribosomal subunits. Each subunit is composed of assembled ribosomal RNA, ribosomal proteins, and ribosomal associated proteins [39, 40]. The ribosome is responsible for facilitating the process of translating mRNA to protein. Briefly, translation occurs through the action of three

main sites (i.e., the aminoacyl [A]- site, peptidyl [P]- site, and exit [E]- site) within the ribosome. The A- site is where aminoacylated transfer (t)RNA (a complex of an amino acid and tRNA) are recruited, the P- site is where the amino acids attach to tRNA to form peptide bonds with incoming aminoacylated tRNA in the A- site, and the E- site is where tRNA are removed from their associated amino acids. The continuation of this process is what forms polypeptide chains (i.e., unmodified proteins). All tRNA have three nucleotide bases (anti-codon) that can match with three nucleotide bases from the mRNA (codon). It is this codon coding system that allows for the translation mRNA starting from the codon for methionine (AUG) and ending with 1 of 3 stop codons (UAA, UAG, and UGA), which do not represent an amino acid [41]. Ribosomes can be found at various location within the myofiber, with some found in the sarcoplasm among myofibrils [42], and others found near the sarcoplasmic reticulum [43]. There exists a large heterogeneity in the exact make-up of ribosomes due to differences in ribosomal protein composition, post-translational modification to ribosomal proteins and ribosomal associated proteins, and post-transcriptional modifications to rRNAs [40]. Heterogeneity among ribosomes may indicate specialization that could benefit myofibers through selective translation of specific mRNA at sites advantageous to protein transport and incorporation [44]. In addition, alterations in the concentration of ribosomes are likely to alter the translational capacity of muscle, and several studies have linked the magnitude of RT response to ribosomal rRNA abundances [45, 46]. Likewise, the phosphorylation of ribosomal proteins (e.g., p70-S6K phosphorylating rpS6) can improve the function of ribosomes and increase ribosomal efficiency [47, 48].

Myofibers also have protein complexes responsible for the breakdown of damaged or unneeded proteins, known as proteasomes. The 26S proteasome works in conjunction with another molecule called ubiquitin that acts to mark proteins with a polyubiquitin chain to undergo

proteolysis [49]. Once proteins are ubiquitinated the 19S proteasome subunit recognizes and unfolds the marked protein, the 20S catalytic subunit cleaves peptide bonds in an ATP dependent manner, and the amino acids are discharged from the 26S proteasome [50]. A study from Steffanetti and colleagues showed molecular markers (e.g., atrogin-1, MURF-1, FOXO1, and FOXO3) of the ubiquitin- proteasome pathway (UPP) are altered during exercise, with somewhat divergent outcomes between endurance exercise and resistance exercise [51]. Endurance exercise in trained participants elicited a greater increase in UPP molecular mediators than resistance exercise, suggesting that protein breakdown plays a larger role in endurance exercise adaptation [51]. While the proposed study does not use an endurance exercise model, there are differences in energy demands between higher-load/lower-volume resistance exercise. Thus, there could be observable differences in the methylation status of molecular markers of the UPP, or the nuclear UPP may play a role in the maintenance of DNA methylation enzymes [52].

Muscle contraction itself is dependent on the coordinated function of the motor unit (i.e., motor neurons and all the muscle fibers they innervate). This can be summarized as electrical signals initiated in the central nervous system and propagated through the peripheral nervous system until it interacts with the sarcolemma where an action potential stimulates the sarcoplasmic reticulum (i.e., the organelle that stores skeletal muscle calcium pools) to release calcium into the sarcoplasm (i.e., the aqueous portion of the myofiber not occupied by myofibrils and mitochondria). To accomplish this, action potentials travel down t-tubules to stimulate dihydropyridine receptors, and this leads to a conformational change in ryanodine receptors allowing calcium to flow from the sarcoplasmic reticulum into the sarcoplasm [53]. Once released into the sarcoplasm, calcium binds to receptors located on the c-domain of troponin, altering the position of troponin I which movies tropomyosin away from the actin-myosin binding site

allowing for myofilament interaction [54]. After voluntary muscle contraction ceases, sarcoendoplasmic reticulum calcium ATPase (SERCA) pumps restore the resting membrane potential by transporting cytosolic calcium back into the sarcoplasmic reticulum [55]. There are two primary variants of SERCA pumps within the sarcoplasmic reticulum membrane of adult skeletal muscle, with SERCA1a predominately appearing in fast-twitch muscle fibers and SERCA2b largely appearing in slow-twitch muscle fibers [55, 56]. The ability of SERCA pumps to transport calcium is regulated by the availability of ATP to undergo hydrolysis and phosphorylate SERCA. The acquisition of a phosphate from ATP conformationally changes SERCA and reduces its affinity for calcium ions. While SERCA1a/2b protein content will not be evaluated in the proposed study, reduced availability of ATP and increased metabolite concentrations imposed through failure training may be of consequence to the functional impairment of SERCA pumps, leading to potential avenues through which lower-load/higher-volume compared to higher-load/lower-volume training could induce differing adaptations [57].

The production of ATP at rest, during aerobic exercise, and during recovery from exercise is heavily dependent on the function of mitochondria within the myofiber [58, 59]. Glucose, glycogen[60], amino acids [61], and triglycerides [62] are enzymatically processed (e.g., glycolysis, transamination, and fatty acid oxidation) within the sarcoplasm before being transported into the mitochondrial matrix to be aerobically processed by beta-oxidation and the citric acid cycle. Mitochondrial substrate oxidation ultimately reduces (i.e., the addition of a hydrogen atom) the molecules of nicotinamide adenine dinucleotide (NAD) and flavin adenine dinucleotide (FAD) into NADH and FADH, respectively. NADH and FADH are then used as substrates in oxidative phosphorylation, in which removed hydrogens from NADH and FADH enter the electron transport chain to produce ATP [63]. The generated ATP is then primarily

transported back into the muscle for utilization (e.g., contraction, calcium transport, energy investments, etc.) [64].

Myonuclei and Anabolic Signaling in Myofibers

One organelle not discussed above is the myonucleus. One of the defining characteristics of myofibers, and likely related to its malleable properties, is the feature of being multinucleated. Myofibers can contain hundreds to thousands of myonuclei, and this cell can increase this number to preserve the myonuclear domain, or the area within the myofiber that can be maintained by a single myonucleus [65]. The nuclear genome resides in myonuclei, and this site governs mRNA transcription [66], RNA processing [67], ribosome assembly [68], and controlled RNA export [69]. Given that my dissertation project aims to interrogate epigenetic events that occur in myonuclei in response to resistance exercise, this section will discuss features of this organelle in greater detail relative to the other organelles discussed above. Two topics will be covered in depth including: i) the occurrence and relevance of myonuclear accretion during myofiber hypertrophy in adulthood, and ii) gene regulation through molecular signaling pathways, mechanics of transcriptional machinery, and epigenetic mechanisms.

The addition of myonuclei to postmitotic myofibers during hypertrophic cell growth in adulthood is thought to occur through the fusion of activated satellite cells. In this regard, several studies have shown that longer-term RT increases myonuclear number in proportion to increases in myofiber CSA [70]. Several rodent studies have attempted to illustrate the mechanistic relevance of myonuclear accretion during skeletal muscle hypertrophy. For instance, Bruusgaard et al. [71] reported that myonuclear accretion occurs prior to overload-mediated hypertrophy, and myonuclear number remained elevated even after 14 days after denervation caused atrophy. These

data suggest that myonuclear accretion may mechanistically facilitate myofiber growth given that accretion preceded hypertrophy. However, a study performed by McCarthy and colleagues in 2011 showed that myonuclear accretion is seemingly not necessary for hypertrophy [72]. Specifically, these authors showed that synergist ablation induced hypertrophy occurred with similar magnitudes in both the wildtype mice, who demonstrated myonuclear accretion, and satellite cell depleted mice who showed virtually no myonuclear accretion [72]. To date, these themes (e.g., the permanence of myonuclear accretion during hypertrophy, or the necessity of myonuclear accretion for myofiber hypertrophy) are still heavily debated [73, 74]. Moreover, other data exist that question whether myonuclear accretion is needed to maintain a rigid myonuclear domain. For instance, Millay's laboratory has used the genetic Myomaker inducible knockout mouse model to suggest an inverse relationship exists between myonuclear number and the ability of myonuclei to upregulate mRNA transcription [75]. Applying these data to humans who engage in resistance training would suggest that, although some individuals may initiate RT with lower myonuclear counts per fiber, this would not necessarily impair hypertrophy given that transcriptional output could compensate for lower myonuclear counts. Hence, more data in this area are needed to examine if the myonuclear domain hypothesis is relevant during skeletal muscle hypertrophy during adulthood.

A topic that is more relevant to my proposed project includes phenomena that transiently occur in myofibers and resident myonuclei during an overload stimulus (e.g., one bout of resistance exercise in humans) such as gene regulation through molecular signaling pathways, mechanics of transcriptional machinery, and epigenetic mechanisms. These events will be discussed later in this chapter. However, one topic that will be briefly discussed here is anabolic signaling in myofibers in response to an overload stimulus. Ultimately, the magnitude, duration and frequency of muscle

contraction is what leads to differential downstream phosphorylation and activation of the highly studied anabolic signaling pathway involving mTORC1 signaling, or metabolic-related pathways like MAPK/PGC1-α signaling. Both pathways are thought to lead to an increased expression of proteins from the myonuclear and mitochondrial genomes, regardless of myonuclear accretion or myonuclear domain expansion [4, 31, 58, 71, 72, 76]. While the direct mechanisms connecting mechanical tension produced during a bout of RT and the activation of mTORC1 signaling is currently unknown, the involvement of several factors produced by contraction (e.g., DGK-induced increases in phosphatidic acid, or a dissociation of the TSC2 mTORC1 inhibitor from the mTOR-lysosome complex) are thought to be critical for increasing mTORC1 signaling [77-80]. mTORC1 is implicated to phosphorylate two proteins that have been shown to be important for translation initiation including p70S6K and eukaryotic initiation factor 4E (eIF4E)- binding protein (4E-BP1). One of the foundational studies showing phosphorylation of p70S6K is strongly related to hypertrophic response comes from Baar and Esser in 1999 [70]. These authors used electrical stimulation training in female Wistar rats to simulate six weeks of hindlimb RT, where the muscle hypertrophy observed. Strikingly, tibialis anterior and extensor digitorum longus wet mass was strongly correlated (r=0.998) to changes in p70S6K phosphorylation at 6 hours post exercise (i.e., the time at which phosphorylation changes peaked). Another foundational study from Bodine and colleagues in 2001 provides evidence of there being a causal relationship between mTOR signaling and overload-induced hypertrophy in rodents. These researchers administered rapamycin to mice during different phases of synergist ablation to inhibit mTOR and noted a decrease in activation of p70S6K and a decrease in 4E-BP1 phosphorylation. More strikingly, rapamycin inhibited synergist ablation-induced plantaris hypertrophy up to 14 days following overload. Since these foundational studies, other rodent and human studies have underscored the importance of

mTORC1 signaling in facilitating skeletal muscle hypertrophy [13, 81-85]. This section of the review is meant to inform the reader of how anabolic signaling occurs in myofibers in response to an overload stimulus. However, this aspect of anabolic signaling will not be examined in my project. Instead, what will be discussed later is the emergence of more recent data that underscores the potential importance of signals leading to epigenetic modifications in response to overload stimuli.

RT Adaptation in Skeletal Muscle with Higher-Load and Lower-Load Training

RT is the practice of strategically subjecting adaptable physiological systems to a load- and/or volume-based insults with the purpose of improving future responses to similar stimuli. The type of adaptation elicited from a bout of RT can be manipulated through alterations in relative load (percent of 1-RM), volume (repetitions x sets x load), rest periods (the time between sets in a single exercise and between exercises), as well as the tempo at which repetitions are completed (the time each repetition takes to complete). These variables are highly interrelated such that, when training near or to volitional fatigue, an increased load will decrease the number of repetitions one is able to complete, and visa-versa a reduced load is necessary to achieve a higher number of repetitions. RT uses almost exclusively (~80-100%) anaerobic energy systems to complete exercise lasting from 1-30s, with this value drifting closer to 60% when continued muscular efforts last longer than 2 minutes [86, 87]. Traditionally, higher-load training is implemented into training programs designed to elicit improvements in force production, and lower-load/higher-volume training is primarily used to maximize skeletal muscle hypertrophy and enhance carbohydrate metabolism/ ATP synthesis during repeated muscular efforts [5, 7, 88, 89]. However, this paradigm has been challenged. A study from Burd et al. in 2010 directly compared

leg extension resistance exercise at 30% 1-RM (30 Fail) and 90% 1-RM (90 Fail) to failure, which showed significant differences in the average time under tension per set at ~43 s and 16 s respectively [90]. In addition, the 30 Fail group performed significantly more volume across 4 sets, thus setting the stage for a comparison of the transient responses between higher-load/lower-volume and lower-load/higher-volume training. At 4h post-exercise, both conditions showed a significant elevation in myofibrillar and sarcoplasmic protein synthetic responses. However, the 30 Fail group showed a significantly higher myofibrillar and sarcoplasmic protein synthetic response, compared to the 90 Fail group 24 hours following exercise. Speculatively, the data showing the delayed response differences in protein synthetic rates indicate that skeletal muscle hypertrophy in response to both modes of training would differ. However, several studies, reviews, and meta-analyses have shown that higher-load/lower-volume compared to lower-load/higher volume RT elicit similar increases in strength and hypertrophic outcomes [5, 9, 11, 13, 14, 16, 89-97]. In 2017, Schoenfeld et al. [14] published a systematic review and meta-analysis on this topic, and showed little difference between higher-load (>60% 1-RM) and lower-load (≤ 60%1-RM) RT to failure for hypertrophy, and in this meta-analysis, the cited studies used a wide array of techniques to measure muscle hypertrophy. When the evaluated studies used air displacement plethysmography (i.e., BOD-POD) to estimate whole-body lean mass [98-100], magnetic resonance imaging and computerized tomography to measure muscle-cross-sectional area [13, 92, 101-105], or muscle biopsies to measure fCSA [6, 13, 106], there were no differences in hypertrophic outcomes between higher-load or lower-load groups. While informative, these studies were only concerned with measures of whole muscle, or myofiber CSA, and did not provide a conclusive profile of the molecular adaptations that occurred. However, Lim and colleagues performed a recent 10- week RT study with groups performing leg exercises to failure

at 80% 1-RM (80 Fail) or 30% 1-RM (30 Fail) [5]. The study evaluated biopsy samples and discovered that both modes of training increased type I and II muscle fiber CSA values, showing failure training activates all muscle fiber types, despite a difference in load. In addition, both the 80 Fail and 30 Fail groups significantly increased satellite cell number per type I muscle fiber, while type II fibers increased myonuclei per fiber with an associated decrease in myonuclear domain size. In contrast, the 30 Fail group significantly increased average satellite cell number per fiber in type II muscle fibers, as well as markers of mitophagy, mitochondrial fusion, and mitochondrial fission (i.e., improved function and proliferation of mitochondria). This study was one of the first studies to show different molecular adaptations occur in response to different volume-loads of RT, and this (along with other studies cited herein) motivated our own laboratory to compare molecular adaptations that occur in response to both modes of training.

Our Laboratory's Contributions to the Volume-Load Resistance Training Literature

Our laboratory has conducted several experiments that have directly or indirectly compared the effects of higher-load versus lower-load RT on molecular adaptations in skeletal muscle. First, Haun in 2017 conducted an acute, within-subject design leg extension study that examined molecular signaling events in response to single bouts of 80% 1-RM to failure (80 Fail) and 30% 1-RM to failure (30 Fail) training. The main outcomes of this study were mRNA expression certain genes related to muscle structure and adaptations as well as mTORC1 pathway and AMPK protein phosphorylation. Load independent increases in the mRNA expression of MuRF-1 and PGC1-α and a decrease in MSTN mRNA was observed. Further, no differences were observed between load conditions for phosphorylated (p)-mTOR, p-AMPK, p-p70S6K, p-rpS6, or p-4EBP1. As a secondary aim, electromyography (EMG) data were collected during exercise. Interestingly, there

was a significantly higher EMG signal across all sets for the 80 Fail condition. Moreover, isokinetic torque at the knee was significantly lower in the 30FAIL group versus 80FAIL group 48 hours following each bout. Collectively, these data suggested that no molecular signaling differences occurred between groups within a 90-minute post-exercise window. However, a higher residual post-exercise fatigue was present following 30 Fail training suggesting a greater demand on the neuromuscular system. Thereafter, Haun and colleagues published another study showing that six weeks of extremely high-volume training at ~60% 1-RM increased mean myofiber CSA in lieu of decreases in the relative content (or concentration) of the actin and myosin heavy chain proteins and an upregulation several proteins involved with glycolysis [8]. Our laboratory speculated that very high-volume RT may lead to a disproportionate increase in myofiber size through sarcoplasmic expansion, and this coincides with myofiber metabolic adaptation via an upregulation in sarcoplasmic enzymes responsible for ATP generation. In 2020, Vann and colleagues evaluated the effects of 10 weeks of higher-load RT on muscle protein changes, muscle growth, and strength adaptations [15]. The results suggested that with higher-load RT: i) a fiber-type specific pattern of muscle growth occurred (i.e., type II muscle fibers significantly increased cross-sectional area), ii) there was a more modest decrease in abundance of contractile proteins relative to that reported by Haun and colleagues, and iii) there was an absence of metabolic adaptation as seen with Haun and colleagues. In 2022, Vann and colleagues directly compared higher-load to higher-volume RT through the use of a single-leg RT paradigm where participants used one leg to perform higher-load RT (HL, 82.5% - 95% 1-RM) and the other was assigned to lower-load RT (HV, 60% 1-RM) RT [17]. The main findings of this study were as follows: i) when using MRI to measure VL cross-sectional area, the HV leg underwent hypertrophy, where the HL leg did not, ii) leg extensor strength increased more in the HL leg

compared to HV leg, and iii) 6-week integrated non-myofibrillar protein synthesis was significantly higher in HV compared to HL. Again, this study provides evidence that RT paradigms with different volume-loads seemingly facilitate differential molecular responses. However, it is currently unknown if the divergent molecular adaptations between training paradigms are related to the differential epigenetic mechanisms, and this will be discussed in the purpose statement of this chapter.

Brief Commentaries on Genetics and Epigenetics

Gregor Mendel first described heredity through his work in pea plants during the mid-19th century [107]. However, his work went largely unnoticed until the turn of the century, well after his death. The scientific community began to discuss how living organisms could possibly pass on traits to their progeny, and before the discovery of DNA, there were several hypotheses for what molecules could be responsible. Many scientists in the early- to mid- 20th century believed chromosomes where the functional unit for heredity [108]. The importance of the individual gene was often overlooked and was mistakenly thought to be composed of proteins [109-111]. In 1944, Avery, Macleod, and McCarty provided pivotal evidence that nucleic acids and not proteins were the molecule that contained inheritable genetic information. This was demonstrated with an experiment that used biologically active deoxyribose nucleic acid (DNA) from a virulent type III Pneumococcus to transform the avirulent type II Pneumococcus into a type III Pneumococcus [112]. As the integration of DNA from one type of bacteria to another caused phenotype alterations, it verified that DNA was the key genetic molecule that scientists had been searching for [112]. This discovery set forth a cascade of research surrounding DNA and genetics, including the identification of the four nucleic acids in DNA (adenine, thymine, cytosine, and guanine) as

well as their use in replication among eukaryotic organisms [113-115]. In 1953, the discoveries of Rosalind Franklin led to the foundational Watson and Crick paper describing the three-dimensional structure of DNA, and from there, countless new and invaluable discoveries have since aided our understanding of genetics [116].

Geneticist Adrian Bird was a pioneer in the scientific discipline of epigenetics. In a foundational review article on the topic, Bird described scientific findings in the 1980's, many which were from his own laboratory, that outlined the physiological significance of DNA methylation in eukaryotes [117]. Decades later, the scientific community has come to appreciate that mRNA transcription is regulated, in part, through DNA methylation. Estimates suggest that ~98% of DNA methylation occurs on cytosine residues present in cytosine guanine dinucleotide pairing sites (i.e., CpG sites), and DNA methylation is catalyzed by DNA methyltransferase (DNMT) enzymes whereas de-methylation is catalyzed by ten-eleven translocation (TET) enzymes [27, 118-120]. An upregulation in DNA methylation in a promoter or enhancer region of a gene negatively affects mRNA transcription by either preventing transcription factor binding or compacting DNA and making it transcriptionally inaccessible [120]. A large and recent research emphasis has focused on how different modes of exercise alter the collective DNA methylome in skeletal muscle [21, 121-123], and this will be discussed in the following sections.

Regulation of Transcription and Epigenetic Modifications

The central dogma of molecular biology indicates that genetic information from DNA must be transcribed by RNA polymerase II into messenger RNA (mRNA), mRNA must be translated by ribosomes into proteins, and proteins are translocated and integrated into the cell structures [124]. Several genes not being actively expressed exist in a tightly wound state known

as heterochromatin [125], and in order for DNA to be read by various RNA polymerases, heterochromatin must be conformationally altered to euchromatin. Underlying the transition from heterochromatin to euchromatin is the winding and unwinding action of the DNA-protein complex known as the nucleosome. The nucleosome contains an octamer of histone proteins made up of two sets of H2A, H2B, H3, H4. Additionally, 147 base pairs of DNA is wrapped around each nucleosome [126, 127]. Histone tails consist of several amino acid residues in series. These residues make histones receptive to post-translational modifications from several groups of molecules (i.e., acetyl groups, methyl groups, etc.). Based on the amino acid residue that is modulated and the level of modification (e.g., the addition of 1,2, or 3 methyl groups), histones electrostatically change the availability of DNA transcriptional start sites to general and specific transcription factors [128].

In 2001, the entire euchromatic portion human genome was mapped [129, 130], giving researchers a means to understand not only human genetics and its relationship with phenotype, but also the epigenetic regulation of this relationship. DNA methylation is perhaps the most researched epigenetic modification. Methylation can be described as the addition of methyl groups to either tails of amino acid residues that extend from histones, known as histone methylation, or to the nucleic acid cytosine on DNA, known as DNA methylation [21]. Both types of methylation are derived from the donation of methyl groups from an S-adenosyl methionine (SAM), and SAM can be replenished through the activity of methionine adenosyl transferase (MAT) converting S-adenosylhomocysteine (SAH) to SAM [131]. Histone methylation is a post-translational modification that has been shown to cause confirmational changes to the nucleosomes making DNA either more or less accessible to transcriptional machinery depending on the amino acid residue methylated and the level of methylation (i.e., mono- di-, or tri-methylation) that occurs.

DNA methylation occurs primarily at CpG dinucleotides within the promoter region of genes called CpG islands, albeit DNA methylation can also occur upstream and downstream from the promoter region at CpG shores and CpG shelves, respectively. DNA methylation can also occur less frequently at non-CpG sites, albeit these sites only constitute ~0.02% of 5-methylcytosines [132]. As with histone methylation, DNA methylation affects the ability of specific and general transcription factors to bind to DNA and this can subsequently reduce the ability of RNA polymerases to associate with promoter regions of genes [21, 133]. Active DNA methylation and demethylation are regulated via two main families of enzymes. *De novo* methylation is controlled by DNMT3a/b enzymes, and active removal of methyl groups from cytosines (i.e., demethylation) is facilitated by ten-eleven translocase (TET) enzymes [21, 27, 134, 135]. TET enzymes act to remove methyl group from DNA by oxidation of 5-methylcytosine (5mC) into 5-hydroxymethylcytosine (5-hmC), 5-formylcytosine (5fC), or 5-carboxylcytosine (5caC), which can then be marked for based-excision repair and replaced with an unmethylated cytosine [27]. DNA can also undergo hemi-methylation through DNMT1 enzymes reading DNA and adding methyl groups antisense to existing modified cytosines [136].

DNA Methylation Responses to Resistance Training and Overload

Within the mammalian genome, DNA methylation is the primary epigenetic modification used to alter transcription at the DNA level [21], and several studies in this section will describe how exercise modulates this process. In 2012, Barrés et al. performed seminal work that outlined how acute endurance exercise alters the epigenetic profile in skeletal muscle [133]. The promoter methylation and mRNA profiles of various metabolic genes (i.e., PGC-1α, TFAM, PPAR-δ, PDK4, citrate synthase for metabolic genes and MEF2A and MYOD1 for muscle-specific

transcription factors) were examined from human vastus lateralis biopsies prior to and 20 minutes following a bout of cycle training. The results showed that DNA was globally hypomethylated after exercise, and the DNA methylation of metabolic genes was generally downregulated after exercise as well. Interestingly, these patterns corresponded with an increased abundance of several of the associated mRNA transcripts. The authors also examined a second cohort of nine untrained participants completed that completed a training bout that used either 40% or 80% of their VO2 max, and muscle biopsies were collected before, 0h after, and 3h after exercise. The results showed that the high intensity exercise elicited more hypomethylation than the lower intensity exercise for PGC-1α, TFAM, PPAR-δ, and MEF2A. When these findings were compared to previous mRNA data collected from the same participants, the genes that underwent hypomethylation presented increases in mRNA levels. Rat skeletal muscle was also exposed to ex-vivo stimulation (0.1 ms impulse, every 1s for 5 minutes, repeated every 10 minutes until 60 min of total stimulation). A significant increase in gene expression was evident ~2.5 hours after stimulation, and this was associated with promoter hypomethylation 45 minutes post stimulation. Finally, the authors performed *in vitro* experiments that treated myotubes derived from rat muscle with caffeine as an exercise mimetic. This work showed caffeine decreased promoter methylation in genes that had increased mRNA expression. Additionally, blocking calcium release inhibited the effects of caffeine. These elaborate series of experiments by Barrés and colleagues provided several lines of evidence to suggest that: i) exercise alters DNA methylation in promoter regions, ii) the amplitude of change is seemingly dependent on exercise intensity, and iii) the action of calcium release from the sarcoplasmic reticulum is involved in DNA hypomethylation of the promoter regions of genes associated with exercise adaptation. This report led to a series of experiments examining how different modes of exercise affected DNA methylation in skeletal muscle. For instance, in 2018

Seaborne and colleagues showed that RT altered DNA methylation in adult skeletal muscle [18, 22]. In one of these studies, Seaborne examined eight untrained males prior to and following a single bout of resistance exercise as well as with a seven-week (3d/week) RT program (loading), a 7-week period of no resistance training (unloading), and a seven-week (3d/week) re-training period (re-loading). DNA methylation was evaluated in muscle tissue at 850,000 CpG sites using a methylation array. The single bout portion of the study showed that skeletal muscle presented differential DNA methylation with a greater portion of CpGs being hypomethylated (0,284 CpGs) than hypomethylated (7,600 CpGs). Moreover, 18 CpG sites showed a significantly strong fold-change correlation when comparing loading and reloading ($r = 0.94$, $p < 0.001$). Additionally, there were 4 of the 18 CpG sites that had been identified in the loading, unloading, and reloading analysis (BICC1, GRIK2, ODF2, TRAF1), and these genes are implicated in cytoskeletal organization [137], neurological function [138], microtubule interaction [139], and activation of the NF-κB and MAPK pathways [140], respectively. While the hypomethylation response of these genes to one bout of exercise did not lead to increased gene expression, there was an increased gene expression in STAG1 and TRAF1 after reloading. During chronic training, participants experienced significant hypertrophic adaptations (6.5% increase versus baseline), and after unloading there was a significant decrease in lean mass (-4.5% versus loading), with no significant difference between unloading and baseline. Due to what the authors proposed as a form of "muscle memory", the re-loading period resulted in a 12% increase of lean mass compared to baseline and a 5.9% increase compared to changes seen during initial loading. A follow-up study by this research group showed that one bout of resistance exercise leads to a 57% hypomethylation of CpGs within gene promoter regions [24] Since this seminal RT work, other experiments have shown that overload affects DNA methylation patterns of rRNA genes [141], and RT causes a vast hypomethylation of the

mitochondrial methylome in older participants [31]. Overload models in rodents have also provided informative data in this area. For example, Figueiredo et al. [141] showed an overload stimulus in mice favorably alters the promoter methylation status of genes associated with ribosome biogenesis, and ribosome biogenesis has been causally linked to skeletal muscle hypertrophy [68]. Von Walden et al. [142] used the genetic HSA-GFP mouse model to show 11,210 CpG sites were hypomethylated and 3,491 sites were hypermethylated in the plantaris muscle three days following synergist ablation. Follow-up analyses by these authors indicated that CpG sites in proximity to genes involved in mTORC1 signaling, autophagy, and ribosome biogenesis were hypomethylated, and the mRNAs of several of these genes were upregulated. Wen et al. [143] used this same mouse model to show that four weeks of retraining, which was preceded by an eight-week period of resistance wheel running and 12 weeks detraining, led to enhanced muscle growth (relative to naïve hypertrophy) that corresponded with a myonuclear methylome "memory" signature; notably, these findings are reminiscent of the aforementioned human data from Sharples' group.

Although the aforementioned studies have been informative, aligning DNA methylation to transcriptomic outcomes have yielded mixed results. A 2019 study from Tuner, Seaborne, and Sharples directly compared transcriptomic data from young, healthy males to the acute and chronic DNA methylation data collected in the previously mentioned Seaborne 2018 study [24]. The acute data revealed there were 1802 differentially expressed genes, with 866 having elevated expression and 936 having depressed expression. Interestingly, of the 866 genes with increased mRNA expression, 270 were hypomethylated and 216 were hypermethylated. Laker et al. [144] also aligned transcriptome and methylome data in humans prior to and following three resistance exercise bouts over a nine-day period. RNA-sequencing indicated that training altered the

expression of 2,616 mRNAs, while methylome analysis using RRBS (i.e., sequencing) indicated 474 genomic regions were differentially methylated. Interestingly, only 54 genes showed concomitant alterations in DNA methylation and mRNA expression patterns following training. Simply stated, these data suggest DNA methylation changes during resistance training may only affect ~2% of genes that are altered at the mRNA level. The aforementioned disparities between methylome and transcriptome data could be due to the timing of tissue acquisition [145]. Specifically, load-induced DNA methylation patterns are seemingly transient (i.e., within three hours following an exercise bout), and these events may affect mRNA expression patterns hours to days thereafter. However, this relationship has not been extensively explored and more data are needed to validate this hypothesis.

Purpose statement

Key concepts were presented in this chapter. First, it is evident that different molecular (and potentially hypertrophic) adaptations can occur with higher load versus higher volume resistance training, and our laboratory has contributed several studies to this body of literature in support of this hypothesis. Second, resistance training can transiently and chronically alter the DNA methylome and transcriptome. Third, limited data suggest select mRNAs respond similarly following a single bout of higher-load versus lower-load resistance exercise. It is not currently known, however, if higher-load versus lower-load RT elicits similar or different methylome-wide or transcriptome-wide responses in skeletal muscle. Therefore, the purpose of this study is to observe the transient changes in DNA methylation statuses with two different modes of failure training using either 30% of maximal strength (30FAIL) or 80% of maximal strength (80FAIL). To accomplish this aim, previously trained college-aged males (n=11) were recruited for this study.

These participants reported to the laboratory in a fasted state and performed either a 30FAIL or 80FAIL resistance exercise bout with the barbell back squat exercise (4 sets) and bilateral leg extensor exercise (4 sets). Biopsies were collected prior to the bout as well as 3 hours and 6 hours following the bout. One week following this bout participants reported to the laboratory during a similar time of day to perform the other style of training, and biopsies were collected at similar timepoints. Outcomes from this study will add to the current body of literature given that it will be the first comprehensive methylome and transcriptome interrogation between these styles of training.

Chapter III

Methods

Ethical Approval and Pre-screening

This study was conducted with prior review and approval from the Auburn Institutional Review Board and in accordance with the most recent revisions of the Declaration of Helsinki (IRB approval #: 20-081 MR 2003).

The participants recruited for this study were young males from the local area that met the following criteria: i) aged 18-35, ii) a body mass index ([BMI] body mass in kilograms/ height in meters^2) not exceeding 35 kg/m^2, iii) no known cardio-metabolic disease (e.g., obesity, diabetes, hypertension, heart disease) or any condition contraindicating participation in resistance training, donating muscle biopsies, or receiving finger sticks, iv) have participated in lower-body training at least once per week over the last 6 months, v) have a self-reported barbell back-squat one repetition maximum of ≥ 1.5x body weight. Following verbal and written consent, participants then completed testing for maximal strength on the barbell-back squat (estimated by a three-repetition maximum) as well as body composition testing for BMI.

Study Design

The study design schematic is available in Figure 3.1. Participants completed a within subject design that included a total of five visits to the laboratory. At visit 1, an informed consent and health history questionnaire were completed. This was followed by testing to determine maximal strength for the barbell back squat and knee extension. At Visit 2, participants completed a battery of baseline (PRE) tests that included measures of height, weight, and vastus lateralis (VL)

thickness. Participants also donated a muscle biopsy from the VL prior to the completion of a single bout of resistance exercise using a randomly assigned experimental load (i.e., 30% or 80% estimated 1-RM). Then, at both 3 hours (3h POST) and 6 hours (6h POST) following the exercise bout, participants received additional muscle biopsies from the VL. Finally, after approximately 7 days, participants completed another bout of resistance exercise using the experimental load not completed at visit 2 (i.e., if visit 2 used 30%, then visit 4 used 80%) with biopsies occurring at PRE, 3h POST, and 6h POST. Visits 3 and 5 were follow-up visits to observe and re-bandage biopsy incisions.

Figure 3.1. ***Study Design***

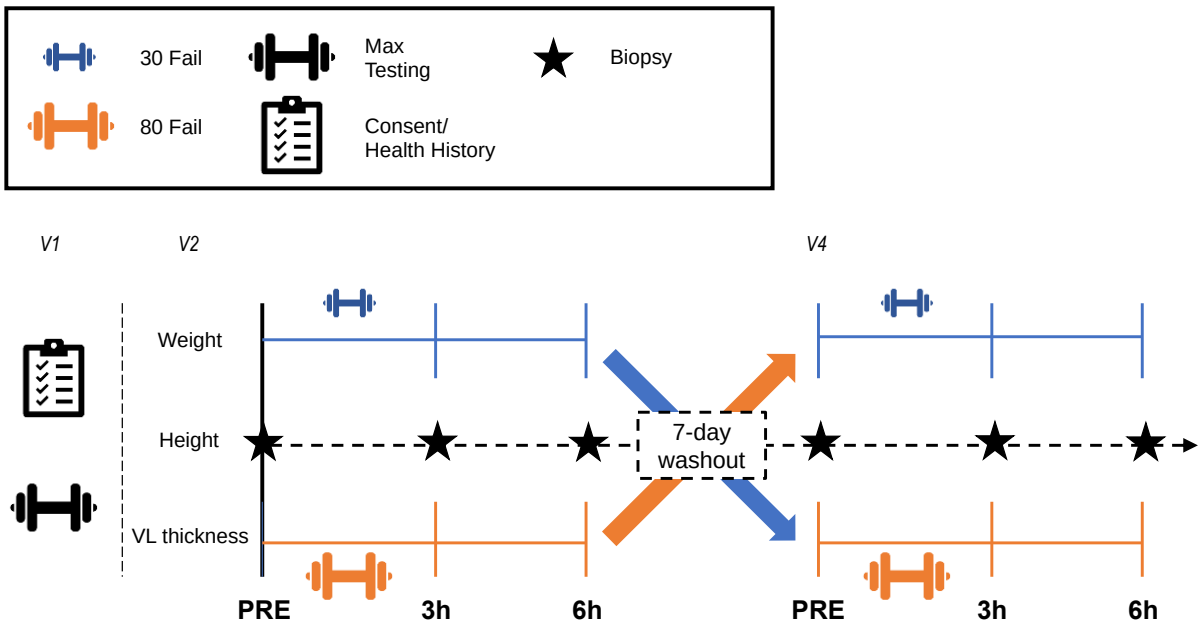

Legend: This schematic represents the timeline for participant consent, max testing, PRE-phenotype testing, experimental resistance exercise bout, cross-over washout period, and timepoints for all biopsies. Abbreviations: 30 Fail, 30% one repetition maximum to failure; 80 Fail; 80% one repetition maximum; VL, *vastus lateralis;* V1, Visit 1.

Testing Sessions

Estimated 1-RM Testing. During the initial visit, participants completed testing to determine their estimated 1-RM ([est. 1-RM]. Est. 1-RM was derived from a 3-repetition maximum test for barbell back squats (squats) and knee extensions. An est. 1-RM was used instead of a true 1-RM to reduce the risk of error/ injury and increases the accuracy of the strength measures. The estimated 1-RM was tested as follows: i) participants completed a general warm-up of 25 jumping jacks and 10 body weight squats, ii) for a specific warm-up, 50% of their most recent, self-reported squat max was performed for 10 reps, iii) subsequently, additional warm-up reps were completed at approximately 60% (8-10 reps), 70% (5-8 reps), 80% (3-5 reps), 90% (1-3 reps) and 95% (1 rep) of their self-reported 1-RM. Then, using NSCA guidelines, testing weights were selected by a Certified Strength and Conditioning Specialist (CSCS), beginning with a load that could easily be performed for 3 reps. Est. 1-RMs were assessed within six attempts, and with each successful attempt the CSCS was informed of how many more reps could be completed (reps in reserve [RIR]), with that number being added to the total reps completed (e.g., reps completed [3] + RIR [2] = 5) this number was considered an estimated rep max for the given load. The estimated rep max was then used to determine the next 3-RM attempt through the National Strength and Conditioning Association (NSCA) guidelines on rep max to 1-RM percentage conversions. This was repeated until the participant either did not complete 3 full repetitions, the parameters of the exercise were not met, or the participant declined an increase in load.

Hydration Testing. Urine specific gravity was used to assess hydration. During visits 2 and 4, participants gave a urine sample (approx. 5ml) that was assessed for urine specific gravity (USG) testing using a handheld refractometer (ATAGO; Bellevue, WA, USA). All participants had a

USG level ≤ 1.020, and this was used as a threshold of sufficient hydration to continue testing [146].

Body Composition Testing. Height and body mass were evaluated using a digital column scale (Seca 769; Hanover, MD, USA). Height was measured to the closest 0.5 cm and body mass to the closest 0.1 kg. Supine bioelectrical impedance spectroscopy was used to estimate fat-free mass and fat mass. The procedure was done according to manufacturer instructions. The technique was also explained in more depth by Esco et al. [147] and Moon et al. [148]. Briefly, after participants rested in a supine position for 5 to 10 minutes, the Imp SFB7 (ImpediMed Limited, Queensland, AU) applied electrical currents, ranging from 50-500kHz, via a tetra-polar electrode configuration. All electrodes placed on the right side of the body (2 electrodes being placed above and below the wrist, 5 cm apart, and 2 being placed above and below the anterior portion of the ankle, 5 cm apart). These signals were then calculated automatically by the device and converted to an estimate of fat-free mass and fat mass.

Vastus lateralis morphological assessment. Ultrasound was used to measure VL muscle thickness (cm) as reported in Sexton et al. [149]. Briefly, real-time B-mode ultrasonography (NextGen LOGIQe R8, GE Healthcare, Chicago, IL, USA), facilitated by a multi-frequency linear-array transducer (L4-12T, 4–12 MHz, GE Healthcare, USA), was utilized in capturing an image of VL thickness (cm^2) in the transverse plane, at approximately 50% the distance between the mid-inguinal crease and the proximal patella. Participants were instructed to lie supine, with knee and hip fully extended, for a minimum of 5 minutes before image acquisition. The image depth was adjusted until the edge of the femur was in view, which allowed for a full-thickness view of the VL. All ultrasound images were taken using a generous amount of water-soluble transmission gel. Following collection of images, freely available analysis software (ImageJ; National Institute of

Health, Bethesda, MD, USA) was used to quantify VL thickness. VL thickness was measured from the VL superficial aponeurosis to the deep aponeurosis via the straight-line function. All ultrasound images were taken and analyzed by the same investigator with a previously established test-retest reliability (ICC 0.96; SEM 0.09 cm; MD 0.24 cm)

Skeletal Muscle Biopsy and Processing. During visits 2 and 4, at PRE, 3h POST, and 6h POST skeletal muscle biopsies were collected from the vastus lateralis using a 5-gauge biopsy needle, where local anesthesia was used. Approximately 50-100 mg of tissue was collected in total with 20-40 mg being adhered to a cork block via tragacanth gum and preserved in an insulating layer of optimum cutting temperature media that was frozen in liquid nitrogen-cooled 2-methylbutane, then stored -80°C to be later used for histology. Remaining tissue was flash frozen in liquid nitrogen and stored at -80°C for later use.

Resistance Exercise Bouts to Failure

During visits 2 and 4, participants completed a resistance exercise bout (squats and knee extensions) where they were randomly assigned to either 80% and 30% of their Est. 1-RM for 4 sets to failure at visits 2 and 4 or at visits 4 and 2. Failure was determined as either: i) an inability to complete a full repetition, ii) technical errors that would compromise safety (e.g., difficulty keeping balance, failure to maintain appropriate posture, etc.), or iii) the participant spent longer than 4 seconds between repetitions. Upon arrival, participants completed a general warm-up of 25 jumping-jack and 10 body weight squats, followed by a specific warm-up of 10 repetitions at 30-50% and 5-8 reps at 75% of the experimental load assigned to them (i.e., 80% or 30% of Est. 1-RM). Stronger participants were allowed to complete an additional warm-up set using 85% of their assigned experimental load. Participants then initiated their sets to failure, and upon completion,

they were given 5 minutes of rest. Additionally, participants were given approximately 5 min of rest between squats and knee extensions. After the bout of exercise was completed, participants were instructed to return to the laboratory 3 hours and 6 hours later. Participants reporting nausea, malaise, and light-headedness were given supplemental nutrition (i.e., a granola bar [calories: 170, total fat: 8 g, carbohydrates: 20 g, protein: 4 g] and 355 ml of sports drink [calories: 80, carbohydrates: 21 g]) to reduce symptoms, and upon completion of training at visit 4, those individuals were given the exact same supplemental nutrition regardless of symptoms.

Biochemical Assays

DNA, RNA, and Protein Isolations. Skeletal muscle samples (15-20 mg) were crushed on a liquid nitrogen cooled stage, weighed to the nearest 0.0001 g (Mettler-Toledo; Columbus, OH, USA) and added to 500 μl of Trizol in 2ml polypropylene tubes. The muscle was then homogenized with tight fitting plastic pestles for approximately 30s or until the tissue was fully crushed. Samples were then placed in a -80°C freezer overnight to increase RNA yield. The following day samples were removed from -80°C freezer and allowed to thaw completely at room temperature, after which 100 μl of bromochloropropane (BCP) was added to the sample and shaken well for 15s, then incubated at room temperature for 2 minutes before being centrifuged at 12,000 g for 15 minutes. Once removed from the centrifuge, samples were kept on ice for the remainder of the procedures. Centrifugation divided the sample into three distinct phases including the top aqueous phase containing RNA, the center meniscus containing DNA, and the bottom layer containing a protein phase. Approximately 200 μl of the liquid phase was removed and placed in a new tube with 500 μl of 100% ethanol, and the RNA was subsequently purified and quantified. The remaining DNA and protein were then separated by first adding 300 μl of 100% ethanol.

Samples were then shaken for 15 seconds, incubated for 3 minutes at room temperature, and subsequently centrifuged at 5000 g for 10 minutes at room temperature. This produced a DNA pellet and a protein supernatant. The supernatant (protein-Trizol-ethanol mixture) was removed and placed in new tubes. The DNA pellet was frozen at -80°C for future purification and quantification. After moving the supernatant to new tubes, 650 µl of 100% ethanol was added to precipitate the protein. The samples were then vortexed, mixed with 100 µl of BCP, and vortexed again. Then, to facilitate phase separation, 600 µl of deionized water was added and vortexed vigorously. The samples were then centrifuged at 12,000 g for 5 minutes to collect a protein pellet from the solution. The resulting supernatant was removed and the pellet air dried at room temperature for 1-2 minutes. The protein pellet was then resuspended in 2x SDS sample loading buffer + 5M Urea (1:2 dilution of 10M Urea, 2:5 dilution of 5x SDS sample loading buffer, 1:10 deionized water, and 1:100 50x protease inhibitor) where it was allowed to dissolve at room temperature. The suspended protein was then quantified using a commercial assay (RC DC™ Protein Assay, catalog #5000122; Bio-Rad; Hercules, CA, USA).

Total Protein Quantification. To quantify total protein, the Bio-Rad RC DC™ Protein Assay was performed according to the manufacturer's instructions. A BSA protein standard was used to create a standard curve. Then 100 µl of standards and samples were added to 2.0 ml polypropylene tubes, 500 µl of RC Reagent I was added to each tube, and tubes were vortexed and incubated at room temperature for 1 min. 500 µl RC Reagent II was then added to each tube, vortexed, and centrifuged at 15,000 g for 5 minutes. The supernatant was discarded, and the tubes were inverted to drain them completely. 510 µl of Reagent A was then added, and each tube was vortexed and incubated at room temperature for 5 min. The samples were then vortexed, and 4 ml

of DC Reagent B was then added to each tube. Samples were then incubated at room temperature for 15 minutes, transferred to a microplate, and absorbances were read at 750 nm.

DNA Purification and Quantification. DNA isolated previously was further purified using a commercial kit (DNeasy Blood and Tissue Kit, catalog #69504; Qiagen; Germantown, MD, USA) according to manufacturer protocol with a minor modification to the elution step. Briefly, 180 µl of ATL buffer and 20 µl of proteinase K were added to each sample, vortexed for 20 seconds, and incubated at 56°C for 8 hours. Then 200 µl each of AL buffer and 100% ethanol were added and then vortexed. The mixture was then transferred to DNeasy Mini spin columns placed in 2 ml polypropylene flow-through tubes. The tubes were then centrifuged at 6,000 g for 1 minute and flow-through tubes were discarded and replaced. Then, 500 µl of Buffer AW1 was added, and tubes were centrifuged at 6,000 g for 1 minute. Flow-through tubes were discarded and replaced. Then, 500 µl of Buffer AW2 was added, and tubes were centrifuged at 20,000 g for 3 minutes to dry the DNeasy membrane containing DNA. Flow-through tubes were discarded and replaced with the final 1.7 ml polypropylene DNA collection tubes. Finally, 200 µl of Buffer AE was added, incubated for 5 minutes at 37°C, and centrifuged at 10,000 g for 1 minute at room temperature to elute DNA. To maximize DNA yield, solution from final DNA collection tubes were reapplied to spin columns and centrifuged at 10,000 g for 1 minute at room temperature. The eluted DNA was then assessed in duplicate for quality and quantity using an absorbance of 260/280 nm provided by a desktop spectrophotometer (NanoDrop Lite; Thermo Fisher Scientific; Waltham, MA, USA). The purified DNA was then sent to a commercial laboratory (TruDiagnostic; Lexington, KY, USA) for the methylation analysis described below.

DNA Bisulfite Conversion. Bisulfite conversion was performed using an Infinium HD Methylation Assay bisulfite conversion kit (EZ DNA Methylation Kit, Zymo Research, CA, USA).

Briefly, 50 μl suspensions (5 μl M-Dilution and 500 ng DNA diluted in distilled water) were added to a conversion plate and incubated at 37°C for 15 minutes. Then, 100 μl of prepared CT Conversion Reagent was mixed with each sample, and the conversion plate was then incubated for 12-16 hours at 50°C in the dark. After incubation, samples were further incubated at 4°C for 10 minutes. Then, 400 μl of M-Binding Buffer and samples were added to a Silicon-A Binding Plate placed on a collection plate. The plates were then centrifuged at 3000 g for 5 minutes, and the flow-through was discarded. Then, 400 μl of M-Wash Buffer was added, and the plate was centrifuged at 3,000 g for 5 minutes. Then, 200 μl M-Desulphonation Buffer was added to the plate, incubated for 15-20 minutes at room temperature, and centrifuged at 3,000 g for 5 minutes. Then, 500 μl of M-Wash Buffer was added to each well and centrifuged at 3,000 g for 5 minutes, and another 500 μl of M-Wash Buffer was added and centrifuged at 3,000 g for 10 minutes. Finally, the binding plate was placed on an elution plate and 30 μl of M-Elution Buffer was added to each well. The plate was then centrifuged at 3,000 g for 3 minutes to elute DNA from the binding plate. Bisulfite Converted DNA (BCD) was stored at -80°C until DNA methylation analysis.

DNA Methylation EPIC BeadChip array amplification. The Infinium MethylationEpic BeadChip Array was performed per the manufacturer's (Illumina) instructions. BCD (4 μl) was transferred from the BCD plate to the matching wells of a MSA4 plate, combined with 20 μl of MA1 and 4 μl of 0.1 NaOH, covered with a cap mat, and mixed by vortexing at 1600 rpm for 1 minute and pulse centrifugation at 280 g. The plate was then incubated for 10 minutes at room temperature, and the cover was removed before the plate was placed upside down. Then, 68 μl of RPM and 75 μl of MSM were added to each well and resealed with the cap mat. The plate was

again vortexed at 1,600 rpm for 1 minute and pulse centrifuged at 280 g. The MSA4 plate was incubated in an Illumina Hybridization Oven at 37°C for 24 hours.

Fragmentation, Precipitation, and Resuspension of Amplified DNA. After amplification of BCD, fragmentation began by subjecting the plate to pulse centrifugation at 280 g for 1 minute. The cap mat was removed and 50 μl of FMS was added to each well in the MSA4 plate. After replacing the cap mat, the plate was vortexed at 1,600 rpm, pulse centrifuged at 280 g for 1 minute, and incubated at 37°C for 1 hour. To precipitate DNA, 100 μl of PM1 was added to each well, the plate was resealed, vortexed at 1,600 rpm for 1 minute, and incubated at 37°C for 5 minutes. The cap mat was removed and discarded before 300 μl of 2-propanol was added to each sample well. The plate was sealed with a new cap mat, inverted 10 times to mix the solution, and incubated at 4°C for 30 minutes. The plate was then centrifuged at 3,000 g for 20 minutes at 4°C. After ensuring a blue pellet was formed and adhered to the bottom of each well, the plate was inverted to drain supernatant. The plate was then tapped while upside down to ensure all wells were drained. The plate was then dried and inverted in a tube rack for 1 hour at room temperature. While inverted, the plate was wiped dry of any residual fluid. DNA was then resuspended by first adding 46 μl of RA1 to each well of the MSA4 plate. The plate was sealed with heat seal foil and subsequently incubated in the hybridization over for 1 hour at 48°C. After, this the pellet was resuspended by vortexing the plate at 18,000 rpm and pulse centrifugation at 280 g.

BeadChip hybridization, extension, and staining. After resuspension of the precipitated, fragmented DNA, the plate was incubated at 95°C for 20 minutes to facilitate denaturing of the DNA. The plate was then left at room temperature for 30 minutes and pulse centrifuged at 280 g. Samples were then added carefully from MSA4 plate onto prepared BeadChips for hybridization. After DNA was fully dispersed, BeadChips were inserted into hybridization chambers and the

chambers were incubated in Illumina Hybridization Oven at 48°C for 16 hours. Afterwards, BeadChips were washed in 200 ml of PB1 and prepared for the staining process. The BeadChips were subjected to a single base-pair extension at precisely 44°C by placing assembled flow-through chamber assemblies into the chamber rack. The reservoir of each flow through chamber was then filled and incubated with the following steps: i) five rounds of 150 μl of RA1 with 30-second incubations, ii) 450 μl of XC1 with a 10-minute incubation, iii) 450 μl of XC1 with a 10-minute incubation, iv) 200 μl of TEM with a 15-minute incubation, v) 2 rounds of 450 μl of 95% formamide/1mM EDTA with 1-minute incubations, vi) a 5-minute incubation, vii) an adjustment of the chamber rack temperature as specified on the STM tube, and viii) two rounds of 450 μl of XC2 with an incubation of 1 minute. After the chamber rack reached the correct temperature, the process of staining BeadChips commenced. Each flow-through chamber was filled and incubated with the following steps repeated, which were repeated five times: i) 250 μl of STM with 10-minute incubations, ii) two rounds of 450 μl of XC3 with 1-minute incubations, iii) 5-minute wait period. The BeadChips were washed of staining reagents by being submerged in PB1 for 5 minutes before being submerged in XC4 for 5 minutes. The BeadChips were then dried for 50-55 min before being imaged by the Illumina iScan® System (Illumina, San Diego, CA, USA)

Muscle Histological Sectioning. Muscle samples, collected and preserved in OCT as described above, were sectioned at a thickness of 10 μm in a cooled (-20°C) cryostat (Leica Biosystems; Buffalo Grove, IL, USA) and electrostatically adhered to positively charged histology slides. The slides were then stored at -80°C until immunohistochemical staining.

Immunohistochemistry. Slides with muscle sections adhered were removed from the -80°C freezer and allowed to equilibrate and dry, while covered, at room temperature for 1.5 hours. Sections were then outlined using a hydrophobic pen to retain solutions for the following

incubation steps. First a 1x phosphate buffer solution (1x PBS) was applied for 10 minutes to rehydrate muscle sections. The 1x PBS was then removed and a 3% peroxide solution was added to the sections to incubate for 15 minutes. Subsequently, the peroxide was removed, and the slides were washed in a 1x PBS solution for 3 x 5 minutes on a rocker. 1x TrueBlack Lipofuscin Autofluorescence Quencher solution (biotium; Fremont, CA, USA) was added and incubated for 1 minute and washed in 1x PBS for 3 x 5 minutes. The sections were then blocked with a 10% normal goat serum and 5% normal horse serum for at least 1 hour, then washed in 1x PBS for 5 minutes. Once blocked, the primary antibody was applied (1:20 Mandra, 1:20 of BA_D5, 9:20 and 9:20 5% normal horse serum, all diluted in 1x PBS; all antibodies from Developmental Studies Hybridoma Bank; Iowa City, IA, USA) and incubated overnight. After primary antibody incubation, slides were washed four times in 1x PBS for 5 minutes. A secondary antibody was applied (1:100 goat, anti-mouse IgG1 594, 1:100 goat, anti-mouse IgG2B 488, diluted with 1x PBS) and incubated for 1 hour. The slides were then washed 4 x 5 minutes in 1x PBS. A DAPI fluorescent dye (1:10,000 DAPI, diluted in deionized water) was then applied for 15 minutes and washed 2 x 3 minutes. A 1:1 PBS-glycerol solution was then applied around the sections as a cover slip adherent, and coverslips were applied thereafter. Following mounting, digital images were immediately captured with a fluorescent microscope (Nikon Instruments, Melville, NY, USA) using a 10x objective. Standardized measurements of type I and type II fCSAs, as well as myonuclei number were performed using open-sourced software (MyoVision 2.0) [150, 151]. A pixel conversion ratio value of 0.964 μm/pixel was used to account for the size and bit-depth of images, and a detection range of detection from 500 to 12,000 μm^2 was used to ensure artifact was removed (e.g., large fibers which may have not been in transverse orientation, or structures between dystrophin stains which were likely small vessels). Test-retest reliability for mean fCSA

was previously determined in our laboratory comparing two separate images from the same sample using 26 muscle samples resulting in an ICC, SEM and MD of 0.91, 459 μm^2, and 1,271 μm^2, respectively.

Nuclear isolations. Nuclear extractions from frozen muscle tissue were performed using a commercial kit (Nuclear Extraction Kit, catalog# ab113474; Abcam; Waltham, MA, USA). Briefly, skeletal muscle samples (15-20 mg) were crushed on a liquid nitrogen cooled stage and added to 1x Pre-Extraction Buffer containing DTT solution (10x pre-extraction diluted 1:10 with distilled water, DTT diluted 1:1000). The tissue was then homogenized, incubated on ice for 15 minutes, and centrifuged for 10 minutes at 12,000 rpm at 4°C. The supernatant was then removed and 1x Pre-Extraction Buffer containing DTT solution and Protease Inhibitor Cocktail (10x pre-extraction diluted 1:10 with distilled water, DTT and PIC diluted 1:1000) was added and incubated for 15 minutes with a 5-second vortex every 3 minutes. The suspension was centrifuged for 10 minutes at 14,000 rpm at 4°C. The supernatant was transferred to a new tube and the concentration was measured with a bicinchoninic acid (BCA) assay.

BCA assay. Nuclear proteins were batch processed for protein concentrations using a BCA kit (Thermo Fisher Scientific; Waltham, MA, USA). Isolated Nuclear protein were quantified in duplicates, and samples (20 µl of 3x diluted sample + 200 µl of Reagent A + B) were subjected to a microplate assay protocol. The average coefficient of variation for nuclear extract protein concentration was 5.88%.

DNMT activity assay. DNMT activity was performed on nuclear extracts using a commercial assay (Colorimetric DNMT Activity Quantification Kit, catalog# ab113467; Abcam). Briefly, nuclear extracts, without the inhibitor, and Adomet Working buffer were added to a strip-well microplate then tightly covered with an adhesive film and incubated at 37°C for 90 minutes.

The reaction solution was then removed, and each well was washed with 1x Wash Buffer 3 times. Diluted Capture Antibody was added to each well and covered with aluminum for incubation at room temperature for 60 minutes. The Diluted Capture Antibody was then removed, and each well was washed 3 times with 1x Wash Buffer. Diluted Detection Antibody was added to each well and the plate was covered with aluminum foil and incubated at room temperature for 30 minutes. The Diluted Detection Antibody was removed, and each well was washed 4 times with 1x Wash Buffer. Diluted Enhancer Solution was then added to each well and the plate was covered with aluminum foil and incubated at room temperature for 30 minutes. The Diluted Enhancer Buffer was removed and washed 5 times with 1x Wash Buffer. Finally, Developer Solution was added to each well and incubated at room temperature, in a dark container, for 10 minutes. Stop Solution was then added to each well, and absorbance was immediately read at 450 nm and 655 nm using a plate reader (Synergy H1; Biotek; Winooski, VT, USA). Activity was expressed as absorbance units per microgram nuclear protein. The average coefficient of variation for absorbance values was 4.23%.

TET activity assay. TET activity was performed on nuclear extracts using a commercial assay (TET Hydroxylase Activity Quantification Kit, catalog# ab156913; Abcam). Briefly, Binding Solution was added to each well and 0.5x TET Substrate were added to each blank and sample wells in a strip-well plate. The solution was covered and incubated at 37°C for 90 minutes. The binding solution was removed, and each well was washed 3 times with 1x Wash buffer. Then Final TET Assay Buffer, without the inhibitor, were added to sample wells. The wells were tightly covered with Parafilm M and incubated at 37°C for 90 minutes. The reaction solution was removed from each well and washed three times with 1x Wash Buffer. Then, Diluted Capture Antibody was added to each well and covered with aluminum foil for incubation at room temperature for 60 minutes. The Diluted Capture Antibody was removed, and each well was washed 3 times with 1x

Wash Buffer. Dilution Detection Antibody was then added to each well, covered with aluminum foil, and incubated at room temperature for 30 minutes. The Diluted Detection Antibody was removed, and each well was washed 4 times with 1x Wash Buffer. Diluted Enhancer Solution was then added to each well and plates were covered with aluminum foil and incubated for 30 minutes at room temperature. The Diluted Enhancer Solution was then removed, and each well was washed 5 times with 1x Wash Buffer. Finally, Fluorescence Development Solution was added to each well and incubated at room temperature for 2-4 minutes. The plate was read at 530ex/590em nm for fluorescence, and activity was expressed as fluorescence units per microgram nuclear protein. The average coefficient of variation for fluorescence values was 7.67%.

Western Blotting. After a BCA assay was performed to determine the concentration of protein in nuclear lysates, the samples were combined with DiH20 and 4x Laemmli buffer achieve a protein concentration of 1 μg/ μl. Following this, 15 μl of each sample was loaded onto a commercially available pre-casted gradient (4-15%) SDS-polyacrylamide gel (Bio-Rad Laboratories, Hercules, CA, USA) which were submerged in a 1x SDS-PAGE running buffer (Ameresco, Framingham, MA, USA). The loaded gel then underwent electrophoresis at 180V for 50 min and was transferred onto a polyvinylidene difluoride membrane (PVDF) at 200 mA for 2h. The membrane was then washed in ponceau stain for 10 minutes, rinsed with DiH2O and imaged to confirm consistent protein loading in each lane. The membrane was then blocked for 1h with 5% nonfat milk powder in Tris-buffered saline containing 0.1% Tween-20 (TBST; Ameresco, Framingham, MA, USA) and subsequently washed with TBST for 3 rounds of 5 min. Then, membranes were incubated overnight at 4°C with 15ml of either a rabbit TET1 (TET1, 1:1000; catalog# ab191698;Abcam, Cambridge, UK), rabbit TET2 (TET2, 1:1000; catalog# 45010S; Cell Signaling Technology, Danvers, MA, USA), or rabbit TET3 (TET3, 1:1000; catalog# 85016S;

Cell Signaling Technology, Danvers, MA, USA) antibodies in TBST with 5% bovine serum albumin (BSA). After primary anti-body incubation, membranes were washed with TBST for 3 rounds of 5 minutes and incubated for 1h, at room temperature, with 15ml of a horseradish-peroxidase (HRP)-linked anti-rabbit IgG (1:2000; catalog #: 7074S; Cell Signaling Technologies, Danvers, MA, USA) secondary antibody in TBST with 5% BSA. Then prior to imaging the membranes were washed in TBST for 3 rounds of 5 min. The membranes were developed by adding 1-2 ml of an enhanced chemiluminescent reagent (Luminata Forte HRP substrate; EMD Millipore, Billerica, MA, USA) to each membrane. Band density was captured using a gel documentation system that includes the associated software (ChemiDoc; Bio-RAD Laboratories, Hercules, CA, USA). Due to non-specific binding with the TET1 antibody, and lack of quantifiable bands with TET2 and TET3, no further analysis of membrane band density was performed.

Statistical Analyses

Statistical analysis was performed in SPSS v26.0 (IBM Corp, Armonk, NY, USA) and Partek Genomic Suite V.7 (Partek Inc., MO, USA. Prior to analyses, Shapiro-Wilks tests of normality were performed on all dependent variables outside of DNA methylation and mRNA expression values. Two-way ANOVAs were used to assess main effects and potential interactions of condition (30 Fail vs 80 Fail) x time (PRE, 3h POST, and 6h POST) for non-methylation data (e.g., changes in VL thickness values, training volume, etc.). For any main effect that violated the assumption of sphericity, a Greenhouse-Geiser correction was applied.

DNA Methylation Analysis. Following quantification of DNA MethylationEPIC BeadChip array, the Partek Genomic Suite V.7 (Partek Inc., MO, USA) was used to process the MethylationEpic _v-1-0_B4 manifest file as described by Maasar et al. 2021 [152]. Briefly, an

average detection p-value was assessed for all samples to ensure values below 0.01 [153], and any probes outside of this range were removed from analysis. Raw signals for the methylated and unmethylated probes were assessed for the difference between average median methylated and average median unmethylated probes were measured to ensure the recommended difference of 0.5 or less [153]. After the data was imported to Partek Genomics Suit, single nucleotide polymorphisms (SNPs) associated probes and cross-reactive probes, identified in validation studies [154], were removed from analysis. Functional normalization using a noob background correction was performed for background normalization [155]. Then, principal component analyses (PCA), density plots, and box and whisker plots were used for quality control (i.e., no samples exceeded 2.2 standard deviations or presented abnormal distributions). Following normalization and quality control analysis, differentially methylated position analysis was performed. β-values were converted into M-values to represent a more valid distribution of data for analysis of differential methylation [156]. Because both treatments were completed by each participant, paired Samples t-tests were used to assess 30 Fail versus 80 Fail at PRE, 3h POST, and 6h POST, and significant DMPs at PRE were removed as confounding DMPs. An ANOVA was also used to determine the main effects for condition (30 Fail and 80 Fail over time) and for time (PRE vs 3h POST, PRE vs 6h POST, and 3h POST vs 6h POST). Differentially methylated CpG positions (DMPs) were subjected to a significance value of $p < 0.01$. Additionally, an analysis to quantify differentially methylated regions (DMRs) that contained at least 2 DMPs within a short genomic region/ locus was performed using the Bioconductor package DMRcate (DOI: 10.18129/B9.bioc.DMRcate).

Transcriptome Analysis. Following the quantification of gene expression with the Clariom-S microarray, raw .CEL files were uploaded into the Transcriptome Analysis Console v4.0.2

(TAC) (Thermo Fisher Scientific). The *H. sapiens* genome was used to generate the reference annotations. Two-way repeated measure (2x2) ANOVAs, with the eBayes correction factor applied, were performed for interactions between bouts from PRE to 3h POST and PRE to 6h POST, for each gene. For this statistical analysis, gene expression was considered significant if a Δfold-change of ±1.5 was exceeded, if the p-value for interaction was less than 0.01, and if the expression at PRE was not significantly different between conditions (p-value less than 0.05). From this analysis, a list of significant genes was generated for use in pathway analysis. Additionally, pairwise comparisons were conducted within each bout for significant time effects. A gene target was considered significant if gene expression exceeded a ±1.5-fold-change from PRE and the p-value for time was less than 0.01. These gene lists were subjected to gene pathway enrichment analysis using the publicly available gene ontology PANTHER17.0 pathway analysis [157, 158].

Chapter IV

Genome-wide DNA Methylation and Transcriptome-wide Responses to a Bout of Higher- Versus Lower-load Resistance Training in Previously Trained Men

Casey L. Sexton[1], Joshua S. Godwin[1], Mason C. McIntosh[1], Bradley A. Ruple[1], Shelby C. Osburn[1], Nicholas J. Kontos[1], Blake R. Hollingsworth[1], Philip J. Agostinelli[1], Andreas N. Kavazis[1], Tim N. Ziegenfuss[2], Hector L. Lopez[2], Ryan Smith[3], Kaelin C. Young[1,4], Varun B. Dwaraka[3], Andrew D. Fruge[5], C. Brooks Mobley[1], Adam P. Sharples[6,*], Michael D. Roberts[1,7,*]

Affiliations: [1]School of Kinesiology, Auburn University, Auburn, AL, USA; [2]The Center for Applied Health Sciences, Canfield, OH, USA; [3]TruDiagnostic, Lexington, KY, USA; [4]Pacific Northwest University of Health Sciences, Yakima, WA, USA; [5]College of Nursing, Auburn University, Auburn, AL, USA; [6]Institute for Physical Performance, Norwegian School of Sport Sciences, Oslo, Norway; [7]Edward Via College of Osteopathic Medicine, Auburn, AL, USA

[*]Address co-correspondence to:
Adam P. Sharples, PhD
Professor, Department of Physical Performance
Norwegian School of Sport Sciences
E-mail: a.p.sharples@googlemail.com

Michael D. Roberts, PhD
Associate Professor, School of Kinesiology
Director, Molecular and Applied Sciences Laboratory
Auburn University
E-mail: mdr0024@auburn.edu

ABSTRACT

We sought to determine how genome-wide DNA methylation and transcriptome responses in skeletal muscle differed between one bout of lower-load versus higher-load resistance exercise. Previously trained college-aged males (n=11, age: 23±4 years old, percent body fat: 11.4 ± 6.4%, training experience: 4 ± 3 years, squat strength relative to body weight: 1.7 ± 0.3) performed two bouts of resistance exercise separated by one week. The higher-load bout consisted of 4 sets of back squats and 4 sets of leg extensions to failure using 80% of their estimated one-repetition maximum (Est. 1-RM) (80 Fail), whereas the lower-load bout consisted of this same paradigm using 30% of their Est. 1-RM (30 Fail). Vastus lateralis muscle biopsies were collected before (PRE), 3 hours (3hPOST), and 6 hours (6hrPOST) after each exercise bout. DNA and RNA were batch-isolated from muscle tissue and analyzed for genome-wide DNA methylation and mRNA expression, respectively, using the 850k Illumina MethylationEPIC array and Clariom S mRNA array. The total number of repetitions performed were significantly greater during the 30 Fail versus 80 Fail bout ($p<0.001$); however, total training volume (sets x reps x load) was not significantly different between conditions ($p=0.571$). While 30 Fail training generally led to greater hypomethylation across various promoter regions, the transcriptome-wide responses between bouts were largely similar. Both bouts altered mRNAs involved in inflammatory signaling (e.g., Toll receptor signaling, CCKR signaling, chemokine and cytokine signaling), apoptosis signaling, gonadotropin-releasing hormone signaling, and integrin signaling. Although several studies have examined the muscle-molecular responses to higher- versus lower-load resistance training, this is the first multi-omics comparison of these paradigms. Our transcriptomic data suggest that the molecular signaling events during the early post-exercise period are largely

similar, and this may explain why similar longer-term phenotypes (e.g., myofiber hypertrophy) result from these two resistance training-to-failure modalities.

Keywords: resistance exercise, training volume, DNA methylation, transcriptomics

INTRODUCTION

Adaptations within skeletal muscle cells, also called myofibers, are a result of overcoming environmental stimuli (i.e., mechanical tension, producing ATP to meet increased energy demands, repairing damage, etc.). Resistance training (RT) increases myofiber hypertrophy, whole-tissue hypertrophy, and strength [1]. It has been recognized that RT produces specific molecular signaling based on training intensity (i.e., 0-100% one-repetition maximum (1RM)) and volume (i.e., sets x repetitions x load) [4]. Further, RT using high loads (≥65% 1RM) at moderate to low volumes (i.e., 1-5 sets of 1-8 repetitions) generally results in increased force production capabilities of skeletal muscles, while lower-load training (i.e., <65% 1RM) with high volume (i.e., >3 sets of >10 repetitions) tends to favor glycolytic and mitochondrial adaptations over strength adaptations [5-9]. These diverging phenotypes are facilitated through a milieu of molecular changes that alter gene expression and increase protein synthesis depending on myofiber needs [2, 3]. Interestingly, despite the specific adaptation seen with higher- load and higher-volume RT, several studies to date have observed that a wide range of loads (i.e., high-loads ≥65-80% 1RM) and low loads (20-<65 1-RM) can achieve a similar magnitude of skeletal muscle hypertrophy through training to failure [5, 10-14].

While the use of RT at higher- and lower- loads to failure generates similar magnitudes of muscle growth, divergent molecular adaptations may occur between these two modes of resistance training. For example, in a 2019 study from Lim and colleagues, several aspects of muscle phenotype were examined after 10 weeks of RT at either 80% or 30% 1RM to failure or at 30% 1-RM, volume equated to the 80% 1RM to failure group. The authors determined there were similar amounts of hypertrophy, strength increases, and satellite cell number increases across both groups, but select mitochondrial adaptations more evident in the 30% 1-RM to failure group [5].

Additionally, Haun and colleagues reported that a six-week, lower-load (i.e.,65% 1-RM) extremely high-volume (i.e., week 6 volume: 32 sets of 10 reps, per exercise), full body training program in trained college aged males produced muscle hypertrophy with a disproportionate expansion of the non-myofibrillar protein pool [8]. The authors also reported significant upregulation in proteins involved with glycolysis as measured through proteomics. Vann and colleagues subsequently examined the effects of a 10-week, higher-load (i.e., >85% 1-RM) moderate- to low-volume, whole body training program in trained college-aged males and reported that myofibril protein accretion scaled with increases in mean fiber cross-sectional area [15]. Moreover, the sarcoplasmic protein adaptations observed by Haun and colleagues were not observed by Vann et al. This collective evidence has led our laboratory to hypothesize that, during higher-volume RT conditions, myofiber hypertrophy occurs due to a disproportionate increase in sarcoplasmic volume [16]. Moreover, we have hypothesized that higher-volume RT leads to a more robust metabolic adaptation phenotype. In 2022, Vann and colleagues tested these hypotheses by using a within-subject six-week unilateral leg RT design that compared higher-load (HL; 82.5% to 95% 1-RM, 9 sets of 5 reps each wk) to a lower-load/higher-volume condition (HV; 60% 1-RM, 5 sets of 10 reps at week 1 to 10 sets of 10 reps at week 6) [17]. Compared to the HL-trained leg, there was a significant increase in vastus lateralis muscle cross-sectional area (measured by magnetic resonance imaging) for the HV-trained leg, and six-week integrated sarcoplasmic protein synthesis rates were significantly higher in the HV-trained leg. These differing responses necessitate more research into the molecular signaling responses to higher-load and lower-load resistance training.

Ultimately, the unique molecular signaling events observed during different training paradigms produce differentially expressed genes (DEGs) that are a specific response to the

imposed demands of RT [159]. This observed DEG response may be a result of multiple epigenetic mechanisms that physically alter the accessibility of DNA, which produces phenotypic variation outside of what can be explained by the sequence of DNA alone [25, 117, 133]. DNA methylation is one of the most studied epigenetic mechanisms in humans, and recent research has shown a variety of exercise modes, including RT, can alter the methylation status of DNA [18, 22]. In mammalian species, DNA methylation primarily occurs at cytosine and guanine dinucleotide-rich sites (CpGs). Methylation events are facilitated through the activity of DNA methyltransferase (DNMT) 3a/3b, which methylate DNA, and ten-eleven translocation methylcytosine dioxygenases (TETs) which de-methylate DNA [21, 117]. Several metabolic events that occur during RT (i.e., glycolysis, the citric acid cycle, etc.) are thought to alter TET activity [27], as well as affect the pool of methyl groups available for donation during the methylation process [21]. Alterations in the methylation status of these positions have been inversely associated with DEGs, where hypomethylation leads to increased gene expression and hypermethylation causes gene silencing [25, 133]. Given that alterations in DNA methylation have been shown to precede changes in gene expression, differential methylation is often thought of as one of the first molecular events that either initiates or blocks the cascade of DNA transcription and mRNA translation. However, it currently is not known whether differential genome-wide and gene-specific methylation responses to higher- and lower-load RT exists. Therefore, the purpose of this study was to examine how an acute bout of higher- versus lower-load RT to failure affected genome-wide DNA methylation and mRNA transcription in skeletal muscle. Moreover, we sought to compare these -omics data to determine whether DNA methylation events after each RT paradigm were associated with mRNA responses. Herein, lower-load and higher-load failure training is defined as 30% 1-RM (30 Fail) and 80% 1-RM (80 Fail), respectively. Given previous findings, we hypothesized that 30 Fail

training would elicit greater DNA hypomethylation relative to 80 Fail training, and this would correspond to an increased expression of genes associated with energy metabolism.

RESULTS

Participant characteristics

Male participants enrolled in the study (n =11) were 23 ± 4 years old with a body mass of 86 ± 12 kg and a height of 180 ± 7 cm, resulting in a BMI of 27 ± 3 kg/m^2. Resistance training experience (i.e., training age) was 4 ± 3 years and the estimated 1RM for the barbell back squat was 143 ± 33 kg (relative to body weight: 1.7 ± 0.3 kg 1RM/ kg body mass). Average vastus lateralis in all participants was 2.99 ± 0.36 cm, and mean fCSA values from biopsied VL tissue averaged 4259 ± 882 μm^2 (type I fiber percent: 34.6 ± 16.6, type II fiber percent: 65.4 ± 16.6; Table 1).

Table 4.1. ***Participant Characteristics***

Variables	Mean ± SD
Age (years)	23 ± 4
Training Age (years)	4 ± 3
Body Mass (kg)	86 ± 12
Height (cm)	180 ± 7
BMI (kg/m^2)	27 ± 3
Squat 1-RM (kg)	143 ± 33
Squat (kg)/ Body Mass (kg)	1.65 ± 0.28
VL thickness (cm)	2.99 ± 0.36
Average fCSA (μm^2)	4259.35 ± 882
Type I Fiber Percent	34.6 ± 16.6
Type II Fiber Percent	65.4 ± 16.6

Legend: data are for the 11 participants and presented as mean ± standard deviation (SD) values. Abbreviations: BMI, body mass index; 1-RM, one repetition maximum; VL, *vastus lateralis*;

fCSA, fiber cross-sectional area. All data were collected prior to first experimental resistance training bout

Training Volume Differences Between the 30 Fail and 80 Fail Bouts

All participants engaged in the 30 Fail and 80 Fail bouts, which were separated by one week, and this is described in greater detail in the methods section. Total lower body training volume was not significantly different between 30 Fail and 80 Fail bouts (p = 0.57, Fig. 1C). However, training volume for the barbell back squat showed a condition by set interaction ($F_{3,30}$ = 11.53, p <0.001, η_p^2 = 0.535; Fig. 1A), a main effect of condition ($F_{1,10}$ = 67.380, p <0.001, η_p^2 = 0.871) where more volume was performed in the 30 Fail condition than the 80 Fail condition (30 Fail:1809 ± 202 kg, 80 Fail: 973 ± 134 kg), and a main effect of set was also evident ($F_{1.40,13.99}$ = 39.46, p <0.001, η_p^2 = 0.798) where average volume decreased across all sets for both conditions (set 1: 2066 ± 224 kg, set 2: 1402 ± 183 kg, set 3: 1150 ± 155 kg, set 4: 947 ± 131 kg). Dependent samples t-tests indicated there was significantly more volume performed on the squat in the 30 Fail condition versus the 80 Fail condition during each set (set 1: p < 0.01, set 2: p =0.002, set 3: p = 0.001, set 4: p = 0.005) and for total squat volume (p < 0.001). Leg extension training volume showed a main effect of condition ($F_{1,10}$ = 6.406, p <0.05, η_p^2 = 0.390; Fig. 1B) where 80 Fail completed more volume on average than the 30 Fail condition (80 Fail: 2200 ± 389, 30 Fail: 1634 ± 254). A dependent samples t-test showed there was significantly more total leg extension volume completed in the 80 Fail condition compared to the 30 Fail condition (p = 0.030).

Total repetitions completed was significantly different between 30 Fail and 80 Fail bouts (p < 0.001, Fig. 1F). The number of repetitions performed for the squat showed a condition by set interaction ($F_{1.38,13.58}$ = 25.229, p <0.001, η_p^2 = 0.716; Fig. 1D), a main effect of condition ($F_{1,10}$ =

172.992, $p < 0.001$, $\eta_p^2 = 0.945$) where on average more repetitions were performed during the 30 Fail condition than the 80 Fail condition (30 Fail: 42 ± 3, 80 Fail: 8 ± 1), and a main effect of set ($F_{1.31,13.1} = 44.925$, $p < 0.001$, $\eta_p^2 = 0.818$) where average reps decreased across all sets for both conditions (set 1: 38 ± 2, set 2: 25 ± 2, set 3: 21 ± 2, set 4: 17 ± 2). Dependent samples t-tests indicated there were significantly more repetitions completed in the 30 Fail condition than the 80 Fail condition during each squat set ($p < 0.001$) and for total squat repetitions ($p < 0.001$). The repetitions performed across sets during leg extensions showed a main effect of condition ($F_{1,10} = 33.058$, $p <0.001$, $\eta_p^2 = 0.768$; Fig. 1E) where there were significantly more repetitions completed per set on average with the 30 Fail condition compared to the 80 Fail condition (30 Fail: 24 ± 3, 80 Fail: 13 ± 2). Dependent samples t-test showed there were significantly more repetitions performed for the leg extension in the 30 Fail condition compared to the 80 Fail condition ($p <0.001$).

Figure 4.1. ***Resistance Exercise Volume and Repetitions***

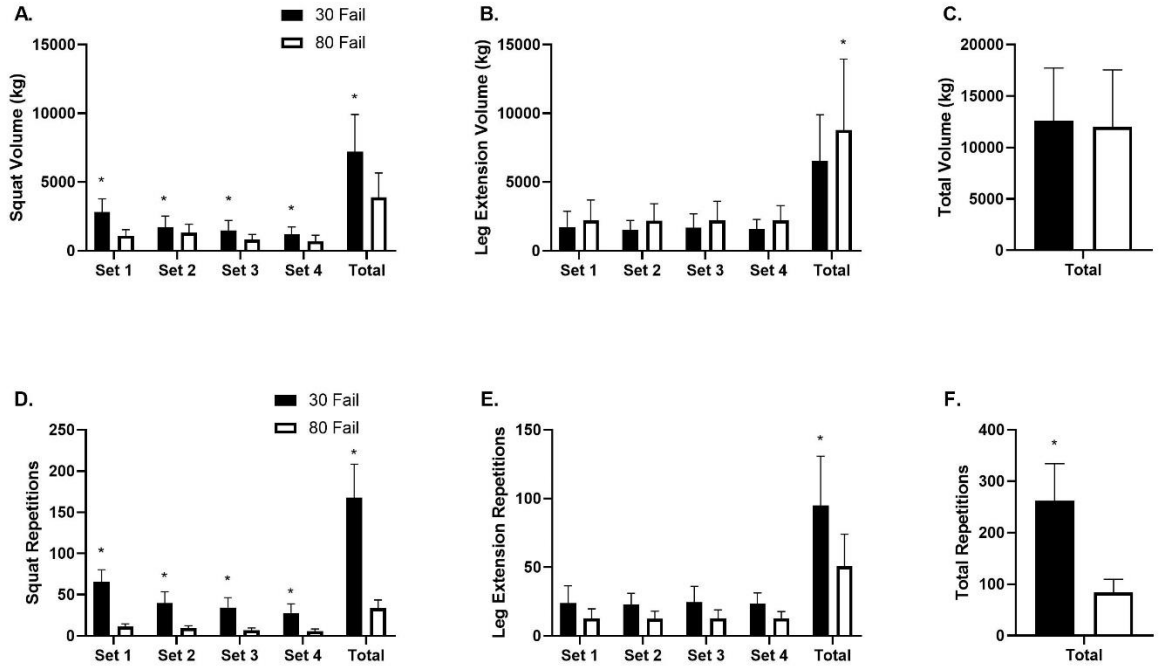

Legend: Data are presented as mean±SD for: **panel A)** squat volume across sets and total squat volume (*n* = 11), **panel B)** leg extension volume across sets and total leg extension volume (*n* = 11), **panel C)** total volume for both exercises (*n* = 11), **panel D)** squat repetitions across sets and total squat repetitions (*n* = 11), **panel E)** Leg extension repetitions across sets and total leg extension repetitions (*n* = 11), **panel F)** total repetitions performed for both exercises (*n* = 11); *, indicates significant difference between conditions per set and in totality (*p < 0.05)*. Abbreviations: 30 Fail, 30% one repetition maximum to failure; 80 Fail; 80% one repetition maximum.

DNA Methylation Changes following 30 Fail and 80 Fail Bouts

There were over 849,690 probed CpG sites to identify significant differentially methylated positions (DMPs) and differentially methylated regions (DMRs) (±1.5-fold, p<0.01). There were 3958 significantly DMPs at baseline ($p < 0.01$). Of these 3958 DMPs, only 156 possessed a

differentially methylated status at 3h and/or 6h after resistance exercise. Therefore, these 156 DMPs were removed from analyses to ensure that changes in each condition were due to the exercise stimuli and not due to altered variation at baseline. There were 4186 DMPs at 3h, with 2535 DMPs (60.6%) being hypermethylated and 1651 CpGs (39.4%) being hypomethylated. Of these 4186 DMPs, 793 DMPs (18.9%) were in a CpG island within a promoter region, and of these 793 DMPs, 21 CpGs (2.6%) were hypermethylated and 772 CpGs (97.4%) were hypomethylated. At 6h post-exercise there were 3488 DMPs, with 1608 DMPs (46.1%) being hypermethylated and 1880 DMPs (53.9%) being hypomethylated. Of these 3488 DMPs, 858 DMPs (24.6%) resided in CpG islands within a promoter region, and of these, 189 were hypermethylated (22%) and 669 were hypomethylated (88%). A summary of these data can be found in Figure 2 below.

Figure 4.2. ***Global and Island/Promoter Methylation Differences Between Bouts***

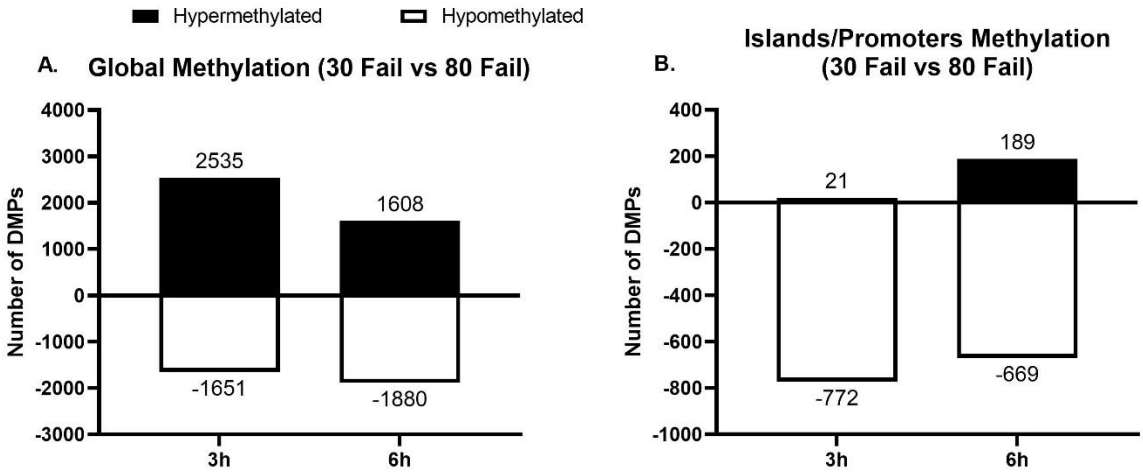

Legend: Data are presented as total number of significant DMPs in 30 Fail compared to 80 Fail for: **panel A)** Global DMPs described as hypomethylated or hypermethylated, **panel B)** Islands/Promoters DMPs described as hypomethylated or hypermethylated. All DMPs are significant to $p < 0.01$. Abbreviations: 30 Fail, 30% one repetition maximum to failure; 80 Fail;

80% one repetition maximum; DMPs, differentially methylated CpG position; Islands/Promoters, CpG islands within promoter regions.

Regarding DMRs between the 30 Fail and 80 Fail bouts, there were 155 DMRs with at least 2 significant DMPs 3h post-exercise ($p < 0.01$), 9 of these DMRs contained 3 DMPs (associated genes: DIP2B, AHCYL, TMEM134, FAM216A, SLC8B1, SERF2, TOM1L2, TEX14, and TXN2), and only 1 DMR contained 4 DMPs (associated gene: EIF4B). Further, only 49 of these 155 DMRs were in CpG islands within promoter regions, with 2 genes containing 3 DMPs (associated genes: FAM216 and TOM1L2) and only 1 gene containing 4 DMPs (associated gene: EIF4B).

At 6h post-exercise there were 67 DMRs with at least 2 significant DMPs between the 30 Fail and 80 Fail bouts. Three DMRs contained 3 DMPs (associated genes: SIN3A, RBM39, and PEG10), and only 1 DMR contained 4 DMPs (associated gene: MAP3K3). Of these 67 DMRs, 65 DMRs were in CpG islands within promoter regions, with these DMRs containing 3 or more DMPs.

TET and DNMT Activity

Given the robust alteration in DNA methylation with both training bouts, we opted to interrogate global TET and DMNT activities from nuclear lysates. There was a significant main effect of time for TET activity ($F_{1.163,10.467} = 6.638$, $p = 0.007$ $\eta_p^2 = 0.424$; Fig. 3A) where average TET activity increased following exercise (Pre: 275.42 ± 31.34, 3h: 520.35 ± 69.45, 6h: 569.10 ± 71.01), but there was no significant main effect of condition ($p = 0.163$) or condition by time

interaction (p = 0.190). For DNMT activity there were no significant main effects of time (p = 0.271) or condition (p = 0.096; Fig. 3B), or condition by time interaction (p = 0.174).

Figure 4.3. ***Nuclear TET and DNMT Activities***

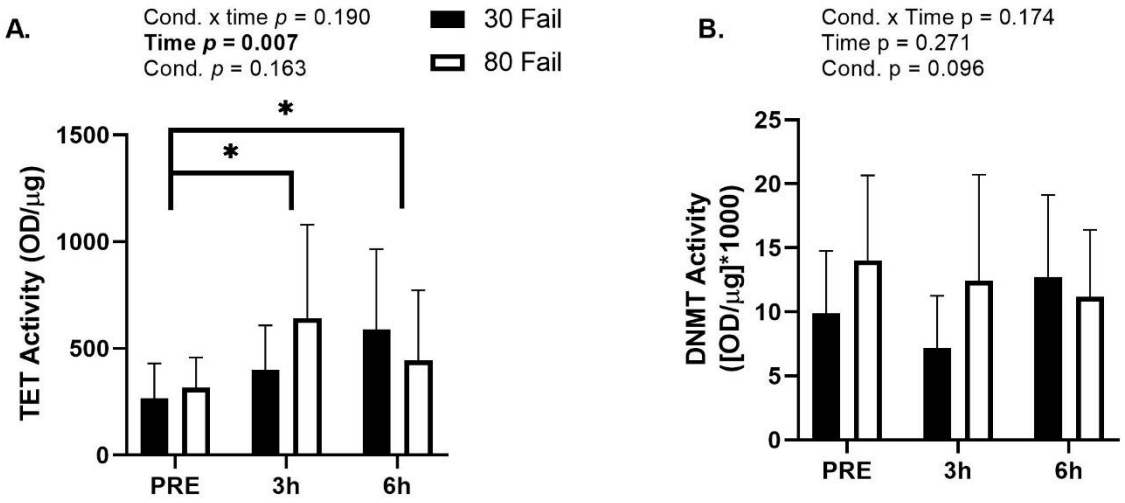

Legend: All data are presented as mean±SD for: **panel A)** Global TET activity from PRE to 3h POST and 6h POST resistance exercise and **panel B)** DNMT activity from PRE to 3h POST and 6h POST resistance exercise; *, indicates a significant change from PRE. Abbreviations: 30 Fail, 30% one repetition maximum to failure; 80 Fail; 80% one repetition maximum; TET, Ten-Eleven Translocase; DNMT, DNA Methyltransferase.

mRNA expression data

There were 21,488 genes probed to identify significant differentially expressed genes (±1.5-fold, p<0.01; termed 'DEGs'). There were 889 significantly DEGs at baseline between conditions (p < 0.05); thus, these DEGs were removed from analyses to ensure that changes in each condition were due to the exercise stimuli and not due to altered variation at baseline.

From Pre to 3h post-exercise with 30 Fail training 1428 mRNAs were upregulated and 1201 mRNAs were downregulated (Fig. 4A). Bioinformatics indicated that mRNAs in the following pathways were significantly enriched ($p<0.001$, FDR < 0.05): i) Toll receptor signaling (fold-enrichment = 2.78), ii) CCKR signaling (fold-enrichment 2.35), iii) apoptosis signaling (fold-enrichment = 2.31), iv) interleukin signaling (fold-enrichment = 2.19), v) gonadotropin-releasing hormone receptor signaling (fold-enrichment = 1.86), vi) integrin signaling (fold-enrichment = 1.82), vii) inflammation mediated by chemokine and cytokine signaling (fold-enrichment = 1.79). From Pre to 6h post-exercise with 30 Fail training 932 mRNAs were upregulated and 924 mRNAs were downregulated (Fig. 4B). Bioinformatics indicated that mRNAs in the following pathways were significantly enriched: i) CCKR signaling (fold-enrichment 2.44), ii) gonadotropin-releasing hormone receptor signaling (fold-enrichment = 2.13).

From Pre to 3h post-exercise with 80 Fail training 1492 mRNAs were upregulated and 1353 mRNAs were downregulated (Fig. 4C). Bioinformatics indicated that mRNAs in the following pathways were significantly enriched: i) Toll receptor signaling (fold-enrichment = 2.78), ii) VEGF signaling (fold-enrichment = 2.30), iii) apoptosis signaling (fold-enrichment = 2.00), iv) CCKR signaling (fold-enrichment = 2.35), v) angiogenesis (fold-enrichment = 1.77), vi) integrin signaling (fold-enrichment = 1.76), vi) gonadotropin-releasing hormone receptor signaling (fold-enrichment = 1.75), vii) Inflammation mediated by chemokine and cytokine signaling (fold-enrichment = 1.68). From Pre to 6h post-exercise with 80 Fail training 974 mRNAs were upregulated and 577 mRNAs were downregulated (Fig. 4D). Bioinformatics indicated that mRNAs in the following pathways were significantly enriched: i) p38 MAPK signaling (fold-enrichment 2.44), ii) CCKR signaling (fold-enrichment = 2.57), iii) TGF-beta signaling (fold-

enrichment = 2.53), iv) gonadotropin-releasing hormone receptor signaling (fold-enrichment = 2.30).

Figure 4.4. ***Time Effect mRNAs Between Bouts with Pathway Enrichment***

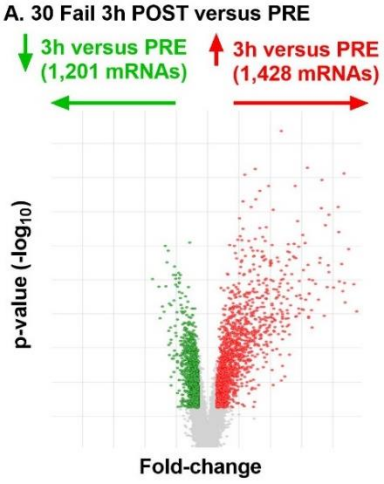

Pathway Analysis: 30 Fail Main Time Effect PRE – 3h

PANTHER Pathways	REFLIST (20589)	Gene List (2427)	(expected)	fold Enrichment	raw P-value	(FDR)
Toll receptor signaling pathway (P00054)	61	20	7.19	2.78	3.39E-04	9.03E-03
CCKR signaling map (P06959)	173	48	20.39	2.35	1.28E-06	1.03E-04
Apoptosis signaling pathway (P00006)	125	34	14.73	2.31	7.02E-05	3.74E-03
Interleukin signaling pathway (P00036)	89	23	10.49	2.19	1.67E-03	3.35E-02
Gonadotropin-releasing hormone receptor pathway (P06664)	237	52	27.94	1.86	1.45E-04	5.80E-03
Integrin signaling pathway (P00034)	200	43	23.58	1.82	6.95E-04	1.59E-02
Inflammation mediated by chemokine and cytokine signaling pathway (P00031)	261	55	30.77	1.79	1.99E-04	6.36E-03

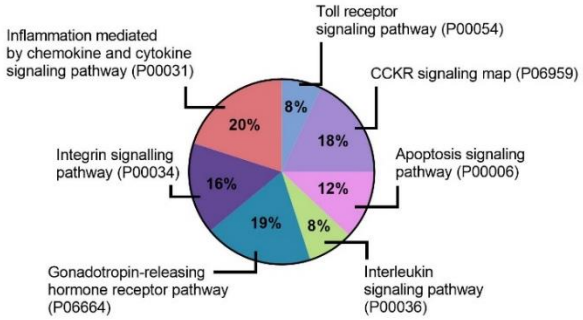

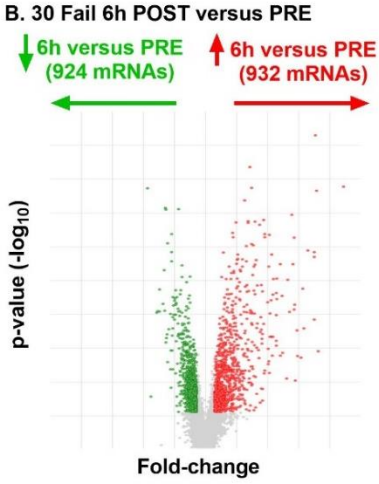

Pathway Analysis: 30 Fail Main Time Effect PRE – 6h

PANTHER Pathways	REFLIST (20589)	Gene List (2427)	(expected)	fold Enrichment	raw P-value	(FDR)
CCKR signaling map (P06959)	173	35	14.36	2.44	9.61E-06	1.54E-03
Gonadotropin-releasing hormone receptor pathway (P06664)	237	42	19.67	2.13	3.32E-05	1.77E-03

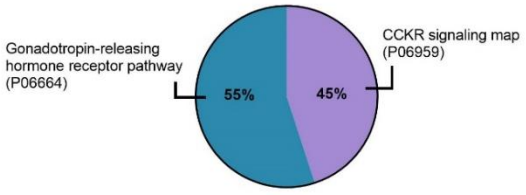

C. 80 Fail 3h POST versus PRE

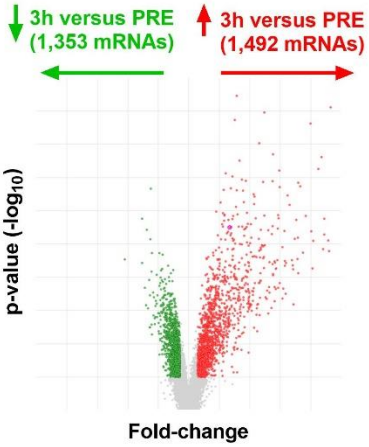

Pathway Analysis: 80 Fail Main Time Effect PRE – 3h

PANTHER Pathways	REFLIST (20589)	Gene List (2427)	(expected)	fold Enrichment	raw P-value	(FDR)
Toll receptor signaling pathway (P00054)	61	19	7.8	2.44	2.01E-03	4.02E-02
VEGF signaling pathway (P00056)	68	20	8.69	2.3	2.02E-03	3.60E-02
Apoptosis signaling pathway (P00006)	125	32	15.98	2	8.97E-04	2.87E-02
CCKR signaling map (P06959)	173	52	22.12	2.35	4.32E-07	3.45E-05
Angiogenesis (P00005)	181	41	23.14	1.77	1.85E-03	4.22E-02
Integrin signaling pathway (P00034)	200	45	25.57	1.76	1.09E-03	2.90E-02
Gonadotropin-releasing hormone receptor pathway (P06664)	237	53	30.3	1.75	5.05E-04	2.69E-02
Inflammation mediated by chemokine and cytokine signaling pathway (P00031)	261	56	33.37	1.68	8.87E-04	3.55E-02

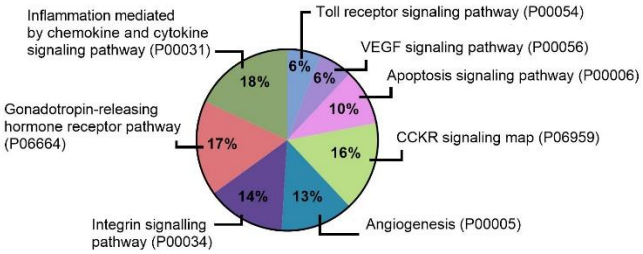

D. 80 Fail 6h POST versus PRE

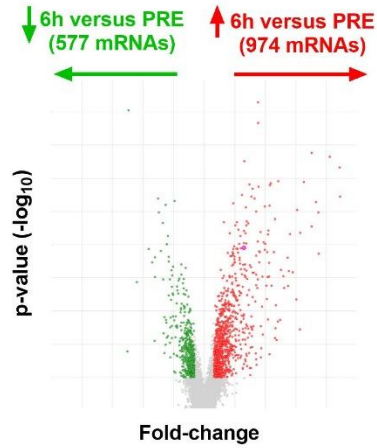

Pathway Analysis: 80 Fail Main Time Effect PRE – 6h

PANTHER Pathways	REFLIST (20589)	Gene List (2427)	(expected)	fold Enrichment	raw P-value	(FDR)
p38 MAPK pathway (P05918)	41	10	2.86	3.5	1.46E-03	4.68E-02
CCKR signaling map (P06959)	173	31	12.06	2.57	1.01E-05	8.11E-04
TGF-beta signaling pathway (P00052)	102	18	7.11	2.53	1.06E-03	4.25E-02
Gonadotropin-releasing hormone receptor pathway (P06664)	237	38	16.52	2.3	1.11E-05	5.92E-04

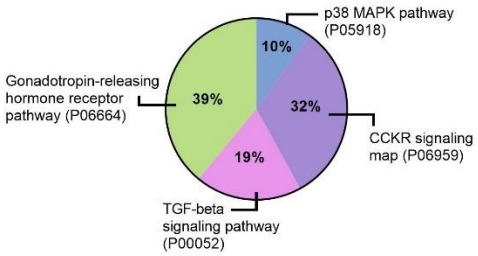

Legend: Differentially expressed genes (DEGs) viewed as volcano plots, pathway analysis of DEG enrichment within biological processes, and gene representation among enriched pathways. P**anel A)** 30 Fail training DEGs from PRE to 3h POST, **panel B)** 30 Fail training DEGs from PRE to 6h POST, **panel C)** DEGs from PRE to 3h POST with 30 Fail training, and **panel D)** DEGs from PRE to 3h POST with 30 Fail training. All DEGs have a fold-change of ±1.5 and $p < 0.01$, pathway analysis was significant if raw p-value < 0.01, and False Discovery Rate (FDR) $p < 0.05$. Abbreviations: 30 Fail; 30% one repetition maximum to failure; 80 Fail; 80% one repetition maximum; REFLIST, reference gene list across human genome; FDR, false discovery rate.

Regarding condition by time interactions (delta-delta fold-change ±1.5, p<0.01), there were only 11 significant DEGs from Pre to 3h post-exercise (Fig. 5 A and B), and 17 significant DEGs between bouts from Pre to 6h post-exercise (Fig. 5 C and D). Given the low number of differentially expressed genes between bouts over time, no pathways were predicted to differ between bouts at the 3h or 6h post-exercise time points.

Figure 4.5. ***DEGs 30v80 PRE to 3h and PRE to 6h***

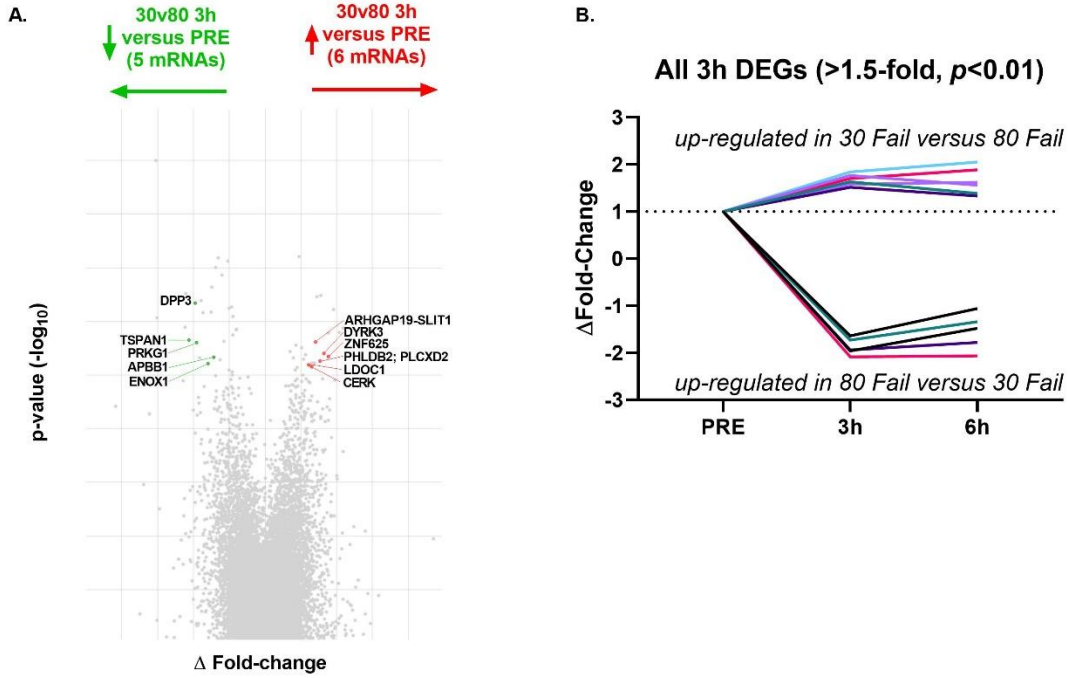

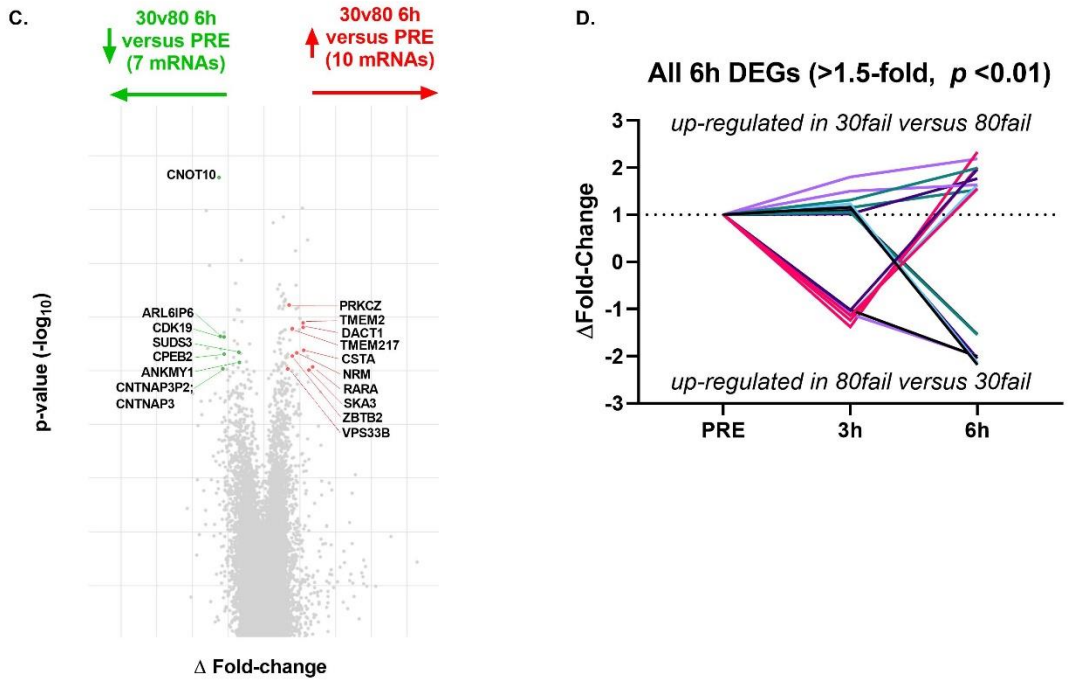

Legend: All data are significant DEGs in 30 Fail versus 80 Fail for: **panel A)** the ΔFold-change in gene expression plotted against p-value (-$\log_{10}$ transformed) at 3h POST versus PRE, **panel B)** the ΔFold-change over time for significant DEGs at 3h POST versus PRE, **panel C)** the ΔFold-change in gene expression plotted against p-value (-$\log_{10}$ transformed) at 6h POST versus PRE, and **panel D)** the ΔFold-change over time for significant DEGs at 6h POST versus PRE; significance threshold set at ±1.5 ΔFold-change, $p < 0.01$. Abbreviations: 30 Fail, 30% one repetition maximum to failure; 80 Fail; 80% one repetition maximum; DEGs, differentially expressed genes.

Preliminary Overlapping Genome-wide Methylome and Transcriptome Results

Overlap results from the methylome and transcriptome data can be found in Figure 6. Notably, these analyses are preliminary given that only DEGs between conditions over time were queried for methylation changes over time. Of the 11 DEGs between bouts from Pre to 3h post-exercise, only 1 DEG (gene symbol: CERK; Fig. 6A) was also associated with a significant DMP. Of the 17 DEGs that differed between bouts from Pre to 6h post-exercise, there were significant methylation events at 3h post-exercise that coincided with significant alterations in mRNAs at 6h post-exercise (Fig. 6 B-E). One DEG was associated with 2 separate, nonconsecutive DMPs (gene symbol: PRKCZ; Fig 7B), 2 DEGs (gene symbols: TMEM217 and NRM; Fig. 6 C and D) were

associated with 1 DMP each, and 1 DEG (gene symbol: CPEB2; Fig. 6E) was associated with a single DMP found within the promoter region.

There were also significant methylation events 6h post-exercise that coincided with significant alterations in mRNAs 6h post-exercise (Fig. 6 F-H). Two DEGs (gene symbols: PRKCZ and RARA; Fig. 6 F and G) were associated with 1 DMP each (PRKCZ associated methylation was unique at 6h POST), and 1 DEG (gene symbol: CPEB2; Fig. 6 H) was associated with a DMP within a CpG island in the gene's promotor region. There were no DEGs from Pre to 6h that were associated with any DMRs at 3h or 6h post-exercise.

Figure 4.6. ***Transcriptome and Methylation Overlap***

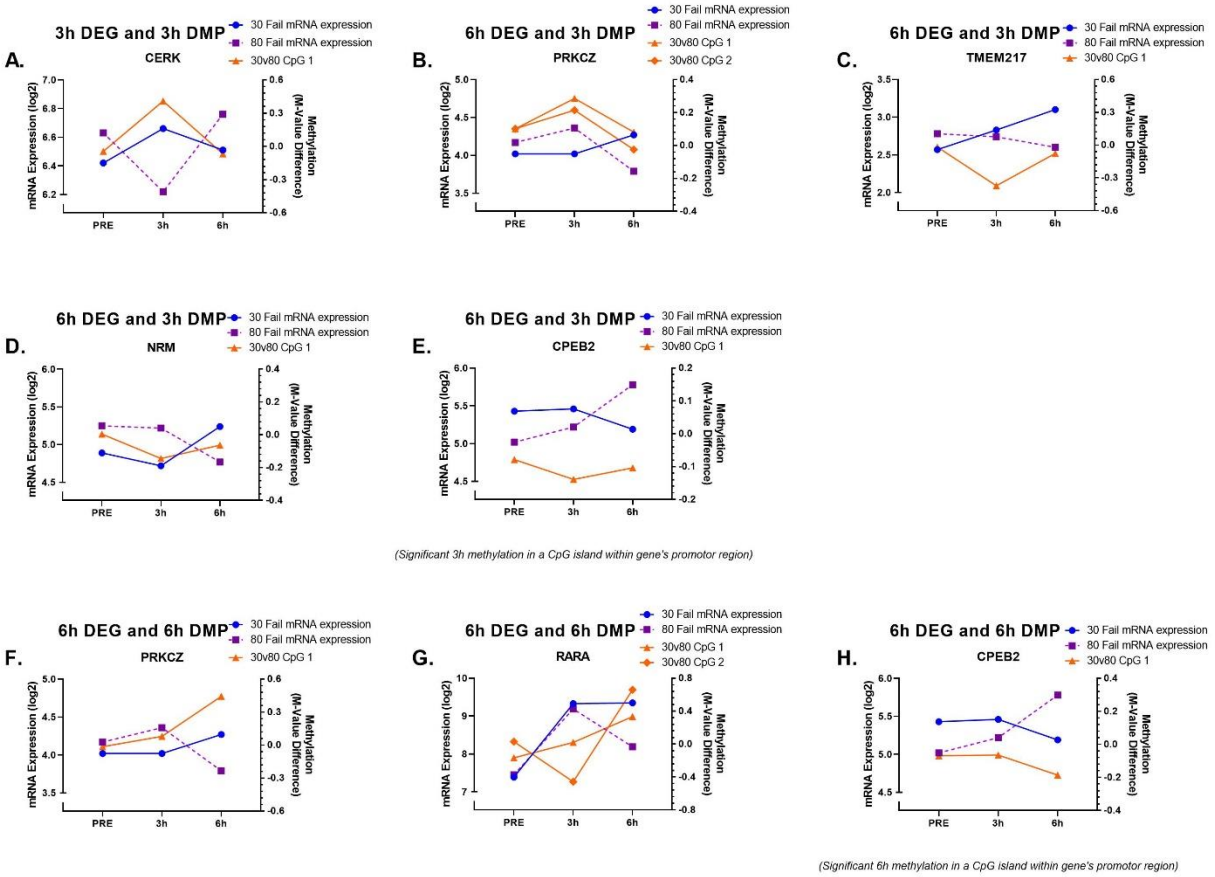

Legend: All figures represent genes found within the transcriptome and methylome analysis for: **panel A)** overlap of 3h DMP and 3h DEG, **panel B-E)** overlap of 3h DMPs and 6h DEGs, **panel F-H)** overlap of 6h DMPs and 6h DEGs; All DMPs significantly different at their respective timepoints $p < 0.01$, DEGs had significance threshold set at ±1.5 ΔFold-change, $p < 0.01$. All figures contain gene comparisons to unique CpG sites. Abbreviations: 30 Fail, 30% one repetition maximum to failure; 80 Fail; 80% 1 repetition maximum; DEGs, differentially expressed genes.

DISCUSSION

This study is the first to compare the acute transcriptome and methylome changes between two different resistance exercise paradigms. Our genome-wide methylation analyses revealed several novel findings. First, 30 Fail and 80 Fail responses indicated that thousands of CpG sites

were differentially methylated across the genome, and at 3h post-exercise more CpGs were hypermethylated than hypomethylated (2535 vs 1651) whereas at 6h post-exercise more sites were hypomethylated than hypermethylated (1880 vs 1608). Additionally, 97% of DMPs in CpG islands within promoters were hypomethylated 3 hours following exercise regardless of condition, showing a robust transient effect of a resistance exercise stimulus on genome-wide promoter methylation status. Lastly, with CpG islands found in promoter regions, a vast majority were hypomethylated for 30 Fail versus 80 Fail at both post-exercise time points (3h: 772 versus 21, 6h: 669 vs 189. We also demonstrated that nuclear TET activity significantly increased following exercise regardless of 30 Fail or 80 Fail training. Finally, our transcriptomic data indicated that there were only 11 mRNAs from PRE to 3h post-exercise and 17 mRNAs from PRE to 6h post-exercise that showed a significant condition by time interaction; however, there were thousands of genes that changed over time for both 30 Fail (Pre to 3h: 2,629 DEGs, Pre to 6h: 1,856 DEGs) and 80 Fail (Pre to 3h: 2,845, PRE to 6h: 1,551).

One of the more interesting observations herein was that higher- load and lower-load resistance exercise led to different global and CpG island/promoter DNA methylation responses. Our data shows that 30 Fail training transiently increased global methylation compared to 80 Fail training but was associated with robust hypomethylation of CpG islands/promoters. While this study is the first to evaluate differential methylation from different resistance exercise modalities, a 2021 study from Maasar and colleagues deployed a similar study design that compared varied modalities of run training [152]. The authors reported that skeletal muscle DNA became largely hypomethylated on a global scale and within key metabolic pathways in response to a higher intensity sprint training versus conventional bout. However, muscle biopsies were taken 30 minutes and 24 hours following exercise and, given that the exercise stimuli were completely

different, it is difficult to draw comparisons between our data and these data. Seaborne and colleagues performed the only other study to measure acute DNA methylation changes with resistance exercise [18]. Their participants were untrained and underwent an acute bout of resistance training with muscle samples collected 30 minutes post-exercise. Approximately 10,000 CpG sites became hypomethylated and 7,500 CpG sites became hypermethylated. Comparing our results to these two studies is challenging given that one study compared different aerobic exercise bouts, and the latter study reported the acute DNA methylome response to a bout of RT not to failure. However, all three of these studies conceptually demonstrate that robust alterations in skeletal muscle DNA methylation occur rapidly in response to a single bout of exercise.

Another interesting and novel finding is that the observed changes in DNA methylation may have resulted from a post-exercise increase in nuclear TET activity. While various studies have examined alterations in skeletal muscle DNA methylation in response to acute and chronic resistance training, this is the first study to analyze how nuclear DNMT and TET activities were altered accordingly. In an eloquent series of experiments from Wang and colleagues [160], the authors reported that TET2 knockout mice experienced severe muscle dysfunction. The authors used these data as well as *in vitro* experiments to conclude that TET2 activity is essential for muscle regeneration as well as myoblast differentiation and fusion. Although it is difficult to compare our data with these preclinical data, the observed alterations in skeletal muscle TET activity during periods of resistance training may ultimately drive changes in DNA methylation, and this may be important for downstream phenotype adaptations. In this regard, rodent models using TET inhibition during periods of mechanical overload are needed to test this hypothesis.

The mRNA response to a single exercise bout does not provide information on other molecular events that can drive skeletal muscle anabolism (e.g., translational signaling or the

protein synthetic response). Notwithstanding, several acute and chronic exercise studies have used transcriptomic data to model signaling events or pathways that are potentially altered [161, 162]. Unlike the aforementioned DNA methylation data, which showed that the 30 Fail bout led to a more robust hypomethylation profile, the transcriptomic response was largely similar between bouts. Specifically, several of the mRNA changes were similar from Pre-to-3h post-exercise and Pre-to-6h post-exercise within the 30 Fail and 80 Fail bouts, and only 11 mRNAs differed between conditions from Pre-to-3h post-exercise and 17 mRNAs differed between bouts from Pre-to-6h post-exercise. Our bioinformatics results also indicated that both training bouts significantly altered mRNAs involved in inflammatory signaling (e.g., Toll receptor signaling, CCKR signaling, chemokine and cytokine signaling), apoptosis signaling, gonadotropin-releasing hormone signaling, and integrin signaling. If extrapolating these transcriptomic data to potential chronic training outcomes, we surmise that the overall phenotypic responses may be largely similar between the 30 Fail and 80 Fail training bouts.

There were, however, some differences between bouts worthy of discussion. First, PRKCZ mRNA was up-regulated at 6h in the 30 Fail versus the 80 Fail bout, and CDK19 mRNA was up-regulated at 6h in the 80 Fail versus the 30 Fail bout. PRKCZ has been shown to bind to and inhibit Akt *in vitro* [163], and Akt acts as a protein kinase to activate the mammalian target of rapamycin (mTOR) signaling cascade to increase muscle protein synthesis [164]. CDK19 is involved with the mediator complex and therefore, along with other proteins, interacts with RNA polymerase II [165]. To our knowledge, neither of these genes have been studied in skeletal muscle during any form of exercise. Hence, it is unknown if the differential post-exercise responses in these two mRNAs between 30 Fail and 80 Fail training would lead to different phenotype outcomes. Our bioinformatics analyses also indicated that the VEGF/angiogenesis, p38 MAPK,

TGF-beta signaling pathways were predicted to be more affected following the 80 Fail bout, and the Interleukin signaling pathway was predicted to be more affected following the 30 Fail bout. Both the VEGF and angiogenesis signaling pathways are associated with the formation of new capillaries [166]. Due to the extended duration of sets and increased metabolic requirements assumed for 30 Fail training, it is counterintuitive that 80 Fail training would preferentially affect these pathways. However, given that no research has investigated the effects of each form of training on muscle capillarization, this may be worthy of interrogation. The interleukin signaling pathway being significantly enriched following the 30 Fail bout suggests a potential increase in inflammation and myokine formation [167]. It stands to reason 30 Fail training could induce an increased inflammatory response from the greater number of muscle contractions and time under tension [168]. The TGF-beta signaling pathway has been associated with extracellular matrix remodeling in skeletal muscle [169], and the 80 Fail condition perhaps upregulated this gene network due to greater mechanical tension transferred through the extracellular matrix during muscle contraction. Nevertheless, the associations stated above are speculatory given that they are predictions provided by the acute transcriptomic responses to one bout of 30 Fail and 80 Fail training, and further research is needed to determine if these acutely enriched pathways, over a training program, would translate into the proteins required to realize true physiological adaptations.

While DNA methylation is regarded as the prominent epigenetic event that either permits or inhibits gene transcription [117, 133], the mRNA response to exercise should be viewed as a more direct measure for potential phenotype outcomes. Although differential methylation responses existed between the 30 Fail and 80 Fail bouts, our transcriptomic findings convolute interpretations. Specifically, our data show the overlap between differential omics responses is

minimal, with only 8 genes displaying overlap between the methylome and transcriptome arrays. Where overlap existed, there were never more than 2 separate, nonsequential CpG sites associated with any gene at each time point. Thus, less than 1% of differentially methylated positions were associated with a differentially expressed gene. Our data largely agree with Laker and colleagues [144] who reported that only 2% of differentially expressed genes from a resistance exercise and high-fat diet intervention were also differentially methylated. To date, very few studies have attempted to evaluate the concomitant epigenetic and transcriptomic responses to resistance exercise. However, Seaborne and colleagues found that an acute bout of resistance exercise in eight untrained males led to 10,000 sites becoming hypomethylated and 7,500 becoming hypermethylated [18]. Interestingly, none of these acutely methylated signatures were associated with changes in mRNA expression until participants had undergone a chronic training paradigm [18]. Additionally, when acute and chronic methylome and transcriptome data were overlapped, ~40% of differentially expressed genes were shown to be associated with altered methylation signatures [18, 22]. Thus, it stands to reason that the epigenetic signatures observed herein may eventually lead to mRNA responses during later post-exercise periods (i.e., 8-72 hours post-exercise). Critically, the -omics overlap analysis herein only included DEGs and DMPs that showed interaction effects. Given that the current -omics overlap analysis is preliminary, and we intend on performing further analysis to examine DEG and DMP overlap with genes showing time effects, there will likely be a greater association between genome-wide methylation and mRNA expression responses due to the exercise stimuli.

Experimental Limitations

The present study possesses limitations including limited -omics data overlap, sample size, sample population, and muscle sample collection time points. As stated prior, we intend on performing further -omics overlap analysis to examine DEG and DMP overlap with genes showing time effects, regardless of condition. Indeed, this analysis will likely indicate a greater association between genome-wide methylation and mRNA expression responses relative to the preliminary analyses performed herein. A larger number of more diverse group of participants, with muscle samples collected at various additional timepoints across a 24-72h time frame, may have resulted in molecular differences between conditions. Alternatively stated, the current study examined the early molecular response to each training bout, and missed the post-exercise window (i.e., 12-72 hours) where events such as increased infiltration of immune cells and satellite cell proliferation occur. Hence, replicating this study design with additional timepoints is warranted.

Conclusions

In conclusion, an acute bout of 30 Fail or 80 Fail resistance exercise produced unique DNA methylation responses, albeit largely similar transcriptomic responses. These data continue to add insightful information to the limited body of literature comparing the muscle-molecular effects of different resistance training paradigms.

MATERIALS AND METHODS

Ethical Approval and Pre-screening

This study was conducted with prior review and approval from the Auburn Institutional Review Board and in accordance with the most recent revisions of the Declaration of Helsinki (IRB approval #: 20-081 MR 2003).

The participants recruited for this study were young males from the local area that met the following criteria: i) aged 18-35, ii) a body mass index ([BMI] body mass in kilograms/ height in meters^2) not exceeding 35 kg/m^2, iii) no known cardio-metabolic disease (e.g., obesity, diabetes, hypertension, heart disease) or any condition contraindicating participation in resistance training, donating muscle biopsies, or receiving finger sticks, iv) have participated in lower-body training at least once per week over the last 6 months, v) have a self-reported barbell back-squat one repetition maximum of ≥ 1.5x body weight. Following verbal and written consent, participants then completed testing for maximal strength on the barbell-back squat (estimated by a three-repetition maximum) as well as body composition testing for BMI.

Study Design

The study design schematic is available in Figure 7. Participants completed a within subject design that included a total of five visits to the laboratory. At visit 1, an informed consent and health history questionnaire were completed. This was followed by testing to determine maximal strength for the barbell back squat and knee extension. At Visit 2, participants completed a battery of baseline (PRE) tests that included measures of height, weight, and vastus lateralis (VL) thickness. Participants also donated a muscle biopsy from the VL prior to the completion of a single bout of resistance exercise using a randomly assigned experimental load (i.e., 30% or 80% estimated 1-RM). Then, at both 3 hours (3h POST) and 6 hours (6h POST) following the exercise bout, participants received additional muscle biopsies from the VL. Finally, after approximately 7 days, participants completed another bout of resistance exercise using the experimental load not completed at visit 2 (i.e., if visit 2 used 30%, then visit 4 used 80%) with biopsies occurring at

PRE, 3h POST, and 6h POST. Visits 3 and 5 were follow-up visits to observe and re-bandage biopsy incisions.

Figure 4.7. ***Study Design***

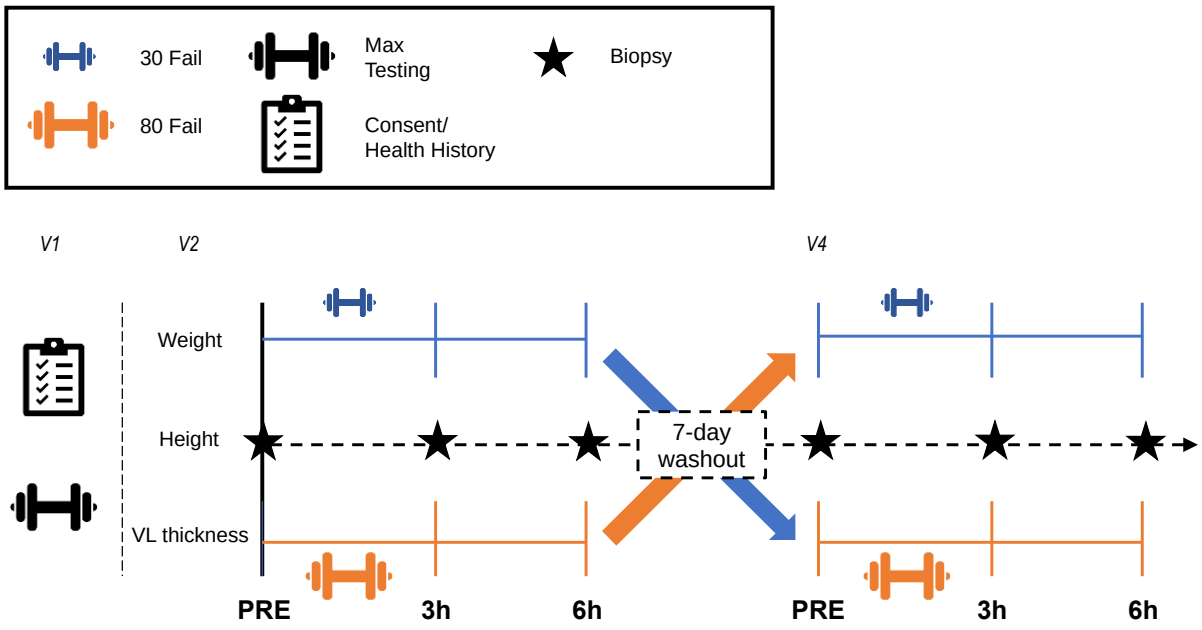

Legend: This schematic represents the timeline for participant consent, max testing, PRE-phenotype testing, experimental resistance exercise bout, cross-over washout period, and timepoints for all biopsies. Abbreviations: 30 Fail, 30% one repetition maximum to failure; 80 Fail; 80% one repetition maximum; VL, *vastus lateralis;* V1, Visit 1.

Testing Sessions

Estimated 1-RM Testing. During the initial visit, participants completed testing to determine their estimated 1-RM ([est. 1-RM]. Est. 1-RM was derived from a 3-repetition maximum test for barbell back squats (squats) and knee extensions. An est. 1-RM was used instead of a true 1-RM to reduce the risk of error/ injury and increases the accuracy of the strength measures. The estimated 1-RM was tested as follows: i) participants completed a general warm-up of 25 jumping jacks and 10 body weight squats, ii) for a specific warm-up, 50% of their most recent, self-reported

squat max was performed for 10 reps, iii) subsequently, additional warm-up reps were completed at approximately 60% (8-10 reps), 70% (5-8 reps), 80% (3-5 reps), 90% (1-3 reps) and 95% (1 rep) of their self-reported 1-RM. Then, using NSCA guidelines, testing weights were selected by a Certified Strength and Conditioning Specialist (CSCS), beginning with a load that could easily be performed for 3 reps. Est. 1-RMs were assessed within six attempts, and with each successful attempt the CSCS was informed of how many more reps could be completed (reps in reserve [RIR]), with that number being added to the total reps completed (e.g., reps completed [3] + RIR [2] = 5) this number was considered an estimated rep max for the given load. The estimated rep max was then used to determine the next 3-RM attempt through the National Strength and Conditioning Association (NSCA) guidelines on rep max to 1-RM percentage conversions. This was repeated until the participant either did not complete 3 full repetitions, the parameters of the exercise were not met, or the participant declined an increase in load.

Hydration Testing. Urine specific gravity was used to assess hydration. During visits 2 and 4, participants gave a urine sample (approx. 5ml) that was assessed for urine specific gravity (USG) testing using a handheld refractometer (ATAGO; Bellevue, WA, USA). All participants had a USG level ≤ 1.020, and this was used as a threshold of sufficient hydration to continue testing [146].

Body Composition Testing. Height and body mass were evaluated using a digital column scale (Seca 769; Hanover, MD, USA). Height was measured to the closest 0.5 cm and body mass to the closest 0.1 kg. Supine bioelectrical impedance spectroscopy was used to estimate fat-free mass and fat mass. The procedure was done according to manufacturer instructions. The technique was also explained in more depth by Esco et al. [147] and Moon et al. [148]. Briefly, after participants rested in a supine position for 5 to 10 minutes, the Imp SFB7 (ImpediMed Limited, Queensland,

AU) applied electrical currents, ranging from 50-500kHz, via a tetra-polar electrode configuration. All electrodes placed on the right side of the body (2 electrodes being placed above and below the wrist, 5 cm apart, and 2 being placed above and below the anterior portion of the ankle, 5 cm apart). These signals were then calculated automatically by the device and converted to an estimate of fat-free mass and fat mass.

Vastus lateralis morphological assessment. Ultrasound was used to measure VL muscle thickness (cm) as reported in Sexton et al. [149]. Briefly, real-time B-mode ultrasonography (NextGen LOGIQe R8, GE Healthcare, Chicago, IL, USA), facilitated by a multi-frequency linear-array transducer (L4-12T, 4–12 MHz, GE Healthcare, USA), was utilized in capturing an image of VL thickness (cm^2) in the transverse plane, at approximately 50% the distance between the mid-inguinal crease and the proximal patella. Participants were instructed to lie supine, with knee and hip fully extended, for a minimum of 5 minutes before image acquisition. The image depth was adjusted until the edge of the femur was in view, which allowed for a full-thickness view of the VL. All ultrasound images were taken using a generous amount of water-soluble transmission gel. Following collection of images, freely available analysis software (ImageJ; National Institute of Health, Bethesda, MD, USA) was used to quantify VL thickness. VL thickness was measured from the VL superficial aponeurosis to the deep aponeurosis via the straight-line function. All ultrasound images were taken and analyzed by the same investigator with a previously established test-retest reliability (ICC 0.96; SEM 0.09 cm; MD 0.24 cm)

Skeletal Muscle Biopsy and Processing. During visits 2 and 4, at PRE, 3h POST, and 6h POST skeletal muscle biopsies were collected from the vastus lateralis using a 5-gauge biopsy needle, where local anesthesia was used. Approximately 50-100 mg of tissue was collected in total with 20-40 mg being adhered to a cork block via tragacanth gum and preserved in an insulating layer

of optimum cutting temperature media that was frozen in liquid nitrogen-cooled 2-methylbutane, then stored -80°C to be later used for histology. Remaining tissue was flash frozen in liquid nitrogen and stored at -80°C for later use.

Resistance Exercise Bouts to Failure

During visits 2 and 4, participants completed a resistance exercise bout (squats and knee extensions) where they were randomly assigned to either 80% and 30% of their Est. 1-RM for 4 sets to failure at visits 2 and 4 or at visits 4 and 2. Failure was determined as either: i) an inability to complete a full repetition, ii) technical errors that would compromise safety (e.g., difficulty keeping balance, failure to maintain appropriate posture, etc.), or iii) the participant spent longer than 4 seconds between repetitions. Upon arrival, participants completed a general warm-up of 25 jumping-jack and 10 body weight squats, followed by a specific warm-up of 10 repetitions at 30-50% and 5-8 reps at 75% of the experimental load assigned to them (i.e., 80% or 30% of Est. 1-RM). Stronger participants were allowed to complete an additional warm-up set using 85% of their assigned experimental load. Participants then initiated their sets to failure, and upon completion, they were given 5 minutes of rest. Additionally, participants were given approximately 5 min of rest between squats and knee extensions. After the bout of exercise was completed, participants were instructed to return to the laboratory 3 hours and 6 hours later. Participants reporting nausea, malaise, and light-headedness were given supplemental nutrition (i.e., a granola bar [calories: 170, total fat: 8 g, carbohydrates: 20 g, protein: 4 g] and 355 ml of sports drink [calories: 80, carbohydrates: 21 g]) to reduce symptoms, and upon completion of training at visit 4, those individuals were given the exact same supplemental nutrition regardless of symptoms.

Biochemical Assays

DNA, RNA, and Protein Isolations. Skeletal muscle samples (15-20 mg) were crushed on a liquid nitrogen cooled stage, weighed to the nearest 0.0001 g (Mettler-Toledo; Columbus, OH, USA) and added to 500 μl of Trizol in 2ml polypropylene tubes. The muscle was then homogenized with tight fitting plastic pestles for approximately 30s or until the tissue was fully crushed. Samples were then placed in a -80°C freezer overnight to increase RNA yield. The following day samples were removed from -80°C freezer and allowed to thaw completely at room temperature, after which 100 μl of bromochloropropane (BCP) was added to the sample and shaken well for 15s, then incubated at room temperature for 2 minutes before being centrifuged at 12,000 g for 15 minutes. Once removed from the centrifuge, samples were kept on ice for the remainder of the procedures. Centrifugation divided the sample into three distinct phases including the top aqueous phase containing RNA, the center meniscus containing DNA, and the bottom layer containing a protein phase. Approximately 200 μl of the liquid phase was removed and placed in a new tube with 500 μl of 100% ethanol, and the RNA was subsequently purified and quantified. The remaining DNA and protein were then separated by first adding 300 μl of 100% ethanol. Samples were then shaken for 15 seconds, incubated for 3 minutes at room temperature, and subsequently centrifuged at 5000 g for 10 minutes at room temperature. This produced a DNA pellet and a protein supernatant. The supernatant (protein-Trizol-ethanol mixture) was removed and placed in new tubes. The DNA pellet was frozen at -80°C for future purification and quantification. After moving the supernatant to new tubes, 650 μl of 100% ethanol was added to precipitate the protein. The samples were then vortexed, mixed with 100 μl of BCP, and vortexed again. Then, to facilitate phase separation, 600 μl of deionized water was added and vortexed vigorously. The samples were then centrifuged at 12,000 g for 5 minutes to collect a protein pellet

from the solution. The resulting supernatant was removed and the pellet air dried at room temperature for 1-2 minutes. The protein pellet was then resuspended in 2x SDS sample loading buffer + 5M Urea (1:2 dilution of 10M Urea, 2:5 dilution of 5x SDS sample loading buffer, 1:10 deionized water, and 1:100 50x protease inhibitor) where it was allowed to dissolve at room temperature. The suspended protein was then quantified using a commercial assay (RC DC™ Protein Assay, catalog #5000122; Bio-Rad; Hercules, CA, USA).

Total Protein Quantification. To quantify total protein, the Bio-Rad RC DC™ Protein Assay was performed according to the manufacturer's instructions. A BSA protein standard was used to create a standard curve. Then 100 µl of standards and samples were added to 2.0 ml polypropylene tubes, 500 µl of RC Reagent I was added to each tube, and tubes were vortexed and incubated at room temperature for 1 min. 500 µl RC Reagent II was then added to each tube, vortexed, and centrifuged at 15,000 g for 5 minutes. The supernatant was discarded, and the tubes were inverted to drain them completely. 510 µl of Reagent A was then added, and each tube was vortexed and incubated at room temperature for 5 min. The samples were then vortexed and 4 ml of DC Reagent B was then added to each tube. Samples were then incubated at room temperature for 15 minutes, transferred to a microplate, and absorbances were read at 750 nm.

DNA Purification and Quantification. DNA isolated previously was further purified using a commercial kit (DNeasy Blood and Tissue Kit, catalog #69504; Qiagen; Germantown, MD, USA) according to manufacturer protocol with a minor modification to the elution step. Briefly, 180 µl of ATL buffer and 20 µl of proteinase K were added to each sample, vortexed for 20 seconds, and incubated at 56°C for 8 hours. Then 200 µl each of AL buffer and 100% ethanol were added and then vortexed. The mixture was then transferred to DNeasy Mini spin columns placed in 2 ml polypropylene flow-through tubes. The tubes were then centrifuged at 6,000 g for 1 minute

and flow-through tubes were discarded and replaced. Then, 500 μl of Buffer AW1 was added, and tubes were centrifuged at 6,000 g for 1 minute. Flow-through tubes were discarded and replaced. Then, 500 μl of Buffer AW2 was added, and tubes were centrifuged at 20,000 g for 3 minutes to dry the DNeasy membrane containing DNA. Flow-through tubes were discarded and replaced with the final 1.7 ml polypropylene DNA collection tubes. Finally, 200 μl of Buffer AE was added, incubated for 5 minutes at 37°C, and centrifuged at 10,000 g for 1 minute at room temperature to elute DNA. To maximize DNA yield, solution from final DNA collection tubes were reapplied to spin columns and centrifuged at 10,000 g for 1 minute at room temperature. The eluted DNA was then assessed in duplicate for quality and quantity using an absorbance of 260/280 nm provided by a desktop spectrophotometer (NanoDrop Lite; Thermo Fisher Scientific; Waltham, MA, USA). The purified DNA was then sent to a commercial laboratory (TruDiagnostic; Lexington, KY, USA) for the methylation analysis described below.

DNA Bisulfite Conversion. Bisulfite conversion was performed using an Infinium HD Methylation Assay bisulfite conversion kit (EZ DNA Methylation Kit, Zymo Research, CA, USA). Briefly, 50 μl suspensions (5 μl M-Dilution and 500 ng DNA diluted in distilled water) were added to a conversion plate and incubated at 37°C for 15 minutes. Then, 100 μl of prepared CT Conversion Reagent was mixed with each sample, and the conversion plate was then incubated for 12-16 hours at 50°C in the dark. After incubation, samples were further incubated at 4°C for 10 minutes. Then, 400 μl of M-Binding Buffer and samples were added to a Silicon-A Binding Plate placed on a collection plate. The plates were then centrifuged at 3000 g for 5 minutes, and the flow-through was discarded. Then, 400 μl of M-Wash Buffer was added, and the plate was centrifuged at 3,000 g for 5 minutes. Then, 200 μl M-Desulphonation Buffer was added to the plate, incubated for 15-20 minutes at room temperature, and centrifuged at 3,000 g for 5 minutes.

Then, 500 μl of M-Wash Buffer was added to each well and centrifuged at 3,000 g for 5 minutes, and another 500 μl of M-Wash Buffer was added and centrifuged at 3,000 g for 10 minutes. Finally, the binding plate was placed on an elution plate and 30 μl of M-Elution Buffer was added to each well. The plate was then centrifuged at 3,000 g for 3 minutes to elute DNA from the binding plate. Bisulfite Converted DNA (BCD) was stored at -80°C until DNA methylation analysis.

DNA Methylation EPIC BeadChip array amplification. The Infinium MethylationEpic BeadChip Array was performed per the manufacturer's (Illumina) instructions. BCD (4 μl) was transferred from the BCD plate to the matching wells of a MSA4 plate, combined with 20 μl of MA1 and 4 μl of 0.1 NaOH, covered with a cap mat, and mixed by vortexing at 1600 rpm for 1 minute and pulse centrifugation at 280 g. The plate was then incubated for 10 minutes at room temperature, and the cover was removed before the plate was placed upside down. Then, 68 μl of RPM and 75 μl of MSM were added to each well and resealed with the cap mat. The plate was again vortexed at 1,600 rpm for 1 minute and pulse centrifuged at 280 g. The MSA4 plate was incubated in an Illumina Hybridization Oven at 37°C for 24 hours.

Fragmentation, Precipitation, and Resuspension of Amplified DNA. After amplification of BCD, fragmentation began by subjecting the plate to pulse centrifugation at 280 g for 1 minute. The cap mat was removed and 50 μl of FMS was added to each well in the MSA4 plate. After replacing the cap mat, the plate was vortexed at 1,600 rpm, pulse centrifuged at 280 g for 1 minute, and incubated at 37°C for 1 hour. To precipitate DNA, 100 μl of PM1 was added to each well, the plate was resealed, vortexed at 1,600 rpm for 1 minute, and incubated at 37°C for 5 minutes. The cap mat was removed and discarded before 300 μl of 2-propanol was added to each sample well. The plate was sealed with a new cap mat, inverted 10 times to mix the solution, and incubated at 4°C for 30 minutes. The plate was then centrifuged at 3,000 g for 20 minutes at 4°C. After ensuring

a blue pellet was formed and adhered to the bottom of each well, the plate was inverted to drain supernatant. The plate was then tapped while upside down to ensure all wells were drained. The plate was then dried and inverted in a tube rack for 1 hour at room temperature. While inverted, the plate was wiped dry of any residual fluid. DNA was then resuspended by first adding 46 μl of RA1 to each well of the MSA4 plate. The plate was sealed with heat seal foil and subsequently incubated in the hybridization over for 1 hour at 48°C. After, this the pellet was resuspended by vortexing the plate at 18,000 rpm and pulse centrifugation at 280 g.

BeadChip hybridization, extension, and staining. After resuspension of the precipitated, fragmented DNA, the plate was incubated at 95°C for 20 minutes to facilitate denaturing of the DNA. The plate was then left at room temperature for 30 minutes and pulse centrifuged at 280 g. Samples were then added carefully from MSA4 plate onto prepared BeadChips for hybridization. After DNA was fully dispersed, BeadChips were inserted into hybridization chambers and the chambers were incubated in Illumina Hybridization Oven at 48°C for 16 hours. Afterwards, BeadChips were washed in 200 ml of PB1 and prepared for the staining process. The BeadChips were subjected to a single base-pair extension at precisely 44°C by placing assembled flow-through chamber assemblies into the chamber rack. The reservoir of each flow through chamber was then filled and incubated with the following steps: i) five rounds of 150 μl of RA1 with 30-second incubations, ii) 450 μl of XC1 with a 10-minute incubation, iii) 450 μl of XC1 with a 10-minute incubation, iv) 200 μl of TEM with a 15-minute incubation, v) 2 rounds of 450 μl of 95% formamide/1mM EDTA with 1-minute incubations, vi) a 5-minute incubation, vii) an adjustment of the chamber rack temperature as specified on the STM tube, and viii) two rounds of 450 μl of XC2 with an incubation of 1 minute. After the chamber rack reached the correct temperature, the process of staining BeadChips commenced. Each flow-through chamber was filled and incubated

with the following steps repeated, which were repeated five times: i) 250 μl of STM with 10-minute incubations, ii) two rounds of 450 μl of XC3 with 1-minute incubations, iii) 5-minute wait period. The BeadChips were washed of staining reagents by being submerged in PB1 for 5 minutes before being submerged in XC4 for 5 minutes. The BeadChips were then dried for 50-55 min before being imaged by the Illumina iScan® System (Illumina, San Diego, CA, USA)

Muscle Histological Sectioning. Muscle samples, collected and preserved in OCT as described above, were sectioned at a thickness of 10 μm in a cooled (-20°C) cryostat (Leica Biosystems; Buffalo Grove, IL, USA) and electrostatically adhered to positively charged histology slides. The slides were then stored at -80°C until immunohistochemical staining.

Immunohistochemistry. Slides with muscle sections adhered were removed from the -80°C freezer and allowed to equilibrate and dry, while covered, at room temperature for 1.5 hours. Sections were then outlined using a hydrophobic pen to retain solutions for the following incubation steps. First a 1x phosphate buffer solution (1x PBS) was applied for 10 minutes to rehydrate muscle sections. The 1x PBS was then removed and a 3% peroxide solution was added to the sections to incubate for 15 minutes. Subsequently, the peroxide was removed, and the slides were washed in a 1x PBS solution for 3 x 5 minutes on a rocker. 1x TrueBlack Lipofuscin Autofluorescence Quencher solution (biotium; Fremont, CA, USA) was added and incubated for 1 minute and washed in 1x PBS for 3 x 5 minutes. The sections were then blocked with a 10% normal goat serum and 5% normal horse serum for at least 1 hour, then washed in 1x PBS for 5 minutes. Once blocked, the primary antibody was applied (1:20 Mandra, 1:20 of BA_D5, 9:20 and 9:20 5% normal horse serum, all diluted in 1x PBS; all antibodies from Developmental Studies Hybridoma Bank; Iowa City, IA, USA) and incubated overnight. After primary antibody incubation, slides were washed four times in 1x PBS for 5 minutes. A secondary antibody was

applied (1:100 goat, anti-mouse IgG1 594, 1:100 goat, anti-mouse IgG2B 488, diluted with 1x PBS) and incubated for 1 hour. The slides were then washed 4 x 5 minutes in 1x PBS. A DAPI fluorescent dye (1:10,000 DAPI, diluted in deionized water) was then applied for 15 minutes and washed 2 x 3 minutes. A 1:1 PBS-glycerol solution was then applied around the sections as a cover slip adherent, and coverslips were applied thereafter. Following mounting, digital images were immediately captured with a fluorescent microscope (Nikon Instruments, Melville, NY, USA) using a 10x objective. Standardized measurements of type I and type II fCSAs, as well as myonuclei number were performed using open-sourced software (MyoVision 2.0) [150, 151]. A pixel conversion ratio value of 0.964 μm/pixel was used to account for the size and bit-depth of images, and a detection range of detection from 500 to 12,000 μm^2 was used to ensure artifact was removed (e.g., large fibers which may have not been in transverse orientation, or structures between dystrophin stains which were likely small vessels). Test-retest reliability for mean fCSA was previously determined in our laboratory comparing two separate images from the same sample using 26 muscle samples resulting in an ICC, SEM and MD of 0.91, 459 μm^2, and 1,271 μm^2, respectively.

Nuclear isolations. Nuclear extractions from frozen muscle tissue were performed using a commercial kit (Nuclear Extraction Kit, catalog# ab113474; Abcam; Waltham, MA, USA). Briefly, skeletal muscle samples (15-20 mg) were crushed on a liquid nitrogen cooled stage and added to 1x Pre-Extraction Buffer containing DTT solution (10x pre-extraction diluted 1:10 with distilled water, DTT diluted 1:1000). The tissue was then homogenized, incubated on ice for 15 minutes, and centrifuged for 10 minutes at 12,000 rpm at 4°C. The supernatant was then removed and 1x Pre-Extraction Buffer containing DTT solution and Protease Inhibitor Cocktail (10x pre-extraction diluted 1:10 with distilled water, DTT and PIC diluted 1:1000) was added and incubated

for 15 minutes with a 5-second vortex every 3 minutes. The suspension was centrifuged for 10 minutes at 14,000 rpm at 4°C. The supernatant was transferred to a new tube and the concentration was measured with a bicinchoninic acid (BCA) assay.

BCA assay. Nuclear proteins were batch processed for protein concentrations using a BCA kit (Thermo Fisher Scientific; Waltham, MA, USA). Isolated Nuclear protein were quantified in duplicates, and samples (20 µl of 3x diluted sample + 200 µl of Reagent A + B) were subjected to a microplate assay protocol. The average coefficient of variation for nuclear extract protein concentration was 5.88%.

DNMT activity assay. DNMT activity was performed on nuclear extracts using a commercial assay (Colorimetric DNMT Activity Quantification Kit, catalog# ab113467; Abcam). Briefly, nuclear extracts, without the inhibitor, and Adomet Working buffer were added to a strip-well microplate then tightly covered with an adhesive film and incubated at 37°C for 90 minutes. The reaction solution was then removed, and each well was washed with 1x Wash Buffer 3 times. Diluted Capture Antibody was added to each well and covered with aluminum for incubation at room temperature for 60 minutes. The Diluted Capture Antibody was then removed, and each well was washed 3 times with 1x Wash Buffer. Diluted Detection Antibody was added to each well and the plate was covered with aluminum foil and incubated at room temperature for 30 minutes. The Diluted Detection Antibody was removed, and each well was washed 4 times with 1x Wash Buffer. Diluted Enhancer Solution was then added to each well and the plate was covered with aluminum foil and incubated at room temperature for 30 minutes. The Diluted Enhancer Buffer was removed and washed 5 times with 1x Wash Buffer. Finally, Developer Solution was added to each well and incubated at room temperature, in a dark container, for 10 minutes. Stop Solution was then added to each well, and absorbance was immediately read at 450 nm and 655 nm using a plate reader

(Synergy H1; Biotek; Winooski, VT, USA). Activity was expressed as absorbance units per microgram nuclear protein. The average coefficient of variation for absorbance values was 4.23%.

TET activity assay. TET activity was performed on nuclear extracts using a commercial assay (TET Hydroxylase Activity Quantification Kit, catalog# ab156913; Abcam). Briefly, Binding Solution was added to each well and 0.5x TET Substrate were added to each blank and sample wells in a strip-well plate. The solution was covered and incubated at 37°C for 90 minutes. The binding solution was removed, and each well was washed 3 times with 1x Wash buffer. Then Final TET Assay Buffer, without the inhibitor, were added to sample wells. The wells were tightly covered with Parafilm M and incubated at 37°C for 90 minutes. The reaction solution was removed from each well and washed three times with 1x Wash Buffer. Then, Diluted Capture Antibody was added to each well and covered with aluminum foil for incubation at room temperature for 60 minutes. The Diluted Capture Antibody was removed, and each well was washed 3 times with 1x Wash Buffer. Dilution Detection Antibody was then added to each well, covered with aluminum foil, and incubated at room temperature for 30 minutes. The Diluted Detection Antibody was removed, and each well was washed 4 times with 1x Wash Buffer. Diluted Enhancer Solution was then added to each well and plates were covered with aluminum foil and incubated for 30 minutes at room temperature. The Diluted Enhancer Solution was then removed, and each well was washed 5 times with 1x Wash Buffer. Finally, Fluorescence Development Solution was added to each well and incubated at room temperature for 2-4 minutes. The plate was read at 530ex/590em nm for fluorescence, and activity was expressed as fluorescence units per microgram nuclear protein. The average coefficient of variation for fluorescence values was 7.67%.

Western Blotting. After a BCA assay was performed to determine the concentration of protein in nuclear lysates, the samples were combined with DiH20 and 4x Laemmli buffer achieve

a protein concentration of 1 μg/ μl. Following this, 15 μl of each sample was loaded onto a commercially available pre-casted gradient (4-15%) SDS-polyacrylamide gel (Bio-Rad Laboratories, Hercules, CA, USA) which were submerged in a 1x SDS-PAGE running buffer (Ameresco, Framingham, MA, USA). The loaded gel then underwent electrophoresis at 180V for 50 min and was transferred onto a polyvinylidene difluoride membrane (PVDF) at 200 mA for 2h. The membrane was then washed in ponceau stain for 10 minutes, rinsed with DiH2O and imaged to confirm consistent protein loading in each lane. The membrane was then blocked for 1h with 5% nonfat milk powder in Tris-buffered saline containing 0.1% Tween-20 (TBST; Ameresco, Framingham, MA, USA) and subsequently washed with TBST for 3 rounds of 5 min. Then, membranes were incubated overnight at 4°C with 15ml of either a rabbit TET1 (TET1, 1:1000; catalog# ab191698;Abcam, Cambridge, UK), rabbit TET2 (TET2, 1:1000; catalog# 45010S; Cell Signaling Technology, Danvers, MA, USA), or rabbit TET3 (TET3, 1:1000; catalog# 85016S; Cell Signaling Technology, Danvers, MA, USA) antibodies in TBST with 5% bovine serum albumin (BSA). After primary anti-body incubation, membranes were washed with TBST for 3 rounds of 5 minutes and incubated for 1h, at room temperature, with 15ml of a horseradish-peroxidase (HRP)-linked anti-rabbit IgG (1:2000; catalog #: 7074S; Cell Signaling Technologies, Danvers, MA, USA) secondary antibody in TBST with 5% BSA. Then prior to imaging the membranes were washed in TBST for 3 rounds of 5 min. The membranes were developed by adding 1-2 ml of an enhanced chemiluminescent reagent (Luminata Forte HRP substrate; EMD Millipore, Billerica, MA, USA) to each membrane. Band density was captured using a gel documentation system that includes the associated software (ChemiDoc; Bio-RAD Laboratories, Hercules, CA, USA). Due to non-specific binding with the TET1 antibody, and lack of quantifiable bands with TET2 and TET3, no further analysis of membrane band density was performed.

Statistical Analyses

Statistical analysis was performed in SPSS v26.0 (IBM Corp, Armonk, NY, USA) and Partek Genomic Suite V.7 (Partek Inc., MO, USA. Prior to analyses, Shapiro-Wilks tests of normality were performed on all dependent variables outside of DNA methylation and mRNA expression values. Two-way ANOVAs were used to assess main effects and potential interactions of condition (30 Fail vs 80 Fail) x time (PRE, 3h POST, and 6h POST) for non-methylation data (e.g., changes in VL thickness values, training volume, etc.). For any main effect that violated the assumption of sphericity, a Greenhouse-Geiser correction was applied.

DNA Methylation Analysis. Following quantification of DNA MethylationEPIC BeadChip array, the Partek Genomic Suite V.7 (Partek Inc., MO, USA) was used to process the MethylationEpic _v-1-0_B4 manifest file as described by Maasar et al. 2021 [152]. Briefly, an average detection p-value was assessed for all samples to ensure values below 0.01 [153], and any probes outside of this range were removed from analysis. Raw signals for the methylated and unmethylated probes were assessed for the difference between average median methylated and average median unmethylated probes were measured to ensure the recommended difference of 0.5 or less [153]. After the data was imported to Partek Genomics Suit, single nucleotide polymorphisms (SNPs) associated probes and cross-reactive probes, identified in validation studies [154], were removed from analysis. Functional normalization using a noob background correction was performed for background normalization [155]. Then, principal component analyses (PCA), density plots, and box and whisker plots were used for quality control (i.e., no samples exceeded 2.2 standard deviations or presented abnormal distributions). Following normalization and quality control analysis, differentially methylated position analysis was

performed. β-values were converted into M-values to represent a more valid distribution of data for analysis of differential methylation [156]. Because both treatments were completed by each participant, paired Samples t-tests were used to assess 30 Fail versus 80 Fail at PRE, 3h POST, and 6h POST, and significant DMPs at PRE were removed as confounding DMPs. An ANOVA was also used to determine the main effects for condition (30 Fail and 80 Fail over time) and for time (PRE vs 3h POST, PRE vs 6h POST, and 3h POST vs 6h POST). Differentially methylated CpG positions (DMPs) were subjected to a significance value of $p < 0.01$. Additionally, an analysis to quantify differentially methylated regions (DMRs) that contained at least 2 DMPs within a short genomic region/ loci was performed using the Bioconductor package DMRcate (DOI: 10.18129/B9.bioc.DMRcate).

Transcriptome Analysis. Following the quantification of gene expression with the Clariom-S microarray, raw .CEL files were uploaded into the Transcriptome Analysis Console v4.0.2 (TAC) (Thermo Fisher Scientific). The *H. sapiens* genome was used to generate the reference annotations. Two-way repeated measure (2x2) ANOVAs, with the eBayes correction factor applied, were performed for interactions between bouts from PRE to 3h POST and PRE to 6h POST, for each gene. For this statistical analysis, gene expression was considered significant if a Δfold-change of ±1.5 was exceeded, if the p-value for interaction was less than 0.01, and if the expression at PRE was not significantly different between conditions (p-value less than 0.05). From this analysis, a list of significant genes was generated for use in pathway analysis. Additionally, pairwise comparisons were conducted within each bout for significant time effects. A gene target was considered significant if gene expression exceeded a ±1.5-fold-change from PRE and the p-value for time was less than 0.01. These gene lists were subjected to gene pathway

enrichment analysis using the publicly available gene ontology PANTHER17.0 pathway analysis [157, 158].

Acknowledgements

The authors would like to thank the participants for devoting their time and willingness to engage in this study.

Funding

M.C. McIntosh was fully supported through a T32 NIH grant (T32GM141739). MDR discretionary laboratory funds were used to fund assay and participant compensation costs.

Author Contributions

CLS and MDR primarily designed and drafted the manuscript. Statistical analysis was conducted by APS, MDR, and CLS, while other gave critical input: KCY, JSG, and CBM. CLS and MDR created the study design, and CLS coordinated the study. All others assisted with testing, study coordination, assays, and any additional aspects of the study.

References

1. Schoenfeld, B.J., *The Mechanisms of Muscle Hypertrophy and Their Application to Resistance Training.* Journal of Strength and Conditioning Research, 2010. **24**(10): p. 2857-2872.
2. Egan, B. and J.R. Zierath, *Exercise metabolism and the molecular regulation of skeletal muscle adaptation.* Cell Metab, 2013. **17**(2): p. 162-84.
3. Lim, C., et al., *Resistance Exercise-induced Changes in Muscle Phenotype Are Load Dependent.* Med Sci Sports Exerc, 2019. **51**(12): p. 2578-2585.
4. Campos, G.E., et al., *Muscular adaptations in response to three different resistance-training regimens: specificity of repetition maximum training zones.* Eur J Appl Physiol, 2002. **88**(1-2): p. 50-60.
5. Kraemer, W.J. and N.A. Ratamess, *Fundamentals of resistance training: progression and exercise prescription.* Med Sci Sports Exerc, 2004. **36**(4): p. 674-88.
6. Haun, C.T., et al., *Muscle fiber hypertrophy in response to 6 weeks of high-volume resistance training in trained young men is largely attributed to sarcoplasmic hypertrophy.* PLoS One, 2019. **14**(6): p. e0215267.
7. Vann, C.G., et al., *Effects of High-Volume versus High-Load Resistance Training on Skeletal Muscle Growth and Molecular Adaptations.* bioRxiv, 2021: p. 2021.07.01.450728.
8. West, D.W.D., et al., *Acute resistance exercise activates rapamycin-sensitive and -insensitive mechanisms that control translational activity and capacity in skeletal muscle.* Journal of Physiology-London, 2016. **594**(2): p. 453-468.

9. Robinson, M.M., et al., *Enhanced Protein Translation Underlies Improved Metabolic and Physical Adaptations to Different Exercise Training Modes in Young and Old Humans.* Cell Metab, 2017. **25**(3): p. 581-592.

10. Grgic, J. and B.J. Schoenfeld, *Are the Hypertrophic Adaptations to High and Low-Load Resistance Training Muscle Fiber Type Specific?* Front Physiol, 2018. **9**: p. 402.

11. Lasevicius, T., et al., *Effects of different intensities of resistance training with equated volume load on muscle strength and hypertrophy.* Eur J Sport Sci, 2018. **18**(6): p. 772-780.

12. Lopez, P., et al., *Resistance Training Load Effects on Muscle Hypertrophy and Strength Gain: Systematic Review and Network Meta-analysis.* Med Sci Sports Exerc, 2021. **53**(6): p. 1206-1216.

13. Mitchell, C.J., et al., *Resistance exercise load does not determine training-mediated hypertrophic gains in young men.* J Appl Physiol (1985), 2012. **113**(1): p. 71-7.

14. Schoenfeld, B.J., et al., *Strength and Hypertrophy Adaptations Between Low- vs. High-Load Resistance Training: A Systematic Review and Meta-analysis.* J Strength Cond Res, 2017. **31**(12): p. 3508-3523.

15. Vann, C.G., et al., *Skeletal Muscle Protein Composition Adaptations to 10 Weeks of High-Load Resistance Training in Previously-Trained Males.* Front Physiol, 2020. **11**: p. 259.

16. Roberts, M.D., et al., *Sarcoplasmic Hypertrophy in Skeletal Muscle: A Scientific "Unicorn" or Resistance Training Adaptation?* Front Physiol, 2020. **11**: p. 816.

17. Vann, C.G., et al., *Effects of High-Volume Versus High-Load Resistance Training on Skeletal Muscle Growth and Molecular Adaptations.* Front Physiol, 2022. **13**: p. 857555.

18. Damas, F., et al., *Resistance training in young men induces muscle transcriptome-wide changes associated with muscle structure and metabolism refining the response to exercise-induced stress.* Eur J Appl Physiol, 2018. **118**(12): p. 2607-2616.

19. Barres, R., et al., *Acute exercise remodels promoter methylation in human skeletal muscle.* Cell Metab, 2012. **15**(3): p. 405-11.

20. Bird, A.P., *CpG-rich islands and the function of DNA methylation.* Nature, 1986. **321**(6067): p. 209-13.

21. Voisin, S., et al., *Exercise training and DNA methylation in humans.* Acta Physiol (Oxf), 2015. **213**(1): p. 39-59.

22. Seaborne, R.A., et al., *Methylome of human skeletal muscle after acute & chronic resistance exercise training, detraining & retraining.* Sci Data, 2018. **5**: p. 180213.

23. Seaborne, R.A., et al., *Human Skeletal Muscle Possesses an Epigenetic Memory of Hypertrophy.* Sci Rep, 2018. **8**(1): p. 1898.

24. Seaborne, R.A. and A.P. Sharples, *The Interplay Between Exercise Metabolism, Epigenetics, and Skeletal Muscle Remodeling.* Exerc Sport Sci Rev, 2020. **48**(4): p. 188-200.

25. Wu, X. and Y. Zhang, *TET-mediated active DNA demethylation: mechanism, function and beyond.* Nat Rev Genet, 2017. **18**(9): p. 517-534.

26. Maasar, M.F., et al., *The Comparative Methylome and Transcriptome After Change of Direction Compared to Straight Line Running Exercise in Human Skeletal Muscle.* Front Physiol, 2021. **12**: p. 619447.

27. Wang, H., et al., *Muscle regeneration controlled by a designated DNA dioxygenase.* Cell Death Dis, 2021. **12**(6): p. 535.

28. Lavin, K.M., et al., *Muscle transcriptional networks linked to resistance exercise training hypertrophic response heterogeneity.* Physiol Genomics, 2021. **53**(5): p. 206-221.

29. Pillon, N.J., et al., *Transcriptomic profiling of skeletal muscle adaptations to exercise and inactivity.* Nat Commun, 2020. **11**(1): p. 470.

30. Powell, D.J., et al., *Ceramide disables 3-phosphoinositide binding to the pleckstrin homology domain of protein kinase B (PKB)/Akt by a PKCzeta-dependent mechanism.* Mol Cell Biol, 2003. **23**(21): p. 7794-808.

31. Saxton, R.A. and D.M. Sabatini, *mTOR Signaling in Growth, Metabolism, and Disease.* Cell, 2017. **168**(6): p. 960-976.

32. Fant, C.B. and D.J. Taatjes, *Regulatory functions of the Mediator kinases CDK8 and CDK19.* Transcription, 2019. **10**(2): p. 76-90.

33. Wagner, P.D., *The critical role of VEGF in skeletal muscle angiogenesis and blood flow.* Biochem Soc Trans, 2011. **39**(6): p. 1556-9.

34. Munoz-Canoves, P., et al., *Interleukin-6 myokine signaling in skeletal muscle: a double-edged sword?* FEBS J, 2013. **280**(17): p. 4131-48.

35. Kanda, K., et al., *Eccentric exercise-induced delayed-onset muscle soreness and changes in markers of muscle damage and inflammation.* Exerc Immunol Rev, 2013. **19**: p. 72-85.

36. Gumucio, J.P., K.B. Sugg, and C.L. Mendias, *TGF-beta superfamily signaling in muscle and tendon adaptation to resistance exercise.* Exerc Sport Sci Rev, 2015. **43**(2): p. 93-9.

37. Laker, R.C., et al., *Transcriptomic and epigenetic responses to short-term nutrient-exercise stress in humans.* Sci Rep, 2017. **7**(1): p. 15134.

38. American College of Sports, M., et al., *American College of Sports Medicine position stand. Exercise and fluid replacement.* Med Sci Sports Exerc, 2007. **39**(2): p. 377-90.

39. Esco, M.R., et al., *Agreement between supine and standing bioimpedance spectroscopy devices and dual-energy X-ray absorptiometry for body composition determination.* Clin Physiol Funct Imaging, 2019. **39**(5): p. 355-361.

40. Moon, J.R., et al., *Estimating body fat in NCAA Division I female athletes: a five-compartment model validation of laboratory methods.* Eur J Appl Physiol, 2009. **105**(1): p. 119-30.

41. Sexton, C.L., et al., *Effects of Peanut Protein Supplementation on Resistance Training Adaptations in Younger Adults.* Nutrients, 2021. **13**(11).

42. Wen, Y., et al., *MyoVision: software for automated high-content analysis of skeletal muscle immunohistochemistry.* J Appl Physiol (1985), 2018. **124**(1): p. 40-51.

43. Viggars, M.R., et al., *Automated cross-sectional analysis of trained, severely atrophied, and recovering rat skeletal muscles using MyoVision 2.0.* J Appl Physiol (1985), 2022. **132**(3): p. 593-610.

44. Maksimovic, J., B. Phipson, and A. Oshlack, *A cross-package Bioconductor workflow for analysing methylation array data.* F1000Res, 2016. **5**: p. 1281.

45. Pidsley, R., et al., *Critical evaluation of the Illumina MethylationEPIC BeadChip microarray for whole-genome DNA methylation profiling.* Genome Biol, 2016. **17**(1): p. 208.

46. Maksimovic, J., L. Gordon, and A. Oshlack, *SWAN: Subset-quantile within array normalization for illumina infinium HumanMethylation450 BeadChips.* Genome Biol, 2012. **13**(6): p. R44.

47. Du, P., et al., *Comparison of Beta-value and M-value methods for quantifying methylation levels by microarray analysis.* BMC Bioinformatics, 2010. **11**: p. 587.

48. Mi, H., et al., *PANTHER version 16: a revised family classification, tree-based classification tool, enhancer regions and extensive API.* Nucleic Acids Res, 2021. **49**(D1): p. D394-D403.

49. Mi, H. and P. Thomas, *PANTHER pathway: an ontology-based pathway database coupled with data analysis tools.* Methods Mol Biol, 2009. **563**: p. 123-40.

REFERENCES (FOR ENTIRETY OF DISSERTATION, SANS Chapter IV)

1. Schoenfeld, B.J., *The Mechanisms of Muscle Hypertrophy and Their Application to Resistance Training.* Journal of Strength and Conditioning Research, 2010. **24**(10): p. 2857-2872.
2. West, D.W.D., et al., *Acute resistance exercise activates rapamycin-sensitive and -insensitive mechanisms that control translational activity and capacity in skeletal muscle.* Journal of Physiology-London, 2016. **594**(2): p. 453-468.
3. Robinson, M.M., et al., *Enhanced Protein Translation Underlies Improved Metabolic and Physical Adaptations to Different Exercise Training Modes in Young and Old Humans.* Cell Metab, 2017. **25**(3): p. 581-592.
4. Egan, B. and J.R. Zierath, *Exercise metabolism and the molecular regulation of skeletal muscle adaptation.* Cell Metab, 2013. **17**(2): p. 162-84.
5. Lim, C., et al., *Resistance Exercise-induced Changes in Muscle Phenotype Are Load Dependent.* Med Sci Sports Exerc, 2019. **51**(12): p. 2578-2585.
6. Campos, G.E., et al., *Muscular adaptations in response to three different resistance-training regimens: specificity of repetition maximum training zones.* Eur J Appl Physiol, 2002. **88**(1-2): p. 50-60.
7. Kraemer, W.J. and N.A. Ratamess, *Fundamentals of resistance training: progression and exercise prescription.* Med Sci Sports Exerc, 2004. **36**(4): p. 674-88.
8. Haun, C.T., et al., *Muscle fiber hypertrophy in response to 6 weeks of high-volume resistance training in trained young men is largely attributed to sarcoplasmic hypertrophy.* PLoS One, 2019. **14**(6): p. e0215267.

9. Vann, C.G., et al., *Effects of High-Volume versus High-Load Resistance Training on Skeletal Muscle Growth and Molecular Adaptations.* bioRxiv, 2021: p. 2021.07.01.450728.

10. Grgic, J. and B.J. Schoenfeld, *Are the Hypertrophic Adaptations to High and Low-Load Resistance Training Muscle Fiber Type Specific?* Front Physiol, 2018. **9**: p. 402.

11. Lasevicius, T., et al., *Effects of different intensities of resistance training with equated volume load on muscle strength and hypertrophy.* Eur J Sport Sci, 2018. **18**(6): p. 772-780.

12. Lopez, P., et al., *Resistance Training Load Effects on Muscle Hypertrophy and Strength Gain: Systematic Review and Network Meta-analysis.* Med Sci Sports Exerc, 2021. **53**(6): p. 1206-1216.

13. Mitchell, C.J., et al., *Resistance exercise load does not determine training-mediated hypertrophic gains in young men.* J Appl Physiol (1985), 2012. **113**(1): p. 71-7.

14. Schoenfeld, B.J., et al., *Strength and Hypertrophy Adaptations Between Low- vs. High-Load Resistance Training: A Systematic Review and Meta-analysis.* J Strength Cond Res, 2017. **31**(12): p. 3508-3523.

15. Vann, C.G., et al., *Skeletal Muscle Protein Composition Adaptations to 10 Weeks of High-Load Resistance Training in Previously-Trained Males.* Front Physiol, 2020. **11**: p. 259.

16. Roberts, M.D., et al., *Sarcoplasmic Hypertrophy in Skeletal Muscle: A Scientific "Unicorn" or Resistance Training Adaptation?* Front Physiol, 2020. **11**: p. 816.

17. Vann, C.G., et al., *Effects of High-Volume Versus High-Load Resistance Training on Skeletal Muscle Growth and Molecular Adaptations.* Front Physiol, 2022. **13**: p. 857555.

18. Seaborne, R.A., et al., *Human Skeletal Muscle Possesses an Epigenetic Memory of Hypertrophy.* Sci Rep, 2018. **8**(1): p. 1898.

19. Sharples, A.P., C.E. Stewart, and R.A. Seaborne, *Does skeletal muscle have an 'epi'-memory? The role of epigenetics in nutritional programming, metabolic disease, aging and exercise.* Aging Cell, 2016. **15**(4): p. 603-16.

20. Jacques, M., et al., *Epigenetic changes in healthy human skeletal muscle following exercise- a systematic review.* Epigenetics, 2019. **14**(7): p. 633-648.

21. Seaborne, R.A. and A.P. Sharples, *The Interplay Between Exercise Metabolism, Epigenetics, and Skeletal Muscle Remodeling.* Exerc Sport Sci Rev, 2020. **48**(4): p. 188-200.

22. Seaborne, R.A., et al., *Methylome of human skeletal muscle after acute & chronic resistance exercise training, detraining & retraining.* Sci Data, 2018. **5**: p. 180213.

23. Turner, D.C., et al., *Mechanical loading of bioengineered skeletal muscle in vitro recapitulates gene expression signatures of resistance exercise in vivo.* J Cell Physiol, 2021. **236**(9): p. 6534-6547.

24. Turner, D.C., R.A. Seaborne, and A.P. Sharples, *Comparative Transcriptome and Methylome Analysis in Human Skeletal Muscle Anabolism, Hypertrophy and Epigenetic Memory.* Sci Rep, 2019. **9**(1): p. 4251.

25. Voisin, S., et al., *Exercise training and DNA methylation in humans.* Acta Physiol (Oxf), 2015. **213**(1): p. 39-59.

26. Wen, Y., et al., *Nucleus Type-Specific DNA Methylomics Reveals Epigenetic "Memory" of Prior Adaptation in Skeletal Muscle.* Function, 2021. **2**(5).

27. Wu, X. and Y. Zhang, *TET-mediated active DNA demethylation: mechanism, function and beyond.* Nat Rev Genet, 2017. **18**(9): p. 517-534.

28. Bagley, J.R., et al., *Epigenetic Responses to Acute Resistance Exercise in Trained vs. Sedentary Men.* J Strength Cond Res, 2020. **34**(6): p. 1574-1580.

29. Davegardh, C., et al., *Sex influences DNA methylation and gene expression in human skeletal muscle myoblasts and myotubes.* Stem Cell Res Ther, 2019. **10**(1): p. 26.

30. Jacobsen, S.C., et al., *Effects of short-term high-fat overfeeding on genome-wide DNA methylation in the skeletal muscle of healthy young men.* Diabetologia, 2012. **55**(12): p. 3341-9.

31. Ruple, B.A., et al., *Resistance training rejuvenates the mitochondrial methylome in aged human skeletal muscle.* FASEB J, 2021. **35**(9): p. e21864.

32. Zurlo, F., et al., *Skeletal-Muscle Metabolism Is a Major Determinant of Resting Energy-Expenditure.* Journal of Clinical Investigation, 1990. **86**(5): p. 1423-1427.

33. Purslow, P.P., *The Structure and Role of Intramuscular Connective Tissue in Muscle Function.* Front Physiol, 2020. **11**: p. 495.

34. Zhang, W., Y. Liu, and H. Zhang, *Extracellular matrix: an important regulator of cell functions and skeletal muscle development.* Cell Biosci, 2021. **11**(1): p. 65.

35. Kjaer, M., *Role of extracellular matrix in adaptation of tendon and skeletal muscle to mechanical loading.* Physiol Rev, 2004. **84**(2): p. 649-98.

36. Huxley, H. and J. Hanson, *Changes in the Cross-Striations of Muscle during Contraction and Stretch and Their Structural Interpretation.* Nature, 1954. **173**(4412): p. 973-976.

37. Huxley, A.F. and R. Niedergerke, *Structural Changes in Muscle during Contraction - Interference Microscopy of Living Muscle Fibres.* Nature, 1954. **173**(4412): p. 971-973.

38. Riley, D.A., et al., *Review of spaceflight and hindlimb suspension unloading induced sarcomere damage and repair.* Basic Appl Myol, 1995. **5**(2): p. 139-45.

39. Nieto, B., et al., *Identification of distinct maturation steps involved in human 40S ribosomal subunit biosynthesis.* Nat Commun, 2020. **11**(1): p. 156.

40. Chaillou, T., *Ribosome specialization and its potential role in the control of protein translation and skeletal muscle size.* J Appl Physiol (1985), 2019. **127**(2): p. 599-607.

41. Doudna, J.A. and V.L. Rath, *Structure and function of the eukaryotic ribosome: the next frontier.* Cell, 2002. **109**(2): p. 153-6.

42. Gauthier, G.F. and A. Mason-Savas, *Ribosomes in the skeletal muscle filament lattice.* Anat Rec, 1993. **237**(2): p. 149-56.

43. Chyn, T.L., et al., *In vitro synthesis of the Ca2+ transport ATPase by ribosomes bound to sarcoplasmic reticulum membranes.* Proc Natl Acad Sci U S A, 1979. **76**(3): p. 1241-5.

44. Mauro, V.P. and G.M. Edelman, *The ribosome filter hypothesis.* Proc Natl Acad Sci U S A, 2002. **99**(19): p. 12031-6.

45. Stec, M.J., et al., *Ribosome biogenesis may augment resistance training-induced myofiber hypertrophy and is required for myotube growth in vitro.* Am J Physiol Endocrinol Metab, 2016. **310**(8): p. E652-E661.

46. Mobley, C.B., et al., *Biomarkers associated with low, moderate, and high vastus lateralis muscle hypertrophy following 12 weeks of resistance training.* PLoS One, 2018. **13**(4): p. e0195203.

47. Mesquita, P.H.C., et al., *Skeletal Muscle Ribosome and Mitochondrial Biogenesis in Response to Different Exercise Training Modalities.* Front Physiol, 2021. **12**: p. 725866.

48. Hammarstrom, D., et al., *Benefits of higher resistance-training volume are related to ribosome biogenesis.* J Physiol, 2020. **598**(3): p. 543-565.

49. Lecker, S.H., et al., *Muscle protein breakdown and the critical role of the ubiquitin-proteasome pathway in normal and disease states.* J Nutr, 1999. **129**(1S Suppl): p. 227S-237S.

50. Attaix, D., et al., *Ubiquitin-proteasome-dependent proteolysis in skeletal muscle.* Reprod Nutr Dev, 1998. **38**(2): p. 153-65.

51. Stefanetti, R.J., et al., *Regulation of ubiquitin proteasome pathway molecular markers in response to endurance and resistance exercise and training.* Pflugers Arch, 2015. **467**(7): p. 1523-1537.

52. von Mikecz, A., *The nuclear ubiquitin-proteasome system.* J Cell Sci, 2006. **119**(Pt 10): p. 1977-84.

53. Fill, M. and J.A. Copello, *Ryanodine receptor calcium release channels.* Physiol Rev, 2002. **82**(4): p. 893-922.

54. Farah, C.S. and F.C. Reinach, *The troponin complex and regulation of muscle contraction.* FASEB J, 1995. **9**(9): p. 755-67.

55. Periasamy, M. and A. Kalyanasundaram, *SERCA pump isoforms: their role in calcium transport and disease.* Muscle Nerve, 2007. **35**(4): p. 430-42.

56. Xu, H. and H. Van Remmen, *The SarcoEndoplasmic Reticulum Calcium ATPase (SERCA) pump: a potential target for intervention in aging and skeletal muscle pathologies.* Skelet Muscle, 2021. **11**(1): p. 25.

57. Nogueira, L., et al., *Ca(2)(+)-pumping impairment during repetitive fatiguing contractions in single myofibers: role of cross-bridge cycling.* Am J Physiol Regul Integr Comp Physiol, 2013. **305**(2): p. R118-25.

58. Parry, H.A., M.D. Roberts, and A.N. Kavazis, *Human Skeletal Muscle Mitochondrial Adaptations Following Resistance Exercise Training.* Int J Sports Med, 2020. **41**(6): p. 349-359.

59. Gan, Z., et al., *Skeletal muscle mitochondrial remodeling in exercise and diseases.* Cell Research, 2018. **28**(10): p. 969-980.

60. Cori, C.F., *Mammalian carbohydrate metabolism.* Physiological Reviews, 1931. **11**(2): p. 143-275.

61. Bergström, J., et al., *Intracellular free amino acid concentration in human muscle tissue.* Journal of applied physiology, 1974. **36**(6): p. 693-697.

62. Wolfe, R.R., et al., *Role of triglyceride-fatty acid cycle in controlling fat metabolism in humans during and after exercise.* American Journal of Physiology-Endocrinology And Metabolism, 1990. **258**(2): p. E382-E389.

63. Zhao, R.Z., et al., *Mitochondrial electron transport chain, ROS generation and uncoupling.* International journal of molecular medicine, 2019. **44**(1): p. 3-15.

64. Brooks, G.A., T.D. Fahey, and K.M. Baldwin, *Exercise physiology : human bioenergetics and its applications*. 4th ed. 2005, Boston: McGraw-Hill. xxi, 876, 7, 22 p.

65. Allen, D.L., R.R. Roy, and V.R. Edgerton, *Myonuclear domains in muscle adaptation and disease.* Muscle Nerve, 1999. **22**(10): p. 1350-60.

66. Kirby, T.J., et al., *Myonuclear transcription is responsive to mechanical load and DNA content but uncoupled from cell size during hypertrophy.* Mol Biol Cell, 2016. **27**(5): p. 788-98.

67. Hinkle, E.R., et al., *RNA processing in skeletal muscle biology and disease.* Transcription, 2019. **10**(1): p. 1-20.

68. Kim, H.G., B. Guo, and G.A. Nader, *Regulation of Ribosome Biogenesis During Skeletal Muscle Hypertrophy.* Exerc Sport Sci Rev, 2019. **47**(2): p. 91-97.

69. Denes, L.T., C.P. Kelley, and E.T. Wang, *Microtubule-based transport is essential to distribute RNA and nascent protein in skeletal muscle.* Nat Commun, 2021. **12**(1): p. 6079.

70. Conceicao, M.S., et al., *Muscle Fiber Hypertrophy and Myonuclei Addition: A Systematic Review and Meta-analysis.* Med Sci Sports Exerc, 2018. **50**(7): p. 1385-1393.

71. Bruusgaard, J.C., et al., *Myonuclei acquired by overload exercise precede hypertrophy and are not lost on detraining.* Proc Natl Acad Sci U S A, 2010. **107**(34): p. 15111-6.

72. McCarthy, J.J., et al., *Effective fiber hypertrophy in satellite cell-depleted skeletal muscle.* Development, 2011. **138**(17): p. 3657-66.

73. Eftestol, E., et al., *Muscle memory: are myonuclei ever lost?* J Appl Physiol (1985), 2020. **128**(2): p. 456-457.

74. Murach, K.A., et al., *Starring or Supporting Role? Satellite Cells and Skeletal Muscle Fiber Size Regulation.* Physiology (Bethesda), 2018. **33**(1): p. 26-38.

75. Cramer, A.A.W., et al., *Nuclear numbers in syncytial muscle fibers promote size but limit the development of larger myonuclear domains.* Nat Commun, 2020. **11**(1): p. 6287.

76. Hawley, J.A., et al., *Integrative biology of exercise.* Cell, 2014. **159**(4): p. 738-49.

77. Jacobs, B.L., et al., *Eccentric contractions increase the phosphorylation of tuberous sclerosis complex-2 (TSC2) and alter the targeting of TSC2 and the mechanistic target of rapamycin to the lysosome.* J Physiol, 2013. **591**(18): p. 4611-20.

78. You, J.S., et al., *A DGKzeta-FoxO-ubiquitin proteolytic axis controls fiber size during skeletal muscle remodeling.* Sci Signal, 2018. **11**(530).

79. Hornberger, T.A., et al., *The role of phospholipase D and phosphatidic acid in the mechanical activation of mTOR signaling in skeletal muscle.* Proc Natl Acad Sci U S A, 2006. **103**(12): p. 4741-6.

80. Jacobs, B.L., et al., *Identification of mechanically regulated phosphorylation sites on tuberin (TSC2) that control mechanistic target of rapamycin (mTOR) signaling.* J Biol Chem, 2017. **292**(17): p. 6987-6997.

81. Karlsson, H.K., et al., *Branched-chain amino acids increase p70S6k phosphorylation in human skeletal muscle after resistance exercise.* Am J Physiol Endocrinol Metab, 2004. **287**(1): p. E1-7.

82. Gundermann, D.M., et al., *Activation of mTORC1 signaling and protein synthesis in human muscle following blood flow restriction exercise is inhibited by rapamycin.* Am J Physiol Endocrinol Metab, 2014. **306**(10): p. E1198-204.

83. Gordon, B.S., et al., *Reduced REDD1 expression contributes to activation of mTORC1 following electrically induced muscle contraction.* Am J Physiol Endocrinol Metab, 2014. **307**(8): p. E703-11.

84. Hamilton, D.L., et al., *Molecular brakes regulating mTORC1 activation in skeletal muscle following synergist ablation.* Am J Physiol Endocrinol Metab, 2014. **307**(4): p. E365-73.

85. Goodman, C.A., et al., *The role of skeletal muscle mTOR in the regulation of mechanical load-induced growth.* J Physiol, 2011. **589**(Pt 22): p. 5485-501.

86. Vianna, J.M., et al., *Aerobic and Anaerobic Energy During Resistance Exercise at 80% 1RM.* J Hum Kinet, 2011. **29A**: p. 69-74.

87. Gastin, P.B., *Energy system interaction and relative contribution during maximal exercise.* Sports Med, 2001. **31**(10): p. 725-41.

88. Mang, Z.A., et al., *Aerobic Adaptations to Resistance Training: The Role of Time under Tension.* Int J Sports Med, 2022.

89. Schoenfeld, B.J., et al., *Effects of Low- vs. High-Load Resistance Training on Muscle Strength and Hypertrophy in Well-Trained Men.* J Strength Cond Res, 2015. **29**(10): p. 2954-63.

90. Burd, N.A., et al., *Low-load high volume resistance exercise stimulates muscle protein synthesis more than high-load low volume resistance exercise in young men.* PLoS One, 2010. **5**(8): p. e12033.

91. Burd, N.A., et al., *Muscle time under tension during resistance exercise stimulates differential muscle protein sub-fractional synthetic responses in men.* J Physiol, 2012. **590**(2): p. 351-62.

92. Fink, J., et al., *Impact of high versus low fixed loads and non-linear training loads on muscle hypertrophy, strength and force development.* Springerplus, 2016. **5**(1): p. 698.

93. Fisher, J.P. and J. Steele, *Heavier and lighter load resistance training to momentary failure produce similar increases in strength with differing degrees of discomfort.* Muscle Nerve, 2017. **56**(4): p. 797-803.

94. Haun, C.T., et al., *Molecular, neuromuscular, and recovery responses to light versus heavy resistance exercise in young men.* Physiol Rep, 2017. **5**(18).

95. Ikezoe, T., et al., *Effects of Low-Load, Higher-Repetition vs. High-Load, Lower-Repetition Resistance Training Not Performed to Failure on Muscle Strength, Mass, and Echo Intensity in Healthy Young Men: A Time-Course Study.* J Strength Cond Res, 2020. **34**(12): p. 3439-3445.

96. Jenkins, N.D., et al., *Neuromuscular Adaptations After 2 and 4 Weeks of 80% Versus 30% 1 Repetition Maximum Resistance Training to Failure.* J Strength Cond Res, 2016. **30**(8): p. 2174-85.

97. Morton, R.W., et al., *Muscle fibre activation is unaffected by load and repetition duration when resistance exercise is performed to task failure.* J Physiol, 2019. **597**(17): p. 4601-4613.

98. Fields, D.A., M.I. Goran, and M.A. McCrory, *Body-composition assessment via air-displacement plethysmography in adults and children: a review.* Am J Clin Nutr, 2002. **75**(3): p. 453-67.

99. Au, J.S., et al., *Arterial Stiffness Is Reduced Regardless of Resistance Training Load in Young Men.* Med Sci Sports Exerc, 2017. **49**(2): p. 342-348.

100. Rana, S.R., et al., *Comparison of early phase adaptations for traditional strength and endurance, and low velocity resistance training programs in college-aged women.* J Strength Cond Res, 2008. **22**(1): p. 119-27.

101. Fink, J., N. Kikuchi, and K. Nakazato, *Effects of rest intervals and training loads on metabolic stress and muscle hypertrophy.* Clin Physiol Funct Imaging, 2018. **38**(2): p. 261-268.

102. Hisaeda, H., et al., *Influence of two different modes of resistance training in female subjects.* Ergonomics, 1996. **39**(6): p. 842-52.

103. Popov, D.V., et al., *[Hormonal adaptation determines the increase in muscle mass and strength during low-intensity strength training without relaxation]*. Fiziol Cheloveka, 2006. **32**(5): p. 121-7.

104. Tanimoto, M. and N. Ishii, *Effects of low-intensity resistance exercise with slow movement and tonic force generation on muscular function in young men.* J Appl Physiol (1985), 2006. **100**(4): p. 1150-7.

105. Van Roie, E., et al., *Strength training at high versus low external resistance in older adults: Effects on muscle volume, muscle strength, and force-velocity characteristics.* Experimental Gerontology, 2013. **48**(11): p. 1351-1361.

106. Morton, R.W., et al., *Neither load nor systemic hormones determine resistance training-mediated hypertrophy or strength gains in resistance-trained young men.* Journal of Applied Physiology, 2016. **121**(1): p. 129-138.

107. Abbott, S. and D.J. Fairbanks, *Experiments on Plant Hybrids by Gregor Mendel.* Genetics, 2016. **204**(2): p. 407-422.

108. Schrödinger, E., *What is life? : the physical aspect of the living cell ; with, Mind and matter ; & Autobiographical sketches*. 1992, Cambridge ; New York: Cambridge University Press. viii, 184 p.

109. Horowitz, N.H. and U. Leupold, *Some Recent Studies Bearing on the One Gene-One Enzyme Hypothesis.* Cold Spring Harbor Symposia on Quantitative Biology, 1951. **16**: p. 65-74.

110. Beadle, G.W. and E.L. Tatum, *Genetic Control of Biochemical Reactions in Neurospora.* Proc Natl Acad Sci U S A, 1941. **27**(11): p. 499-506.

111. Gayon, J., *From Mendel to epigenetics: History of genetics.* C R Biol, 2016. **339**(7-8): p. 225-30.

112. Avery, O.T., C.M. Macleod, and M. McCarty, *Studies on the Chemical Nature of the Substance Inducing Transformation of Pneumococcal Types : Induction of Transformation by a Desoxyribonucleic Acid Fraction Isolated from Pneumococcus Type Iii.* J Exp Med, 1944. **79**(2): p. 137-58.

113. Dahm, R., *Discovering DNA: Friedrich Miescher and the early years of nucleic acid research.* Hum Genet, 2008. **122**(6): p. 565-81.

114. Chargaff, E., *Structure and function of nucleic acids as cell constituents.* Fed Proc, 1951. **10**(3): p. 654-9.

115. Chargaff, E., E. Vischer, and et al., *The composition of the desoxypentose nucleic acids of thymus and spleen.* J Biol Chem, 1949. **177**(1): p. 405-16.

116. Watson, J.D. and F.H.C. Crick, *Molecular Structure of Nucleic Acids - a Structure for Deoxyribose Nucleic Acid.* Nature, 1953. **171**(4356): p. 737-738.

117. Bird, A.P., *CpG-rich islands and the function of DNA methylation.* Nature, 1986. **321**(6067): p. 209-13.

118. Eden, S. and H. Cedar, *Role of DNA methylation in the regulation of transcription.* Curr Opin Genet Dev, 1994. **4**(2): p. 255-9.

119. Jurkowska, R.Z., T.P. Jurkowski, and A. Jeltsch, *Structure and function of mammalian DNA methyltransferases.* Chembiochem, 2011. **12**(2): p. 206-22.

120. Moore, L.D., T. Le, and G. Fan, *DNA methylation and its basic function.* Neuropsychopharmacology, 2013. **38**(1): p. 23-38.

121. Sellami, M., et al., *Regular, Intense Exercise Training as a Healthy Aging Lifestyle Strategy: Preventing DNA Damage, Telomere Shortening and Adverse DNA Methylation Changes Over a Lifetime.* Front Genet, 2021. **12**: p. 652497.

122. Swiatowy, W.J., et al., *Physical Activity and DNA Methylation in Humans.* Int J Mol Sci, 2021. **22**(23).

123. Widmann, M., A.M. Niess, and B. Munz, *Physical Exercise and Epigenetic Modifications in Skeletal Muscle.* Sports Med, 2019. **49**(4): p. 509-523.

124. Ille, A.M., H. Lamont, and M.B. Mathews, *The Central Dogma revisited: Insights from protein synthesis, CRISPR, and beyond.* Wiley Interdiscip Rev RNA, 2022: p. e1718.

125. Babu, A. and R.S. Verma, *Chromosome structure: euchromatin and heterochromatin.* Int Rev Cytol, 1987. **108**: p. 1-60.

126. Luger, K., *Dynamic nucleosomes.* Chromosome Res, 2006. **14**(1): p. 5-16.

127. Mellor, J., *Dynamic nucleosomes and gene transcription.* Trends Genet, 2006. **22**(6): p. 320-9.

128. Bendandi, A., et al., *The role of histone tails in nucleosome stability: An electrostatic perspective.* Comput Struct Biotechnol J, 2020. **18**: p. 2799-2809.

129. Horvath, J.E., et al., *Lessons from the human genome: transitions between euchromatin and heterochromatin.* Human Molecular Genetics, 2001. **10**(20): p. 2215-2223.

130. Lander, E.S., et al., *Initial sequencing and analysis of the human genome.* Nature, 2001. **409**(6822): p. 860-921.

131. Ulrey, C.L., et al., *The impact of metabolism on DNA methylation.* Hum Mol Genet, 2005. **14 Spec No 1**: p. R139-47.

132. Jang, H.S., et al., *CpG and Non-CpG Methylation in Epigenetic Gene Regulation and Brain Function.* Genes (Basel), 2017. **8**(6).

133. Barres, R., et al., *Acute exercise remodels promoter methylation in human skeletal muscle.* Cell Metab, 2012. **15**(3): p. 405-11.

134. Hackett, J.A. and M.A. Surani, *DNA methylation dynamics during the mammalian life cycle.* Philos Trans R Soc Lond B Biol Sci, 2013. **368**(1609): p. 20110328.

135. Hashimoto, H., et al., *Recognition and potential mechanisms for replication and erasure of cytosine hydroxymethylation.* Nucleic Acids Res, 2012. **40**(11): p. 4841-9.

136. Iio, H., et al., *DNA maintenance methylation enzyme Dnmt1 in satellite cells is essential for muscle regeneration.* Biochem Biophys Res Commun, 2021. **534**: p. 79-85.

137. Chicoine, J., et al., *Bicaudal-C recruits CCR4-NOT deadenylase to target mRNAs and regulates oogenesis, cytoskeletal organization, and its own expression.* Dev Cell, 2007. **13**(5): p. 691-704.

138. Guzman, Y.F., et al., *A gain-of-function mutation in the GRIK2 gene causes neurodevelopmental deficits.* Neurol Genet, 2017. **3**(1): p. e129.

139. Donkor, F.F., et al., *Outer dense fibre protein 2 (ODF2) is a self-interacting centrosomal protein with affinity for microtubules.* J Cell Sci, 2004. **117**(Pt 20): p. 4643-51.

140. Shi, J.H. and S.C. Sun, *Tumor Necrosis Factor Receptor-Associated Factor Regulation of Nuclear Factor kappaB and Mitogen-Activated Protein Kinase Pathways.* Front Immunol, 2018. **9**: p. 1849.

141. Figueiredo, V.C., et al., *Genetic and epigenetic regulation of skeletal muscle ribosome biogenesis with exercise.* J Physiol, 2021. **599**(13): p. 3363-3384.

142. Von Walden, F., et al., *The myonuclear DNA methylome in response to an acute hypertrophic stimulus.* Epigenetics, 2020. **15**(11): p. 1151-1162.

143. Wen, Y., et al., *Nucleus Type-Specific DNA Methylomics Reveals Epigenetic "Memory" of Prior Adaptation in Skeletal Muscle.* Function (Oxf), 2021. **2**(5): p. zqab038.

144. Laker, R.C., et al., *Transcriptomic and epigenetic responses to short-term nutrient-exercise stress in humans.* Sci Rep, 2017. **7**(1): p. 15134.

145. Kuang, J., et al., *Interpretation of exercise-induced changes in human skeletal muscle mRNA expression depends on the timing of the post-exercise biopsies.* PeerJ, 2022. **10**: p. e12856.

146. American College of Sports, M., et al., *American College of Sports Medicine position stand. Exercise and fluid replacement.* Med Sci Sports Exerc, 2007. **39**(2): p. 377-90.

147. Esco, M.R., et al., *Agreement between supine and standing bioimpedance spectroscopy devices and dual-energy X-ray absorptiometry for body composition determination.* Clin Physiol Funct Imaging, 2019. **39**(5): p. 355-361.

148. Moon, J.R., et al., *Estimating body fat in NCAA Division I female athletes: a five-compartment model validation of laboratory methods.* Eur J Appl Physiol, 2009. **105**(1): p. 119-30.

149. Sexton, C.L., et al., *Effects of Peanut Protein Supplementation on Resistance Training Adaptations in Younger Adults.* Nutrients, 2021. **13**(11).

150. Wen, Y., et al., *MyoVision: software for automated high-content analysis of skeletal muscle immunohistochemistry.* J Appl Physiol (1985), 2018. **124**(1): p. 40-51.

151. Viggars, M.R., et al., *Automated cross-sectional analysis of trained, severely atrophied, and recovering rat skeletal muscles using MyoVision 2.0.* J Appl Physiol (1985), 2022. **132**(3): p. 593-610.

152. Maasar, M.F., et al., *The Comparative Methylome and Transcriptome After Change of Direction Compared to Straight Line Running Exercise in Human Skeletal Muscle.* Front Physiol, 2021. **12**: p. 619447.

153. Maksimovic, J., B. Phipson, and A. Oshlack, *A cross-package Bioconductor workflow for analysing methylation array data.* F1000Res, 2016. **5**: p. 1281.

154. Pidsley, R., et al., *Critical evaluation of the Illumina MethylationEPIC BeadChip microarray for whole-genome DNA methylation profiling.* Genome Biol, 2016. **17**(1): p. 208.

155. Maksimovic, J., L. Gordon, and A. Oshlack, *SWAN: Subset-quantile within array normalization for illumina infinium HumanMethylation450 BeadChips.* Genome Biol, 2012. **13**(6): p. R44.

156. Du, P., et al., *Comparison of Beta-value and M-value methods for quantifying methylation levels by microarray analysis.* BMC Bioinformatics, 2010. **11**: p. 587.

157. Mi, H., et al., *PANTHER version 16: a revised family classification, tree-based classification tool, enhancer regions and extensive API.* Nucleic Acids Res, 2021. **49**(D1): p. D394-D403.

158. Mi, H. and P. Thomas, *PANTHER pathway: an ontology-based pathway database coupled with data analysis tools.* Methods Mol Biol, 2009. **563**: p. 123-40.

159. Damas, F., et al., *Resistance training in young men induces muscle transcriptome-wide changes associated with muscle structure and metabolism refining the response to exercise-induced stress.* Eur J Appl Physiol, 2018. **118**(12): p. 2607-2616.

160. Wang, H., et al., *Muscle regeneration controlled by a designated DNA dioxygenase.* Cell Death Dis, 2021. **12**(6): p. 535.

161. Lavin, K.M., et al., *Muscle transcriptional networks linked to resistance exercise training hypertrophic response heterogeneity.* Physiol Genomics, 2021. **53**(5): p. 206-221.

162. Pillon, N.J., et al., *Transcriptomic profiling of skeletal muscle adaptations to exercise and inactivity.* Nat Commun, 2020. **11**(1): p. 470.

163. Powell, D.J., et al., *Ceramide disables 3-phosphoinositide binding to the pleckstrin homology domain of protein kinase B (PKB)/Akt by a PKCzeta-dependent mechanism.* Mol Cell Biol, 2003. **23**(21): p. 7794-808.

164. Saxton, R.A. and D.M. Sabatini, *mTOR Signaling in Growth, Metabolism, and Disease.* Cell, 2017. **168**(6): p. 960-976.

165. Fant, C.B. and D.J. Taatjes, *Regulatory functions of the Mediator kinases CDK8 and CDK19.* Transcription, 2019. **10**(2): p. 76-90.

166. Wagner, P.D., *The critical role of VEGF in skeletal muscle angiogenesis and blood flow.* Biochem Soc Trans, 2011. **39**(6): p. 1556-9.

167. Munoz-Canoves, P., et al., *Interleukin-6 myokine signaling in skeletal muscle: a double-edged sword?* FEBS J, 2013. **280**(17): p. 4131-48.

168. Kanda, K., et al., *Eccentric exercise-induced delayed-onset muscle soreness and changes in markers of muscle damage and inflammation.* Exerc Immunol Rev, 2013. **19**: p. 72-85.

169. Gumucio, J.P., K.B. Sugg, and C.L. Mendias, *TGF-beta superfamily signaling in muscle and tendon adaptation to resistance exercise.* Exerc Sport Sci Rev, 2015. **43**(2): p. 93-9.